Aus dem Fachbereich Medizin

der Johann Wolfgang Goethe-Universität

Frankfurt am Main

betreut am

Zentrum der Inneren Medizin

Medizinische Klinik I

Direktor: Prof. Dr. Stefan Zeuzem

Identification and characterization of allosteric inhibitors of Aurora Kinase A for innovative drug discovery for cancer therapy

Dissertation

zur Erlangung des Doktorgrades der Medizin

des Fachbereichs Medizin

der Johann Wolfgang Goethe-Universität

Frankfurt am Main

vorgelegt von

Amanda Herbrand

aus München

Frankfurt am Main, 2018

Dekan:	Prof. Dr. Josef Pfeilschifter
Referent:	Prof. Dr. Dr. Albrecht Piiper
Korreferent/in:	Prof. Dr. Christian Brandts
ggf. 2. Korreferent/in:	
Tag der mündlichen Prüfung:	25.10.2019

Index

I. List of Figures

Figure 3.2: Cross-titrations for AurA and TPX2. The graphs show increasing interaction with increasing concentration of protein and peptide measured. The counts are “arbitrary counts” by the Envision equipment.

Figure 3.3: Substrates tested for 25 ng AurA at 5, 10 and 20 µg. Histone H3 provides the best signal and was chosen as substrate for further activity assays.

Figure 3.4: Linear increase in substrate phosphorylation with increasing amount of AurA. Specific kinase activity remains steady. Each data point of the kinase assay is performed in duplicates.

Figure 3.5: Melting curves of AurA and AurA in conformation with 50 µM of TPX2. Result is a melting point shift $\Delta T_m = 4.2$ °C.

Figure 4.1: Diagrammed order of experiments performed for the identification and characterization of hit-compounds.

Figure 4.2: Identification process of validating hit compounds for displacement of TPX2 from AurA.

Figure 4.3: Curves for all hit compounds identified and confirmed in screening and rescreening.

Figure 4.4: Influence of hit-compounds on phosphorylation of substrate Histone H3. Only Iopanoic acid and Tiratricol achieve a visible reduction of substrate turnover and hence inhibition of AurA. The radioactivity associated to each spot was quantified with phosphoimager technology (see Figure 4.5), which measures radioactivity in a linear range over 6 orders of magnitude.

Figure 4.5: Results for hit-compounds tested on the activity of AurA. Only Iopanoic acid and Tiratricol show a clear inhibitory effect.

Figure 4.6: Overview of melting point shifts of all hit-compounds at a 50µM concentration.

Figure 4.7: Melting point shifts for different concentrations of the compounds.

Figure 4.8: Graphs for the variants of PS 731 tested in AlphaScreen and activity assay. No displacement of TPX2 could be observed, although PS 878, 879 and 882 inhibit the activity of AurA.

Figure 4.9 Effect of compounds on the interaction between AurA and TPX2 peptide. **a)** Impact of MLN8237 on the binding of TPX2 to AurA. MLN8237 potently displaces TPX2 with an IC50 of 0.1 nM; **b)** Comparison of established AurA inhibitors MLN8237 and VX680 to the hit compounds of the screening.

Figure 4.10: Effect of small compounds on the in vitro activity of AurA. EC50 for selected inhibitors from the screening in comparison to known AurA inhibitors that target the ATP-binding site.

Figure 4.11: Comparison of the produced thermal shift depending on the compound concentration.

Figure 4.12: Preliminary graphs for the experiments performed with MST.

Figure 4.13: Results of MTT-assay for the hit-compounds after 48h incubation, growth in [%] relating to the growth of cells only treated with DMSO.

Figure 4.14: Results of MTT-assay for the control compounds and PS 731 after 48h incubation, growth in [%] relating to the growth of cells only treated with DMSO. PS 731 is the most potent inhibitor of growth in this experiment.

Figure 4.15: Scheme of the cell cycle experiments.

Figure 4.16: Example for **a)** normal distribution of genome of untreated cells and **b)** distribution for cells in cell cycle arrest due to treatment with Nocodazole, a spindle toxin that causes arrest in G2/M.

Figure 4.17: Typical figure of a cell cycle arrest in G2/M caused by PS 731. Cells in G2/M have a chromosome set of 4n. Control compounds MLN 8237 and VX 680 showed the same distribution pattern (see Supplement).

Figure 4.18: a) Cell cycle state of all tested hit-compounds in comparison to DMSO treated cells with nearly half of the cells in G1 phase and half in synthesis. All have the same distribution pattern as DMSO with the exception of Oxymetholone. **b)** Comparison of the FACS analysis of DMSO treated cells and cells treated with 25 µM Oxymetholone. In the DMSO graph, the shoulder between G1 and G2/M can be explained by the Thymidine treatment for synchronization. This shoulder vanishes in cells treated with Oxymetholone, 78% of the cells remain in G1. A repetition of this assay with 50 µM Oxymetholone showed the same result.

Figure 4.19: Cells treated with Nocodazole are arrested in G2/M due to its toxicity to the spindles. When cells are treated with 50 µM Oxymetholone and Nocodazole, the difference is negligible.

Figure 4.20: Effect of known AurA inhibitors and PS 731 on the cell cycle. 25 µM of MLN 8237, VX 680 and PS 731 with addition of Nocodazole. MLN 8237, which inhibits AurB at concentrations higher than 1 µM, causes mitotic slippage

II. List of Tables

III. Abbreviations

ADP	Adenosine-diphosphat
AGC kinases	Group of kinases named after their main families, protein kinases A, G and C
AKIs	Aurora kinase inhibitors
APC/C	Anaphase promoting complex
ATM/ ATR kinase	Ataxia Telangiectasia Mutated and Ataxia telangiectasia and Rad3-related protein
ATP	Adenosine-triphosphat
AurA	Aurora kinase A
AurB	Aurora kinase B
AurC	Aurora kinase C
BCR-ABL	breakpoint cluster region-Abelson
Bio-His	Biotinilated Histidine

Bora	Bora, aurora kinase A activator
BRCA2	Breast cancer gene 2
BSA	Bovine serum albumin
cdc2	Human homolog for cyclin-dependent kinase 1 (Cdk1)
cdc25	Cell division cycle phosphatase 25
Cdk 1	Cyclin-dependent kinase 1
Cdk 2	Cyclin-dependent kinase 2
Chk1/ Chk2	Checkpoint kinase 1 and 2
CLL	Chronic lymphatic leukemia
CML	Chroniy myelogenous leukemia
DB	dilution buffer
DFS	Differential Scanning Fluorimetry
DMSO	Dimethylsulfoxide
DNA	Desoxyribonuclein-acid
DTT	Dithiothreitol
e.g.	for example
EC50	Half maximal effective concentration
Eg5	Human mitotic kinesin Eg 5
f.c.	final concentration
FACS	Fluorescence-activated cell scanning
FGFR1	Fibroblast growth factor receptor 1
FLT3	Fms like tyrosine kinase 3
G2/M	Transition phase from synthesis to mitosis
G-CSF	Granulocyte colony-stimulating factor
GSK-3β	Glycogen synthase kinase-3beta
GST	Glutathione S-transferase
H_2O	Water
H3	Histone H3
HeLa	Henrietta Lacks cervix carcinoma cells
HIS-tag	Histidine tag for tracking proteins
HIV	Human immunodeficiency virus
IC50	Half minimal inhibitory concentration
INCENP	Inner centromer protein

MBP	Myelin basic protein
Mg	Magnesium
min, h	Minutes, hours
MST	MicroScale Thermophoresis
NaCl	Natriumchloride
NADH	Nicotinamidadenindinukleotid
ng, µg, mg, g	nano, micro, milli gramm
Ni-NTA	Nickel-chelate Nitrilotriacetic acid
nl, µl, ml, l	nano, micro, milli liter
NLS-domain	Nuclear localization signal
nM, µM, mM, M	nano, micro, milli, molar (mol/l)
N-myc	Neuroblastoma associated Myelocytomatosis virus oncogene
p21	Cyclin-dependent kinase inhibitor 1, tumorsuppressor
p53	Tumorsuppressorgene p53
PBS	Phosphate buffered saline
PCR	Polymerase chain reaction
PDK1	Phosphoinositide- dependent kinase-1
PIF pocket	Pocket on PDK1 for the binding of PIFtide
PIFtide	Synthetic peptide containing the phosphorylated hydrophobic motif of Rsk2
PI-stain	Propidium iodide
PKA	Protein kinase A
PKC	Protein kinase C
PKG	Protein kinase G
PLK1	Polo-like kinase 1
RanGTP	Ras-related Nuclear protein-Guanin-triphosphate
Ras	Rat sarcoma viral oncogene
Ser/Thr	Group of Serin/ Threonin protein kinases
Src kinase	Proto-oncogene tyrosine- protein kinase
TACC	Transforming acidic coiled coil
Thr287 and Thr288	Threonin residues 287 and 288

TPX2	Targeting Protein for Xenopus kinesin- like protein
Tris	Tris(hydroxymethyl)-aminomethan containing buffer
VEGFR2	Vascoendothelial growth factor receptor 2
Wee1	Mitosis inhibitor protein kinase Wee1
wt	Wild type
Xklp2	Xenopus kinesin-like protein 2

1. Abstract

1.1 English version

Cancer is one of the leading causes of death across all countries and its diagnosis still yields fear for the affected patient. Although treatment of cancer has made marvelous progress compared to the agents available thirty years ago, a cure for cancer, however, is still a distant prospect. Modern therapy still is a burden for many patients due to heavy side effects. With the development of agents targeting specific molecular targets on cancer cells, a new field of cancer therapy was opened and a small success story in the history of cancer began.

Aurora kinases represent a relatively new target in cancer therapy. The kinase is a essential part of mitosis and cell cycle progression and its overexpression has been shown to be related to many kinds of malignancies. Allosteric inhibition of a kinase is an increasing pre-clinical approach not yet established in the treatment of patients. In this thesis, we combine allostery with another innovative approach that is drug repurposing. If repurposed, a drug can be permitted to fast track drug admission to clinical trials.

I set up a screening of 1280 FDA approved drugs to identify small molecule compounds that affect the binding of Aurora kinase A and its main physiologic binding partner, TPX2. Further, I characterized the positive hits in vitro for their capabilities to displace TPX2 from Aurora A, to inhibit Aurora kinase activity, to thermally stabilize the protein and performed assays to determine their dissociation constant. Last but not least, I tested the compounds in cells for their effect on the cell viability and cell cycle via flow cytometry. Comparing the hit-compounds with controls I found that ATP-competitive AurA inhibitor MLN 8237 strongly displaces the interaction of Aurora A with TPX2.

Summarized, we identified eight hit compounds allosterically affecting Aurora A, but no compound proved to be active in all assays. Just one compound, PS 731, identified in another screening performed by our group and further characterized in this thesis remains interesting, especially when put in context with recent publications released in the time between the start of experiments for this thesis and its finalization.

1.2 German version

Auch heutzutage stellt Krebs immer noch eine der Haupttodesursachen der Welt dar. Für viele Patienten birgt die Diagnose Krebs große Angst, obwohl die Krebsbehandlung im Vergleich zu den vor dreißig Jahren erhältlichen Mitteln erstaunliche Fortschritte gemacht hat. Ein Heilmittel gegen Krebs ist jedoch noch in weiter Ferne und die moderne Therapie ist für viele Patienten aufgrund schwerer Nebenwirkungen immer noch eine Belastung. Mit der gezielten Entwicklung von Wirkstoffen gegen molekulare Marker auf den Krebszellen wurde ein neues Feld der Krebstherapie eröffnet und eine kleine Erfolgsgeschichte in der Geschichte des Krebses begann.

Aurora Kinasen stellen ein neueres Ziel in der Krebstherapie dar. Die Kinase ist ein wesentlicher Bestandteil von Mitose und Zellzyklusprogression und ihre Überexpression wurde mit einigen malignen Erkrankungen in Verbindung gebracht. Die allosterische Inhibition einer Kinase ist ein neuer Ansatz, der in der Forschung wenig etabliert und bisher in klinischen Studien kaum zu finden ist. In dieser Doktorarbeit kombinieren wir allosterische Inhibition mit einem anderen innovativen Ansatz, der Neuverwendung von bereits zugelassenen Medikamenten für neue Indikationen.

Wir haben ein Screening von etwa 1200, bereits von der amerikanischen Food and Drug Association (FDA) zugelassenen Medikamenten durchgeführt, um niedermolekulare Verbindungen zu identifizieren, die die Bindung von Aurora Kinase A und seinem wichtigsten physiologischen Bindungspartner, TPX2, stören. Des Weiteren haben wir in verschiedenen Experimenten die positiv-getesteten Substanzen aus dem Screening auf ihre Fähigkeiten hin untersucht, die Eigenschaften von Aurora A und das Verhalten in Zellen zu beeinflussen.

Zusammengefasst konnten wir acht Trefferverbindungen identifizieren, die Aurora A allosterisch beeinflussen, aber keine Verbindung erwies sich als aktiv in allen durchgeführten Experimenten. Nur eine Verbindung, PS 731, die in einem anderen von unserer Gruppe durchgeführten Screening identifiziert und in dieser Arbeit weiter charakterisiert wurde, bleibt interessant - insbesondere im Zusammenhang mit neueren Veröffentlichungen in der Zeit zwischen dem Beginn der Experimente für diese These und ihrer Fertigstellung.

2. Introduction

Cancer has always been one of the most challenging diseases for human beings. It has even been called the "emperor of all maladies" [8]. Even with modern medicine, it is one of the leading causes of death in industrialized nations as well as in developing countries according to the WHO [9]. Until 2030, the incidence of cancer is expected to rise to 23.6 million new cases per year, which is an increase of 68% in comparison to 2012 [10].

This trend puts emphasis on the importance of cancer research. Although in the last 30 years a lot of progress has already been made in cancer therapy, new problems arise such as heavy side effects or resistance to some chemotherapeutics. So, there is a need for new drugs against cancer with minimized side effects that can be combined with other potent chemotherapeutics in order to overcome resistances. Also, taylor-made therapies adapted to the genetic profile of a tumor are going to be the future of cancer treatment [11].

Aurora Kinase A (AurA) is a key player in the regulation of cell division and has gained attention of the scientific community over the last years. Drug development on Aurora kinase has been in focus of pharmaceutical industries over the years [3,12]. However, new knowledge on the mechanism of regulation can lead to innovative approaches for the development of more selective drugs. First, I will give an overview of the origin and classification of the family of Aurora kinases, especially their role in the cell cycle and mitosis. Further I will discuss about the interaction of AurA and its partner protein TPX2.

2.1 Family of Aurora protein Kinases

In 2002 Manning et al. identified all human kinases from the whole human genome and mapped them according to their evolutionary origins and hence their relations [1] (see Figure 2.1). This mapping showed eight overall groups, to which every protein kinase could be assigned: seven main branches of the kinome and one group termed "others" that could not been related clearly.

The sub-family of Aurora kinases is classified in this group of "other" kinases. However, when looked upon the kinome tree, they are very close to the group

of AGC kinases indicating an evolutionary relation. Also close to the trunk of AGC kinases sits polo-like kinase 1 (short PLK1), a Serine /Threonine kinase and substrate of Aurora A that has also an important role in cell cycle mechanisms. AGC is short for the original representatives of this group, Protein Kinases A, G and C (PKA, PKG, PKC). Also part of the AGC group is the kinase PDK-1 that will be used for later comparison with AurA. A feature that shows the relation of Aurora kinase to the AGC kinases group is an allosteric binding site that is crucial to the proteins activation [13,14]. For the AGC kinases this site is called the PIF-pocket, a regulatory site on the small lobe of the catalytic domain [15]. The PIF-Pocket binds a C-terminal hydrophobic motif and hence auto-activates the kinase. However, Aurora kinases do not have this hydrophobic motif but an equivalent mechanism of activation by regulatory proteins binding to their small lobe [16].

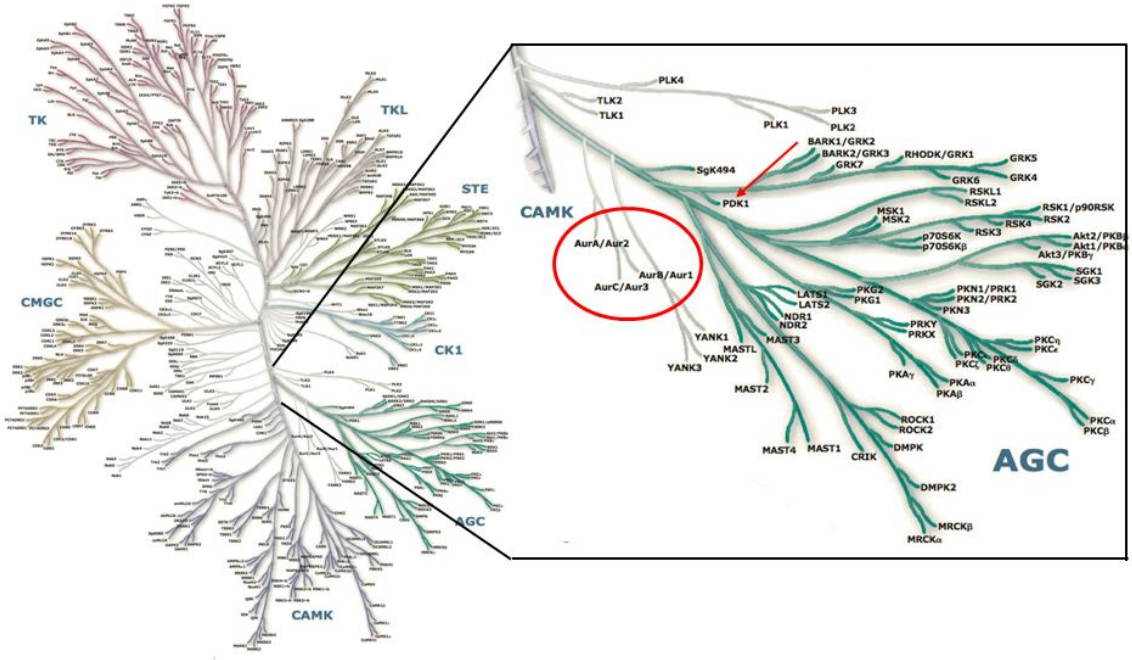

Figure 2.1: Evolutionary tree representation of the human kinome with their eight main groups [1]. The family of Aurora kinase (encircled) is closely related to the AGC kinases, amongst them PDK-1 (arrow).

Aurora kinases are serine/ threonine protein kinases. The family of serine/ threonine kinases consists of 125 members, of whom 21 have been shown to be ill expressed in variant tumors [17].

The sequence of Aurora kinases A, B and C ranges from 309 to 403 amino acids with Aurora C being the shortest and Aurora A being the longest of the

kinases [18]. The structures of the proteins are organized similarly with an N-terminal domain, a protein kinase domain with an activation loop and a C-terminal domain with a D-Box with its degradation signal [19]. The catalytic domain does not differ much between the three kinases. The N-terminal region preceding the catalytic domain ranges between 39 and 129 amino acids and holds high divergence to have better specificity of substrates [18]. Aurora kinases can be found on chromosomes 20q13.2 (AurA), 17p13.1 (AurB) and 10q13 (AurC) respectively [3].

2.1.1 Aurora Kinase A

Aurora kinase A is also known under the names Aurora-2, AIK, AIR-1, AIRK1, AYK1, BTAK, Eg2, MmIAK1 and STK15 but will be called Aurora A (AurA) in this thesis [18]. Main localization of AurA is the centrosome but it is also expressed at the spindle poles during pro- and metaphase and at the microtubules during telophase of the cell division [20,21].

The main tasks of AurA are the regulation of maturation of the centrosomes, the correct separation of the centriole pairs and the assembly of microtubules [21]. Also, AurA seems to have a role in initiating the dissembling of the nuclear membrane during mitosis [22].

Activation of AurA is linked to cdc2/Cyclin B1 [5]. To fulfill its purposes Aurora Kinase A interacts with a range of different proteins, such as D-TACC, Eg5, p53, Bora and TPX2 [23], before it gets degraded by APC/C complex during mitotic exit [24]. Also, AurA is closely linked with the protein kinase PLK1 [25].

2.1.2 Aurora Kinase B

Aurora B (which is also known as Aurora-1, AIM-1, AIK2, AIR-2, AIRK-2, ARK2, IAL-1 and STK12) is mainly localized around the kinetochores. There, AurB regulates the correct attachment of the microtubules to kinetochores and the cytokinesis [26]. It forms a so called chromosomal passenger complex alongside with INCENP (inner centromere protein) and survivin [27],[18]. Also, Aurora B phosphorylates Histone H3 and regulates chromosome condensation and hence progression in cell cycle [28].

Aurora B has been found to be elevated in thyroid anaplastic carcinoma, oral, colon and breast cancer and primary non-small cell lung carcinoma [3,29].

2.1.3 Aurora Kinase C

Aurora C (AurC, AIK3) is the least explored of the Aurora kinases. It plays a role in meiosis more than mitosis and is therefore mainly expressed in testis where it is involved in spermatogenesis [30]. It also has similar tasks as AurB. It has been found that AurC can even take over function of AurB, when AurB is inhibited, and that AurC also interacts with INCENP and is part of the chromosomal passenger protein [27].

Overexpression of AurC can be found in liver and breast cancer [31].

2.2 Structure, regulation and interactions of Aurora Kinase A

To understand the interactions and regulation mechanisms of AurA the structure of AurA needs to be visualized. Human Aurora A consists of 402 amino acids and has a typical composition with a N-terminal domain, a catalytic domain and a C-terminal domain. It has been shown that most part of the N-terminal domain is not necessary for catalytic activity, which only requires the catalytic domain residues 122-402 [14].

The structure of AurA used here is described in Cheetham, Knegtel et al. [2]. The catalytic domain consists of a small lobe, which contains a β-sheet and a glycine-rich loop. The ATP-binding site sits in between the small lobe and the large lobe (see Figure 2.2 a). It has been shown that the ATP binding site is an evolutionary conserved structure that shows similarities to other kinases like Src kinase, CDK2 or GSK-3β making it a challenge to design selective inhibitors for AurA that bind there [2].

Other relevant structures within the catalytic domain are the –helix α-C and the activation loop (res. 273-292). Both, the activation loop and the helix α-C are crucial to modulate the active or inactive conformation of AurA.

The C-terminus consists of a highly conserved sequence with a loop region that holds a degradation motif for the enzymatic decomposition of AurA by APC/C (anaphase promoting complex,[24]).

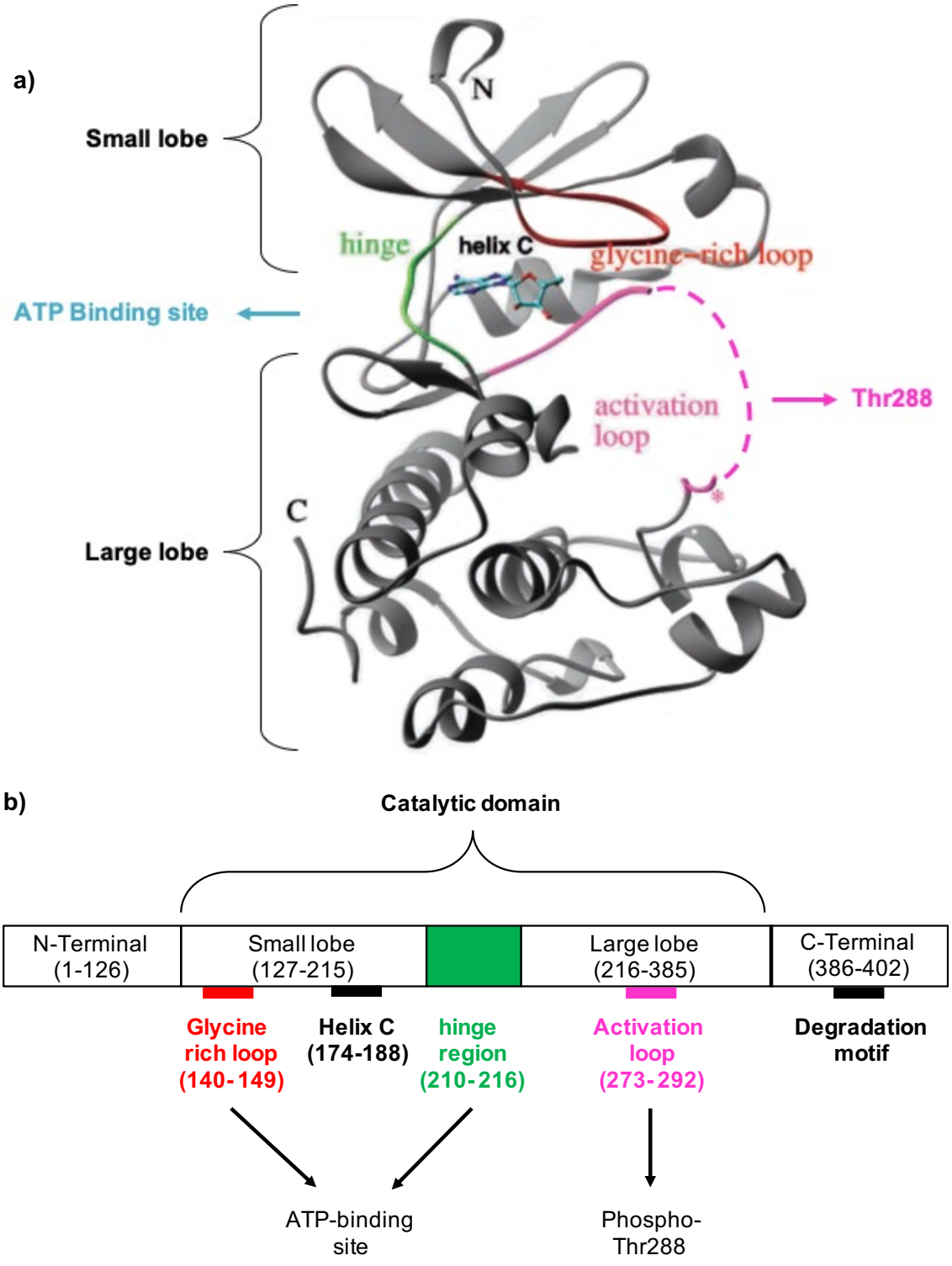

Figure 2.2 a) Structure of Aurora kinase A bound to Adenosine obtained by crystallography[2]. A Glycine-rich loop (red) and the hinge region (green) form a hydrophobic pocket for ATP. The activation loop (pink) with the activating Thr288 could not be resolved properly and is hence filled in with a dotted line. **b)** Domains and relevant sites of Aurora kinase A derived from the description and results in Cheetham, Knegtel et al., 2002 [2].

2.2.1 Regulation of Aurora Kinase A by phosphorylation

Like other related kinases Aurora kinase A is activated by phosphorylation. On the activation loop two threonine residues are available for phosphorylation, Thr287 and Thr288. Thr288 is the relevant residue whose phosphorylation increases the activity of AurA [32]. The phosphorylation of Thr288 is catalyzed by AurA itself making the activation a mechanism of auto-phosphorylation [16]. It has also been shown, that Cdk1 is necessary for full activation of AurA [33]. Also, PLK1 being a substrate of AurA facilitates the recruitment of AurA towards the centrosomes [34]. In combination with the regulation of other downstream substrates of AurA it can be assumed that AurA, PLK1 and Cdk1 perform a positive feedback loop of co-activation [5].

The peptide TPX2 plays another major role in the activation process of AurA and shall be described in the next chapters since its interaction is vital for understanding the aim of this work.

2.2.2 Properties of TPX2

TPX2 is a spindle assembly factor that was first discovered in the eggs of the frog species Xenopus laevis [35]. TPX2 stands for targeting protein for Xklp2, where Xklp2 in turn stands for Xenopus kinesin-like protein 2[36]. In humans, TPX2 binds Xklp2 orthologs like for example kinesin family member 15 (KIF15) [37]. Heidebrecht et al. showed that TPX2 levels rise during G2/M and decrease after completed cytokinesis. In humans, it is a 747 amino acids long protein with three major domains: an AurA binding domain (1-43), a NLS-domain (nuclear localization signal, 313-316) forming a binding motif for importin-α for transportation into the nucleus and a TPX2-domain (324-open) for binding and fixating Xklp2 to the microtubules[38].

TPX2 is released from transport factors in the cytosol and then builds a complex with importin α/ β for nucleation [39]. This process is regulated by RanGTP[40].

2.2.3 Interaction of Aurora Kinase A and TPX2

Although AurA has many binding and interaction partners, TPX2 is probably the most important one. It localizes AurA to the spindle microtubules were AurA

performs most of its tasks [41]. Also, TPX2 promotes auto-phosphorylation and hence activation of AurA [16].

Dodson and Bayliss[42] showed that these two paths of activation of AurA are synergistic and work independently from each other. The state where AurA is bound to TPX2 and is phosphorylated at Thr288 is the most active one, whereas phosphorylation only is still more activating than binding to TPX2 only. However, there is no certain order of achieving full activation [42].

TPX2 binds at two sites at AurA, at the N-terminal lobe of the catalytic domain and at the activation loop [43]. Bound in this conformation TPX2 stabilizes the otherwise mobile hinge region and moves the activation loop into a position that the phosphorylated Thr288 cannot be accessed for dephosphorylation by protein phosphatase 1 and hence be inactivated. Following the model of CDK2 activation by cyclin, the initial model proposed by Bayliss et al.[14] suggested that the activation happens mainly by making Thr288 inaccessible to phosphatases. It has been shown that for the binding of TPX2 to AurA the amino acids 1-43 of TPX2 are sufficient. In this context it makes sense that this area is preserved throughout species. However, binding of TPX2 to the microtubules is not possible anymore with the short sequence 1-43. Eyers et al., in contrast, suggested that the activation of AurA would involve a conformational change, following the general model of activation of PDK1 [16]. In this line, research teams working on PDK1 and AGC kinases have included Aurora activation as one more example of modulation of activity mediated by the site equivalent to the PIF-pocket [44]. More recent work by Bayliss and collaborators accept a model of activation of Aurora, involving a conformational change, being equivalent to the mechanisms described for PDK1 and AGC kinases [45].

2.3 Cell cycle, mitosis and the role of Aurora kinase A

Cell division is what all animate beings have in common. It is the essence of growth and reproduction. Cell division itself is part of the cell cycle, the circle of cell metabolism that is the backbone of life. The cell cycle is divided in four phases that all have a specific purpose or task. The G1 phase is the phase of normal functioning where the cell does its biological duty. After G1, the synthesis phase starts - short S phase. The main task of the S phase is the

duplication of the genomic material to provide one exact copy of the DNA for the daughter cell. When completed the cell goes into G2 phase, the transition phase from synthesis to mitosis. Mitosis (M phase) takes place in five stages (inter-, prometa-, meta-, ana- and telophase) where the doubled chromosomes are equally distributed to make two identical daughter cells [46].

To work properly and without any flaw this whole process requires an elaborate system of interaction partners, of which AurA is a part [47]. To ensure no defect in cell division and in the resulting daughter cells, the cell cycle has certain checkpoints for troubleshooting [48]. Otherwise such defects could easily lead to the evolution of cancer cells.

2.3.1 Cell cycle checkpoints

In the cell cycle there are four checkpoints. Every checkpoint gives a chance to halt the cell in case of defects or dysfunction.

The first checkpoint is in G1 phase, called the restriction point. At this point a cell has to check if it is ready to enter S phase or go into G0, the hibernation state for cells. If the cell passes, it has to run through a second checkpoint at the transit from G1 to S phase where the cell is examined for DNA damage by ATM/ ATR kinase activating the Chk1/ Chk2 pathway for cell cycle arrest [49].

The third checkpoint is in G2 phase. The replication of DNA is completed at this point and is again checked for damages via the ATM/ ATR pathway. During G2, proteins needed for mitosis accumulate in the cell. The most important protein for entering mitosis is Cyclin B1. It is the cardinal point of all pathways leading to mitosis or the opposite - cell cycle arrest [50].

The last checkpoint is during metaphase of mitosis (Spindle assembly checkpoint). Here it is checked if the chromosomes have aligned properly in the equatorial platform of the cell. Spindles should be inserted at the chromosome kinetochores and a bipolar tension is established between the kinetochores and the two spindle poles [48]. Differences in the bipolar tension will be detected and lead to cell cycle arrest until the spindles are attached properly [51]. Then, entry into anaphase can be promoted by the APC/C, its increased activity leads to degradation of Cyclin B1 [52].

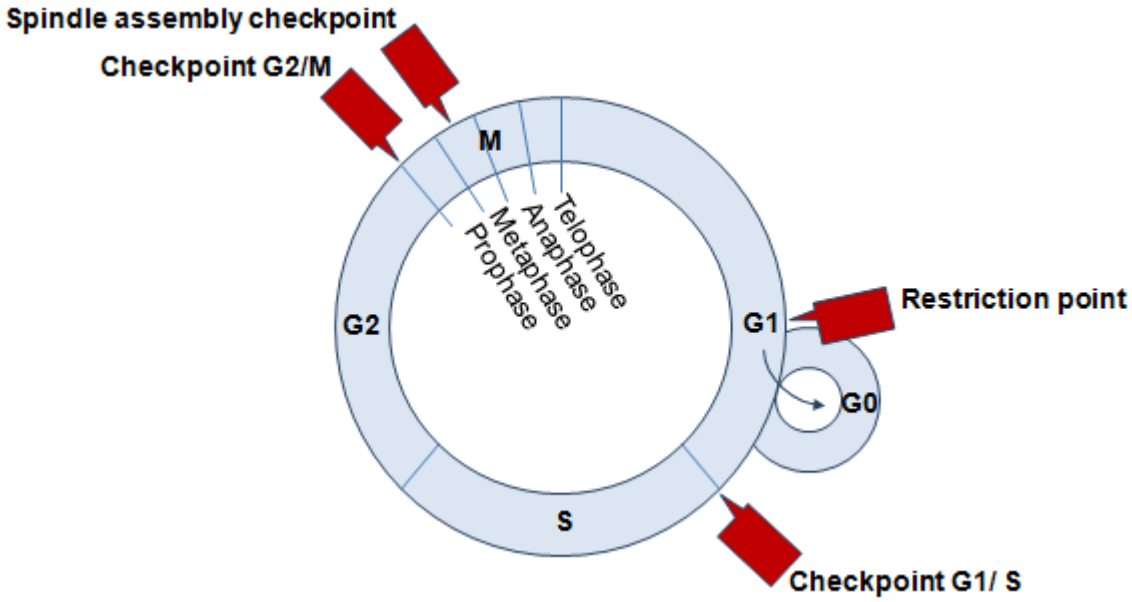

Figure 2.3: Scheme of the cell cycle and its four checkpoints (modified graphic from Kollareddy et al., 2008)[3].

2.3.2 Role of Aurora kinase A during G2 phase

The function of AurA arises from its pathway and interaction partners. During G2 AurA is upregulated and accumulates in the cytosol. It forms a complex with BORA[53], which together activate PLK1, which in turn leads to the activation of the phosphatase cdc25 and Cyclin B1. Also, PLK1 inhibits Wee1, which in turn is an inhibitor of Cdk1 (also called cdc2). Therefore levels of Cyclin B1 rise in the cell and represent the final switch that leads to mitosis [54]. However, starting point of this regulatory mechanism is AurA, which controls mitotic entry with the activation of PLK1 [55] (Figure 2.4).

In case of DNA damage, the ATR/ ATM pathway is activated. ATR/ ATM directly inhibit PLK1 and activate Chk1/ 2 which inhibit cdc25 [56]. Also, with PLK1 inhibited, Wee1 can now inhibit Cdk more effectively [57]. In addition, p53 is activated, which leads to an inhibition of Cyclin B1 via p21 and protein 14-3-3 [58]. Overall, mitotic entry is prevented and the cell arrests in G2 until the damage is resolved.

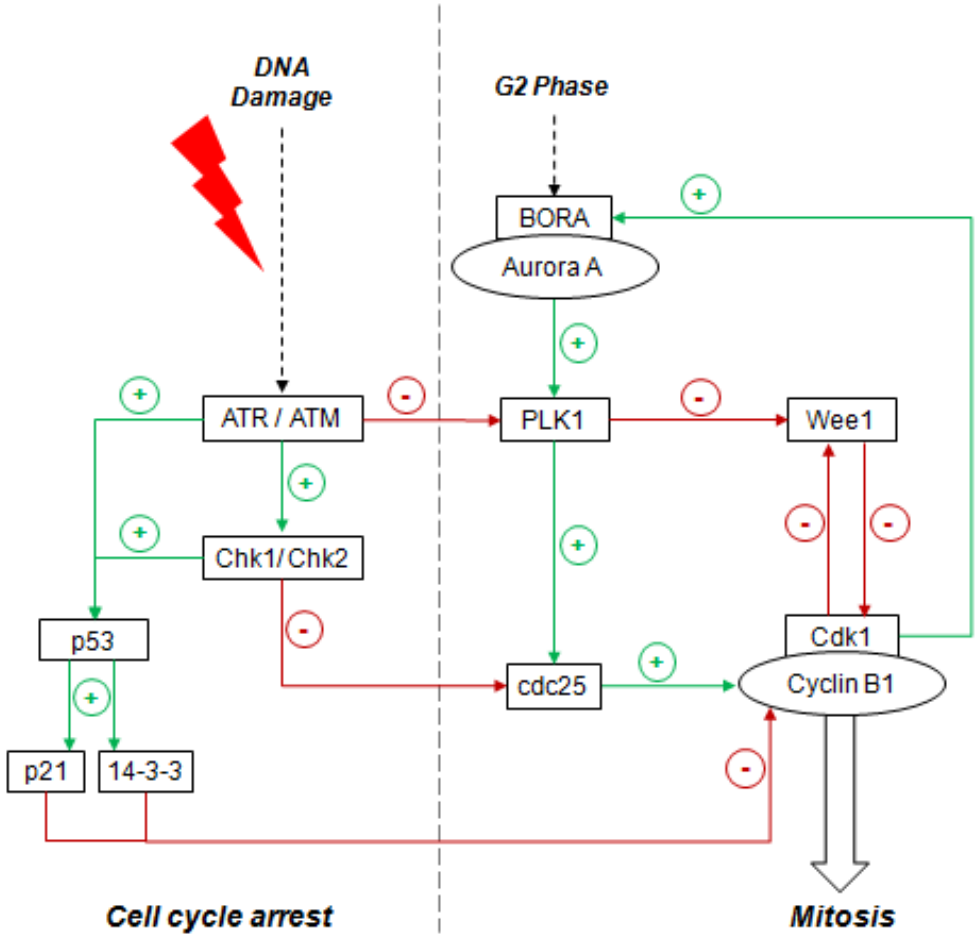

Figure 2.4: Participation of AurA in the G2/M checkpoint (summarized from Wang et al., 2009 [4]; Lens et al., 2010 [5]). Green arrows with a plus symbol indicate an activation pathway, red arrows with a minus symbol indicate inhibition.

2.3.3 Function of Aurora kinases during mitosis and the spindle assembly checkpoint

After entry into mitosis the elevated level of active PLK1 leads to degradation of BORA [59,60]. After initiating mitosis AurA has to be redirected towards the centrosomes and spindles. The drop of BORA releases AurA for its new tasks. AurA forms an activating complex for PLK1 with centrosomal protein Cep192 leading to centrosome maturation [61,62]. Also, AurA is now free to bind to TPX2, which redirects the kinase to the spindles and associates with AurA for assembly of the microtubules [62]. Both, the AurA-Cep192- and the AurA-TPX2 complex take part in the regulation of AurA substrate Eg5 [6364], which is essential for spindle formation in its function as motor protein. At the spindles

AurA phosphorylates its substrate TACC3, which is important for stability of the microtubules [65].

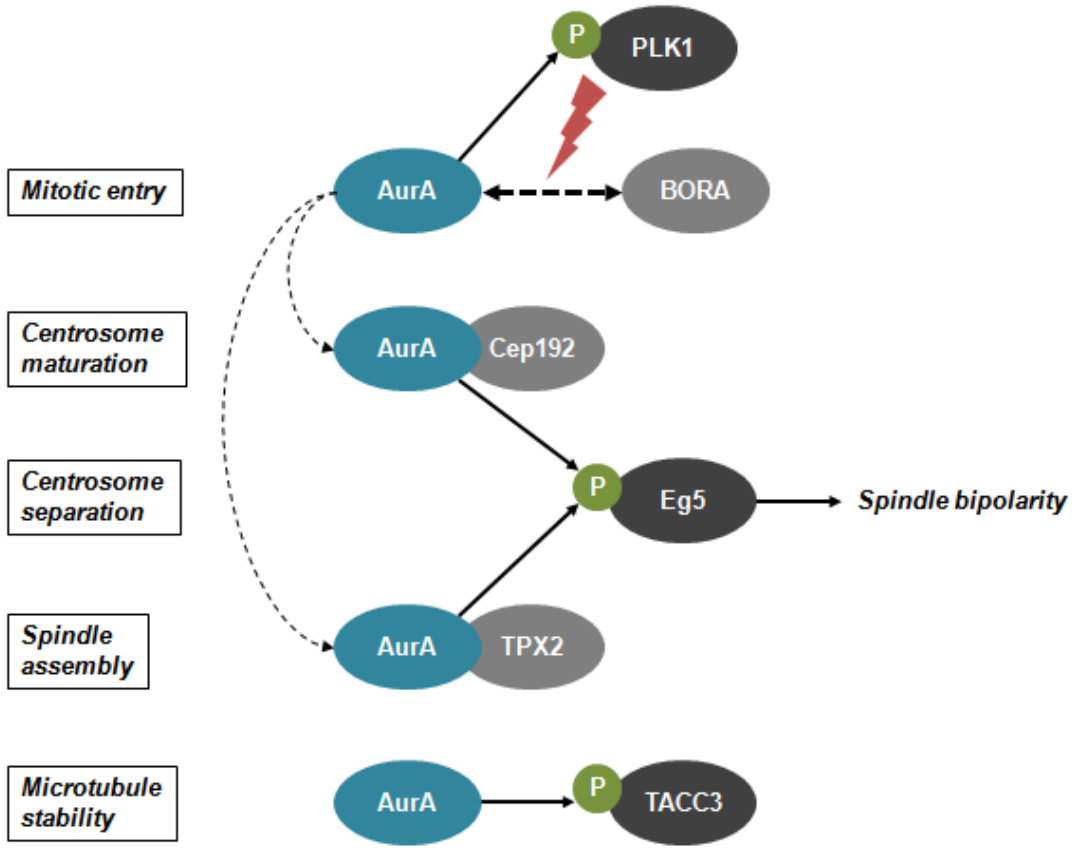

Figure 2.5: Functions and substrates/ cofactors of Aurora kinase A during mitosis. The diagram shows the process from mitotic entry after dissociation from BORA to the full development of the mitotic spindles with cofactors Cep192 and TPX2 (modified from Asteriti et al., 2015 [6]; Barr and Gergely, 2007 [7]).

The results of inhibiting Aurora kinase A are abnormal spindle formations in terms of monopolar spindles due to deficient phosphorylation of Eg5 [66] and chromosome segregation defects [67]. Improperly attached spindles to the kinetochores activate the spindle assembly checkpoint in mid-mitosis and the cells are arrested in cell division [68].

2.3.4 Mitotic slippage

Mitotic slippage is the process of cells exiting mitosis "[...] in the absence of chromosome segregation and cytokinesis, resulting in tetraploid cells [...]" [69]. This phenomenon is achieved by prolonged spindle dysfunction for example induced by mitotic inhibitors [70]. According to Tao et al.[69], cells go to

programmed cell death after mitotic slippage, if the spindle assembly checkpoint is competent.

Mitotic slippage occurs especially after inhibition of Aurora B because of errors in cytokinesis and resulting polyploidy[71]. Inhibition of AurA shows a mere cell cycle arrest and defects in spindle formation [72]. Especially combination of two agents, an AurB inhibitor and another spindle poison, for example paclitaxel and an AurA or PLK1 inhibitor, shows high occurrence of mitotic slippage [5]. It has also been shown that MLN 8237, which is classified as an AurA selective compound, has an effect on AurB at higher concentrations of 1 µM resulting in mitotic slippage [73].

2.4 Aurora Kinase A as oncogene

Oncogenes are a part of the genome, and their deregulation makes a cell more likely to become a cancer cell. Aurora kinase A is a so-called proto-oncogene, which means that it is a normal part of the cell but changes in its regulation, function or quantity can promote cancer.

More recently, Aurora A was described as a prognostic marker for different types of cancer, such as ovarian, lung or colorectal carcinoma[74–76]. Elevated levels of AurA correlate with poor prognosis.

2.4.1 Amplification and overexpression of Aurora kinase A in variant tumor cells

It has been shown that the Aurora A gene is amplified and the kinase is overexpressed in many solid tumors [77,78]. This leads to errors in centrosome segregation and to chromosomal instability. In consequence, cells show aneuploidy, a characteristic feature of cancer cells in general [79].

Tumors who have reportedly a high level of AurA are breast, colon, ovarian, pancreatic, gastric, esophageal, bladder, cervical and head and neck cancer [80–86]. Aur A is connected to tumor suppressors like p53 [87]. p53, the so called guardian of the cell, is phosphorylated by AurA and marked for degradation [88]. So, if AurA is overexpressed, p53 is degraded more and the cell is susceptible for abnormalities.

In ovarian cancer, a connection was found between Aurora A and the suppression of BRCA2 [89]. Furthermore, induced overexpression of AurA in mice lead to mammary gland abnormalities such as hyperplasia or early cellular senescence, depending on the presence of p53 [90,91] or even pre-stages of cancerous cells [92].

2.4.2 N-myc

N-myc is a transcription factor encoded by the MYCN gene. It is activated in a receptor tyrosine kinase pathway via phosphatidylinositol 3-kinase and cdk1/ Cyclin B[93]. N-myc can be overexpressed in childhood neuroblastoma and is associated with drug resistance and poor prognosis [94]. Direct attempts to target N-myc have been unsuccessful [95]. However, N-myc is stabilized by Aurora kinase A[96], which slows degradation of N-myc. High levels of Aurora A in neuroblastoma are also associated with poor prognosis [97].

Because of this relation, tumors with Myc amplification have now become druggable targeting Aurora kinase A [98]. It seems, that inhibiting activity of AurA is not enough for destabilizing the AurA/N-myc complex but a conformational change in terms of an allosteric transition is needed [99,100].

2.5 Protein kinases as targets of modern chemotherapy on the example of Tyrosine kinase inhibitors (EGFR1/HER1, HER2/c-neu)

Traditional chemotherapeutics used in cancer therapies are highly toxic and associated with a lot of side effects. Thus, modern drug development tends towards more specific agents, also called targeted therapies. Useful targets are kinases like for example tyrosine kinases.

Tyrosine kinases, especially receptor tyrosine kinases like EGFR or HER2, are often overexpressed in many different kinds of cancer [101]. Inhibition of receptor tyrosine kinases has proven to be an effective tool against tumors in breast, ovarian, prostate, colon, lung, hepatocellular carcinoma, gastrointestinal stromal tumors, melanoma and even leukemia [102] [103]. So, kinases inhibitors have already been proven to be an effective tool in cancer therapy.

Aurora kinases are within the next promising Ser/Thr protein kinase targets for more specific chemotherapeutical drugs [104,105,104].

2.6 Clinical trials on Aurora Kinase inhibitors

A variety of Aurora kinase inhibitors (AKIs) have been enrolled in clinical trials [3,106,107]. So far, a few of them have reached phase II studies[94]. Most of them are not selective and have an effect on more than one kinase, e.g. PHA-739358[108] (also called Danusertib, inhibits Aurora A, B and C) or ENMD-2076 [109] (inhibits Aurora A, VEGFR2, FGFR1 and FLT3). Common side effects were nausea or neutropenia, which in case of Danusertib could be controlled with additional G-CSF for non-leukemia patients[110]. Another promising, but AurB selective compound is AZD1152 (Barasertib) [111].

Range of application of AKIs could be therapy of refractory cancers. For example, Danusertib also inhibits BCR-ABL and could show effects on Imatinib-refractory CML [112] (chronic myelogenous leukemia). ENMD-2076 achieved response in platinum-resistant ovarian carcinomas [113].

Therefore, co-medication of AKIs and other chemotherapeutic agents could be a possible concept of therapy. It has been shown, that tumors with amplification of AurA are more likely to show resistance to Taxol (e.g. Paclitaxel) [114].

Two known AurA inhibitors have been used in this thesis for comparison and benchmarking, VX 680 and MLN 8237.

2.6.1 VX 680

VX 680 (also known as MK-0457) is an inhibitor for Aurora A, B and C with IC50s of 0,7, 18 and 4,6 nM, respectively [115]. VX680 binds to the ATP-binding site of Aurora A, as determined by crystallography of the complex [116]. However, it's clinical development has been terminated due to severe toxicities [3] and VX 680 is not listed in current reviews about Aurora inhibitors in clinical trials anymore [106].

This compound has been used as a control by our group before, for example in the doctoral thesis of Lisa Eisert or in Schulze, Saladino et al., 2016 [44].

2.6.2 MLN 8237

This compound, also known as Alisertib, is currently one of the most promising in clinical trials on Aurora inhibitors. It is selective for AurA with an IC50 of 1 nM [117], but has also effects on AurB at concentrations higher than 1 µM [73]. It is derived from the compound MLN 8054, which showed too many side effects in patients and was hence eliminated from trials.

MLN 8237 is running in phase I and II trials on different solid tumors as well as Non-Hodgkin lymphoma, chronic myelogenous leukemia and multiple myeloma [106]. MLN 8237 disrupts interactions with N-myc, although another pre-clinical compound, CD532, appears more potent in this regard [98].

2.7 Re-use of known drugs for other fields of application (drug repurposing) by the example of lenalidomide

A drug that has been reused for other fields of application is lenalidomide, a derivative of thalidomide. After the Contergan scandal, thalidomide nearly vanished from prescription lists until it was discovered to be effective against other diseases like leprosy [114] or HIV years later [118,119].

In matters of cancer, it has been shown to be potent against multiple myeloma, which at that time was very difficult to treat [120].

To reduce side effects a structural analogue of thalidomide was derived, lenalidomide, which has even higher effectiveness [121]. Lenalidomide is now standard treatment for therapy refractory multiple myeloma in combination with dexamethasone and deletion 5q-type myelodysplastic syndrome [122].

It is a perfect example of fast-track recycling of an already known drug for other fields of application. Since its teratogenic side effects are widely known, patients have to take good care of contraception during therapy.

2.8 Innovative approach - Model of allostery explained by the example of protein kinase PDK1

Pharmacological regulation of a kinase is possible in two ways: competing directly with the ATP or modulating in an allosteric way. Allostery means that binding to one spot on the kinase causes conformational change at another

binding site [123]. This mechanism is mostly used for securing downstream signaling cascades [124]. A binding partner may dock to the allosteric binding site and hold the kinase either in an active state or bring the catalytic domain in an inactive conformation[125].

Thermodynamically, allostery must be bi-directional. However, the bi-directionality has not been investigated in depth in protein kinases. By using small compounds we could recently demonstrate that this mechanism of allostery works in both ways on the example of kinase PDK1 [44]. The polypeptide PIFtide and small compounds [125–128] bind to the regulatory site of the PIF-pocket and activate the kinase by altering the conformation of the ATP-binding site. Working in the opposite direction, we recently described suitable compounds binding to the ATP binding site that are able to enhance or displace a binding partner bound to the PIF-pocket of the kinase. We called this mechanism “reverse allostery” [44].

Although there were conflicting models on the mechanism of regulation of AurA by TPX2, we supported the model where TPX2 binds to the PIF-pocket-like position on the small lobe of the kinase and has an allosteric effect on AurA stabilizing the catalytic domain in a “close-active” conformation. In our paper on bidirectional allostery, we included the data from this thesis showing that the principle of reverse allostery also applies for AurA. The inhibitor MLN 8237, which is known to bind to the ATP binding site [129], displaces TPX2 potently and is hence an example for reverse allostery on AurA.

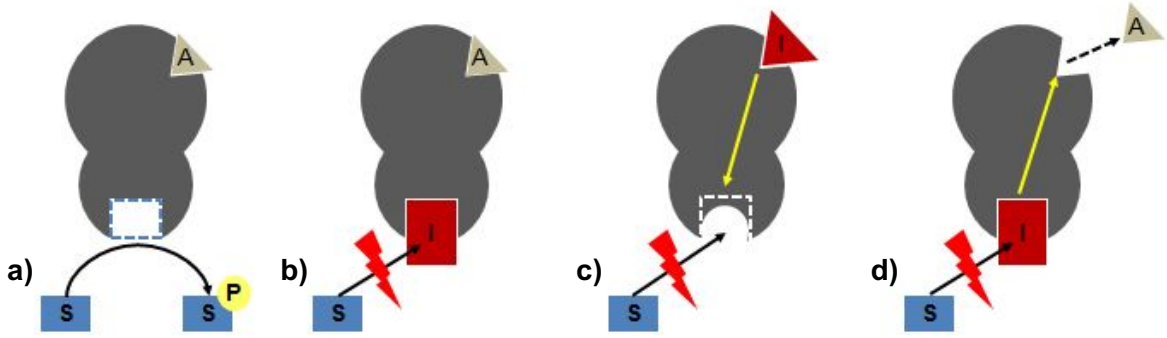

Figure 2.6: Graphic representation of inhibitory mechanisms; **a)** shows a full functioning kinase phosphorylating a substrate S with a bound activating allosteric motif A. **b)** Shows a competitive inhibition (inhibitor marked I). The principle of allosteric inhibition is depicted in **c)**. The mechanism of reverse allostery is shown in **d)**, where a

compound binding to the ATP binding site is displacing the allosteric motive A. However, this compound does not necessarily have to be inhibitory to the kinase.

2.9 Aim of this thesis

This thesis has a multidimensional approach and aims to understand the mechanism of regulation of Aurora kinase and its allosteric processes. The screening performed intents to identify small compounds that affect Aurora kinase allosterically. This way, it may be possible to identify compounds that are more likely to be selective for Aurora kinase A. Selectivity is a parameter to develop a drug with less side effects for cancer therapy. Also, the use of a compound library comprising drugs already approved for use in human beings can enable a fast track development and clinical trials, in case a promising hit is identified.

On a biochemical point of view, this thesis aims on understanding the allostery of Aurora kinase A. Here, the mechanisms are less known than with other kinases, like for example PDK1 from the AGC kinases family. The allosteric regulation of the activity would imply that compounds binding at the ATP-binding site could produce effects at the docking interaction with TPX2 and other proteins. I here describe that the reverse allostery concept recently published for PDK1 by our group is also applicable to AurA and its interaction partner TPX2. By identifying compounds that displace AurA from TPX2 we hope to gain more information on the molecular mechanisms of regulation and information for rational development of innovative drugs to Aurora kinases.

3. Materials and methods

3.1 Materials

Equipment, consumables, substances and software and their producers used during the different assays are listed below in alphabetical order.

3.1.1. Equipment

Equipment	Producer
Cytometer (flow cytometry)	FACSCalibur BD Biosciences
EnVision multilabel plate reader	PerkinElmer
Phosphoimager	Fujifilm FLA-9000
Liquidator manual 96-channel pipetting station	Steinbrenner Laborsysteme GmbH
Monolith NT.115 series (for Microscale Thermophoresis)	NanoTemper Technologies GmbH
8-channel dispenser (1-10µl, 10-100µl)	Eppendorf Multipette
Pipets (0.2-2µl, 2-20µl, 20-100µl, 100-1000µl)	Gilson
Pipetting robot	Eppendorf epMotion 5070
Real time PCR cycler	StepOne Plus Real time PCR System by Thermo Fisher Scientific

3.1.2. Consumable supplies

Consumable	Producer
384-well plate	Greiner
96-well PCR plate	ThermoScientific
96-well plate (conical bottom)	Greiner
Capillaries for MST (premium coated)	NanoTemper Technologies GmbH
His-Tag Labeling Kit RED-tris	NanoTemper Technologies GmbH

NTA for MST (MO-L008)

Liquidator pipetting tips	Mettler Toledo
Pipetting tips (for both Eppendorf and Gilson pipets, all volumes)	Starlab
Tubes	Eppendorf
Whatman p81 paper	Whatman/ GE

3.1.3. Chemicals

Chemical	**Producer**
AlphaScreen beads	PerkinElmer (6760619, LOT: 675278A)
CellTiter-Blue	Promega G8081
DMSO Dimethylsulfoxid	Roth (Rotipuran >99.8%)
DTT (Dithiotreitol)	AppliChem
EasyTides Adenosine 5'-triphosphate, (γ ^{32}P)	PerkinElmer
Ethanol 80 %	Sigma
Magnesiumchloride	Roth
PBS	Thermo scientific
Pluronic F.127	Sigma Aldrich
Propidium iodide (PI-stain)	Sigma (> 94%, P-4170)
Phosphoric acid	Sigma
RNase A solution	Qiagen (#158924)
Sodium chloride	Sigma Aldrich (PharmaGrade, CAS: 7647-14-5)
Sypro orange	Invitrogen
Trizma pH 7.4	Sigma Aldrich
Trypsin	Gibco
Tween 20	Thermo scientific

3.1.4. Proteins

Protein	Producer
6HIS- Aurora A	Recombinant, expressed from bacteria with a pET 28a plasmid, purified with Ni-NTA and gelfiltration; full length protein with His-tag
6HIS- Aurora A, D274N mutant	Recombinant, expressed from bacteria with a pET 28a plasmid, purified with Ni-NTA and gelfiltration; kinase dead mutant with His-tag
GST- Aurora B	ProQinase GmbH (expressed from Baculovirus infected Sf9 cells, purified with GST-affinity chromatography)
Histone H3 (from calf thymus)	Roche (11034758001 via Sigma Aldrich)
Histone Mix type III-S	Sigma H5505

3.1.5. Peptides

Peptide	Producer
TPX-2 (Biotin-MSQVKSSYSYDAPSDFINFSSLDDEGDTQNIDSWFEEKANLEN-NH2)	JPT Peptide Technologies GmbH

3.1.6. Compounds

Compound	Producer
AZD 1152	Sigma Aldrich (CAS: 722544-51-6)
Atractyloside	Sigma (CAS: 102130-43-8)
Balsalazide	Santa Cruz Biotechnology (CAS: 80573-04-2)
Erlotinib	Cayman Chemicals (CAS: 183321-74-6)
Iopanoic acid	LGC Limited (CAS: 96-83-3)
L-Thyronin	Sigma Aldrich (CAS: 6893-02-3)
MLN8237	Selleckchem (CAS: 1028486-01-2)

Oxymetholone	LGC Limited (CAS: 434-07-1)
Pranlukast	Cayman Chemicals (CAS: 103177-37-3)
Derivatives of compound PS731	Alfa Aesar, Maybridge, Enamine, Hit2Lead, Acros, Apollo
Screening library (FDA and EMA approved drugs)	Prestwick (Prestwick Chemical library)
Tiratricol	Abcam (CAS: 51-24-1)
VX 680	Selleck (CAS: 639089-54-6)

3.1.7. Antibodies

The following antibodies were used by Dr. Monika Raab for western blots. Dilution and handling of the antibodies were performed according to the producers guidelines.

Antibody	**Producer**
anti-PLK1 (monoclonal mouse)	Sigma-Aldrich (WH0005347M1)
anti-pT210 PLK1 (monoclonal rabbit)	Abcam (ab155095)
anti-phospho-Aurora A, B and C (monoclonal rabbit)	Cell Signaling Technology (D13A11)
anti-Aurora B (polyclonal rabbit)	Cell Signaling Technology (3094S)
anti-Phospho-Histone H3 (Ser10, polyclonal rabbit)	Millipore (06-570)
anti-Cyclin B1 (polyclonal rabbit)	Sigma-Aldrich (SAB4503501)
anti-β-Actin (monoclonal mouse)	Sigma-Aldrich (A5441/AC-15)
Secondary antibodies (anti-rabbit and anti-mouse)	GE Healthcare: rabbit (NA934V), mouse (NXA931)

3.1.8. Software

Software	**Producer**
Analysis of radioactivity	MultiGauge V3.1

Analysis and Graphics	GraphPad Prism 6.0
Calculation	Microsoft Excel 2007
Cell cycle software	Cell Quest Pro
Bibliography	Citavi
Picture editing	Gimp 2.8.18
Microscale Thermophoresis	Nanotemper software
Text	Microsoft Word 2007
Thermalshift/ PCR cycler software	StepOne Software Version 2.0 Applied BioSystems

3.2 Methods

Various methods have been used to detect interactions between a compound and AurA. The aim was to first identify compounds that displace AurA and TPX2. In the next step those compounds were tested if they had any effect on the activity and stability of the enzyme. Finally the effect on cells and their cell cycle were measured. For further characterization, the thermophoretic properties were analyzed to determine a dissociation constant. All techniques used shall be described in the following sections.

3.2.1 AlphaScreen Interaction Assay

AlphaScreen is a versatile detection assay for various interactions like for example protein-peptide, protein-protein or protein-DNA developed by PerkinElmer. The assay is based on beads that emit light when brought in close proximity. We used a kit containing Streptavidin donor beads and Nickel chelate (Ni-NTA) acceptor beads (Figure 3.1). The Streptavidin binds to biotinylated protein/ peptide and the Nickel to the His-tag of a protein, in our case biotin-TPX2 and His-AurA. If the peptide and the protein bind, the Nickel chelate and Streptavidin beads are brought into close proximity. When this binding complex gets excited with light of 680 nm wavelength, the Streptavidin donor bead releases a singlet oxygen that transmits onto the Nickel chelate acceptor bead causing it to emit light. This light of 520-620 nm wavelength can now be detected. A singlet oxygen can only travel a distance of 200 nm, so if there is no

acceptor in close proximity, no emission takes place. That kind of proximity can only be achieved by binding to a reaction partner. For measurement the EnVision multilabel plate reader was used.

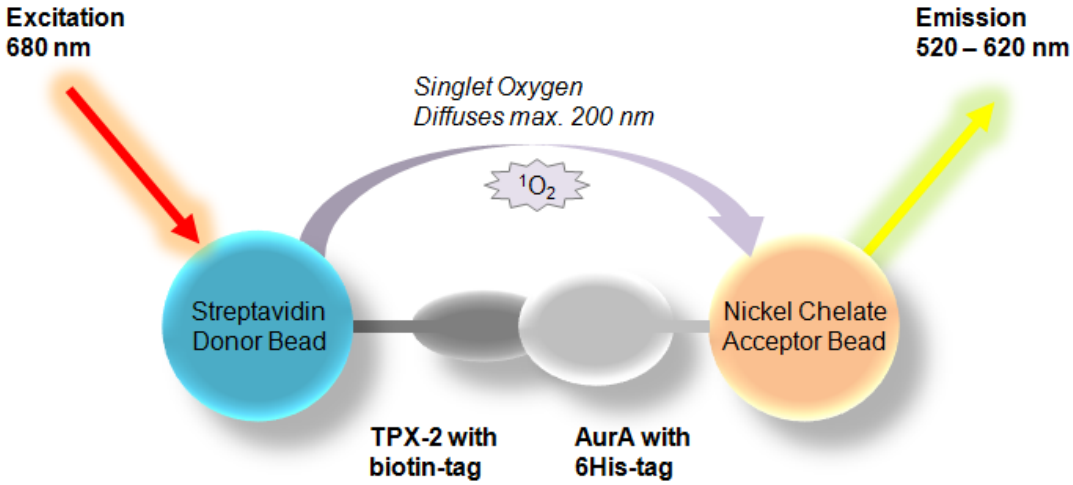

Figure 3.1: Schematic representation of AlphaScreen assay mechanism. If AurA binds TPX2, donor and acceptor beads are brought in close proximity so the singlet oxygen can travel and excite the nickel chelate to emit light.

We used this assay to detect displacement of AurA and TPX2. Without addition of any compound TPX2 and AurA can bind successfully and the detected signal equals a reference value of 100% binding. If a compound displaces TPX2, the beads are not close any more and less light will be emitted. The more potent a compound is the lower the detected signal gets.

A buffer containing 100 mM NaCl, 50 mM Tris, 0.01 % Tween 20, 0.1 % BSA and 2 mM DTT was used for the assay (AlphaScreen dilution buffer). Because of its instability the DTT was added freshly to the buffer before every assay.

The protocol for AlphaScreen consists of three components. A solution of the compound to be tested, a peptide-protein mix and a mix of acceptor and donor beads.

Every compound was tested in a 1: 100 dilution resulting in a concentration of 1% DMSO. Thereby a steady concentration of DMSO was achieved making the results comparable to other compounds and to a DMSO-only reference value. Dilutions from stock were made in DMSO until the desired concentration was obtained. Then 1 µl of compound in DMSO was diluted with 39 µl of dilution buffer (1:40 dilution). Later 10 µl of a peptide-protein mix and 5 µl of beads were

added to 10 µl of this solution obtaining a further dilution of 1: 2,5 making a total dilution of the compound of 1:100.

For the peptide-protein mix an equivalent amount of TPX2 and AurA (wt) was added to a tube with dilution buffer. The tube with the peptide-protein mix was kept on ice until added to the wells with the compound solution.

Last, the acceptor and donor beads were added in a 1: 50 dilution to a tube with dilution buffer. Because of the light sensitivity of the beads this step was done with dimmed lights and the solution was kept in a tube wrapped in aluminium foil. In the end, each well of the 384-well plate would contain 25 µl solution composed of 10 µl dilution buffer with the diluted compound or 1% DMSO, 10 µl of a peptide- protein mix and 5 µl of the diluted acceptor and donor beads (Table 3.1).

The assay is left for incubation for one hour in the dark at room temperature (23°C). Then the plate can be read with the EnVision multilabel reader and the results are interpreted with Microsoft Excel and GraphPad Prism. As described above EnVision multilabel reader detects the binding of AurA to TPX2. Every assay has a set of reference values where only DMSO and no compound is added to AurA and TPX2. The detected counts of all DMSO values are averaged and set as 100% binding. The quotient of the counts of a compound tested and the DMSO reference gives the relative amount of binding of AurA and TPX2 after interaction with the compound. If a compound is tested in different concentrations, we can obtain a curve of decreasing binding with increasing concentrations of the compound (IC50). These calculations were done with Microsoft Excel 2007 and the associated graphs with Graph Pad Prism 6. In the screening process the concentration of the compounds were set at 50 µM. In further testing, concentrations from 200 µM to 3 µM in a 1:2 dilution were used or, if the compound seemed to be very potent, using lower concentrations. The screening of the library was performed in singlicates. All other datapoints were performed in duplicates.

To obtain the right concentrations to be used in the AlphaScreen assay, a so called cross-titration was performed. Concentrations of 100 - 50 - 25 - 12.5 and 0 nM protein and peptide are tested against each other. This way, a

concentration can be identified within the linear range of interaction of AurA and TPX2. Here, the signal should be high enough to discriminate against the background and inhibition or enhancement should be clearly visible. In the steady state a displacement or increased binding of TPX2 would be harder to detect.

The cross-titration was performed with concentrations starting at 12 - 6 - 3 - 1.5 and 0 nM to capture the range of the AurA-TPX2 interaction where counts are still increasing.

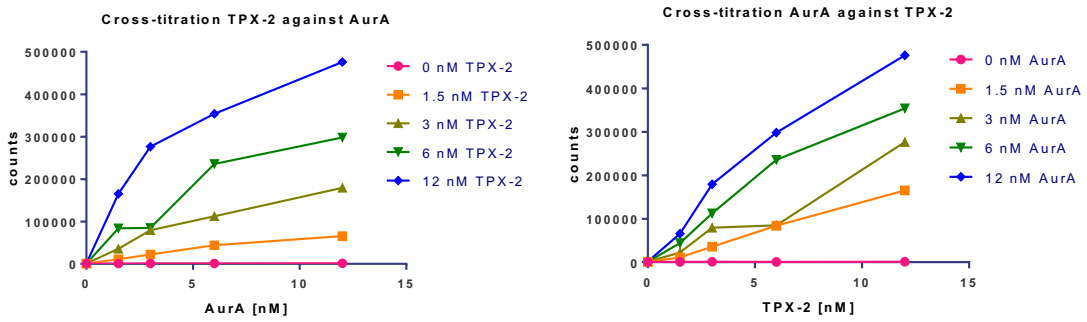

Figure 3.2: Cross-titrations for AurA and TPX2. The graphs show increasing interaction with increasing concentration of protein and peptide measured. The counts are “arbitrary counts” by the Envision equipment.

Concentrations chosen for the following AlphaScreen assays were 2 nM for AurA and 3 nM for TPX2. Those concentrations are in the linear range of the interaction and counts are high enough to give good discrimination against the background. With those concentrations the Prestwick chemical library was screened.

10 µl	100 mM NaCl
	50 mM Tris
	0.01 % Tween 20
	0.1 % BSA
	2 mM DTT
	Diluted compound (200-3 µM f.c., making a total of 1% DMSO)
10 µl	2 nM AurA (wt)
	3 nM TPX2
5 µl	Beads,1:50 diluted in dilution buffer
25 µl	**Final Volume/ well**

Table 3.1: Content of one well measured in AlphaScreen assay.

3.2.2 Protein kinase Activity

The main method in our lab to measure protein kinase activities is with radioactive ATP. The ATP we used has a ^{32}Phosphate isotope instead of its usual non-radioactive gamma-phosphoryl group. This isotope is a beta emitter with a half-life of 14,3 days. Any substrate phosphorylated with this ^{32}P gamma-ATP can be traced later on. For tracing, the phosphorylated substrate is spotted on a phosphocellulose membrane, in our lab we use Whatman p81 paper. The membrane is negatively charged and binds peptides with positive Arginine or Lysine residues. Hence, the protein phosphorylated with ^{32}P-gamma ATP also binds to the membrane. However, negatively charged ATP will not bind. The more substrate is phosphorylated, the more radioactivity is detectable.

For the assay we need to prepare two mixes, a protein-substrate mix and an ATP- Mg mix to start the reaction with. The reaction is set up in a 96-well plate. First of all the protein-substrate mix is prepared. The volume of the protein-substrate mix for each well adds up to 15 µl. The content of each well consists of 1 µl 500 mM Tris solution with 1% β-Mercaptoethanol (Tris buffer), 1 µl containing 1 mg/ml BSA and 50 mM Tris and 0.1 % β-Mercaptoethanol, 1 µl of AurA (25 ng/ well), 2 µl of substrate for phosphorylation (containing 2.5 µg/ well) and 9 µl of H_2O. The remaining µl is reserved for testing compounds. For this assay, the wild type kinase was used.

Compounds will be diluted in DMSO until the desired concentration is reached. For the activity assay a final concentration of compounds of maximal 200 µM (and from there a 1:2 dilution) was used. 1 µl of compound were provided first in the well, then 14 µl of the protein-substrate mix is added on top making it a 5% concentration of DMSO in this assay. Next, the ATP- Mg mix is prepared. Its volume is 5 µl per well and consists of 2 µl of 1mM ATP, 2 µl of 100 mM MgCl and 1 µl of Tris buffer.

2 µl	Tris buffer (500 mM Tris pH 7.5, 1 % β-Mercaptoethanol)
1 µl	Dilution buffer (50 mM Tris pH 7.5, 0.1 % β-Mercaptoethanol, 1 mg/ml BSA)
1 µl	Diluted compound (200-3 µM f.c., making a total of 5 % DMSO)
1 µl	25 ng AurA (wt)
2 µl	2.5 µg substrate H3
9 µl	H_2O
2 µl	1 mM ATP
2 µl	100 mM Mg^{2+}
20 µl	**Final Volume/ well**

Table 3.2: Content of one well measured in the kinase activity assay.

In a proper protective environment, the radioactive ^{32}P gamma-ATP is added to the ATP-Mg mix. Summarized each well contains along with buffer the following reagents: 25 ng Aurora Kinase A, 2.5 µg substrate Histone H3, a compound to inhibit activity of AurA, 5% DMSO, 10 mM Mg, 100 µM ATP and ^{32}P gamma-ATP.

After the compound and the protein-substrate mix are dispensed in the wells of a 96 well plate the reaction is started with addition of 5µl of the radioactive ATP-Mg mix. Next, the assay is incubated for 30 minutes until stopped with a solution of 1:25 hydrogen-phosphatic acid, which denatures the kinase. 4 µl of each well is spotted on a p81 membrane using the epMotion pipetting robot.

Afterwards the paper is washed with 1:100 hydrogen phosphatic acid solution for ten minutes to wash away the left-over ATP. The washing procedure is performed four times. Now everything left on the paper should be the phosphorylated substrate. For a reference value of the total amount of radioactivity, we take 2 µl of any well, dilute 1:100 to get a reasonable signal. 4 µl of this 1:100 solution is now spotted manually on another sheet of p81 membrane that should not be washed. This reference membrane will allow us to calculate the total radioactivity since it contains the maximum amount of radioactive ATP in a well.

After washing and drying the assay membrane is wrapped in film next to the membrane for the total reference value. They are stored over night in a phosphoimager cartridge with a radio sensitive film to trace all radioactive

marked substrates. On the next day the film can be read using the Fuji phosphoimager and the image is analyzed with Multigauge software. The product and hence the specific activity of AurA can directly be derived from the signal strength. If a compound is inhibiting the activity of AurA, less phosphorylation is happening. Therefore less substrate is marked radioactive and the trace is weaker. A background signal has been considered for calculating activity, also a maximum signal possible (total signal). The total signal was obtained in the way described above explaining the multiplication with 100 in the formula. The formula for specific activity that has been used is:

$$Specific\ activity = \frac{Product\ [nmol]}{Protein\ [mg] \times Time[min]}$$

with the product being:

$$Product = \left(\frac{Signal - Background\ signal}{Total\ signal\ \times 100} \right) \times 2$$

This assay can determine if a compound is affecting the activity of AurA. Concentrations from 200 µM to 3 µM in a 1:2 dilution were tested.

Preliminary tests before testing the compounds on AurA have been made to find the right conditions. The substrate for AurA previously used by our group, a Histone mix by Sigma, was not available anymore.

Instead, I tested three possible substrates: Histone H3 from calf thymus, Histone mix, type III-S and MBP, which is a standard substrate for numerous kinase assays. All substrates were tested at 5, 10 and 20 µg with 25 ng of AurA. Histone H3 from calf thymus proves to be a very good substrate for assays with AurA providing a strong signal even at the lowest concentration tested.

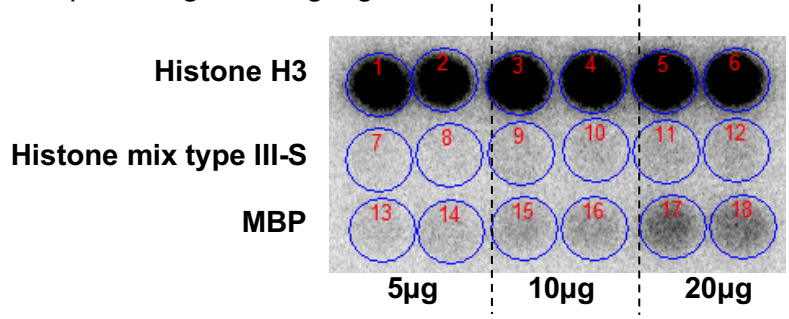

Figure 3.3: Substrates tested for 25 ng AurA at 5, 10 and 20 µg. Histone H3 provides the best signal and was chosen as substrate for further activity assays.

After choosing a suitable substrate, the amount of 25 ng used for AurA had to be confirmed. Therefore, I tested 25 to 1 ng AurA with 5 µg Histone H3. The results showed a linear increase in phosphorylation with increasing amount of enzyme and a good signal-to-noise ratio at 25 ng of AurA. At the same time the specific activity of the enzyme was around 10 nmol/(min*mg).

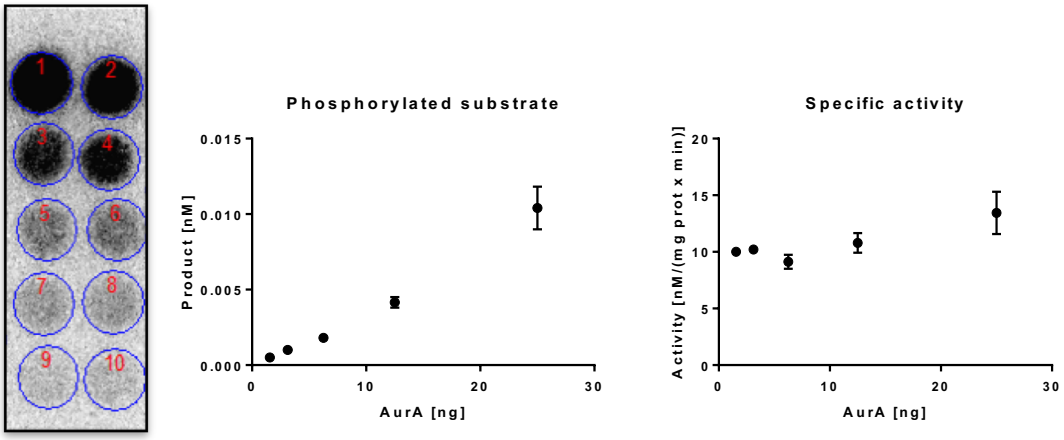

Figure 3.4: Linear increase in substrate phosphorylation with increasing amount of AurA. Specific kinase activity remains steady. Each data point of the kinase assay is performed in duplicates.

3.2.3 Thermal Stability Assay

The thermal stability assay, also called Differential Scanning Fluorimetry (DSF) or thermal shift assay, is an assay to identify whether a compound that is binding to the protein is also stabilizing it in terms of thermal denaturation.

The assay is performed in a 96-well PCR plate in a real time PCR cycler. Only one cycle is needed, increasing the temperature 0,3°C every minute starting at 25°C to 80°C. When heated, the protein unfolds and denatures allowing the dye Sypro orange to bind to its OH-groups. The more unfolded the protein is, the more OH-groups become exposed and the more dye is able to bind, thus fluorescence increases. This procedure is recorded by the StepOne plus real time PCR cycler. Program settings need to be on advanced setup, where a meltcurve function is available. Settings for reporter are "TAMRA" and for the quencher "none". The final volume of the sample is 10 µl. Preparation of the sample is performed as described next.

The compound is prediluted in DMSO to 5 mM. I then aim to reach a final concentration of 50 µM. 1 µl of the compound is diluted with 9 µl of a buffer

containing 10 mM Hepes, 150 mM NaCl. 1 µl of this solution is again taken and placed in a 96-well PCR plate. Then, 9 µl of a protein-mix is added, consisting of 10 mM Hepes, 150 mM NaCl, 1 mM DTT, 1 µM protein and 1% of the dye Sypro orange. For every sample we did duplicates, a DMSO reference value and we tested the compounds without protein to see if they have any intrinsic fluorescence or interaction with the dye.

9 µl	10mM Hepes
	150 mM NaCl
	1 mM DTT
	1 µM AurA (wt)
	1% Sypro orange
	Dilution buffer (10 mM Hepes, 150 mM NaCl)
1 µl	Diluted compound (200-3 µM f.c.)
10 µl	**Final Volume/ well**

Table 3.3: Content of one well measured in the thermal stability assay.

The melting point for AurA we obtained in different experiments varied between 40.9 and 42.3 °C. In my experiments, TPX2 stabilized AurA by binding to the TPX-binding site achieving a thermal shift of 4.2 °C (see Figure 3.5).

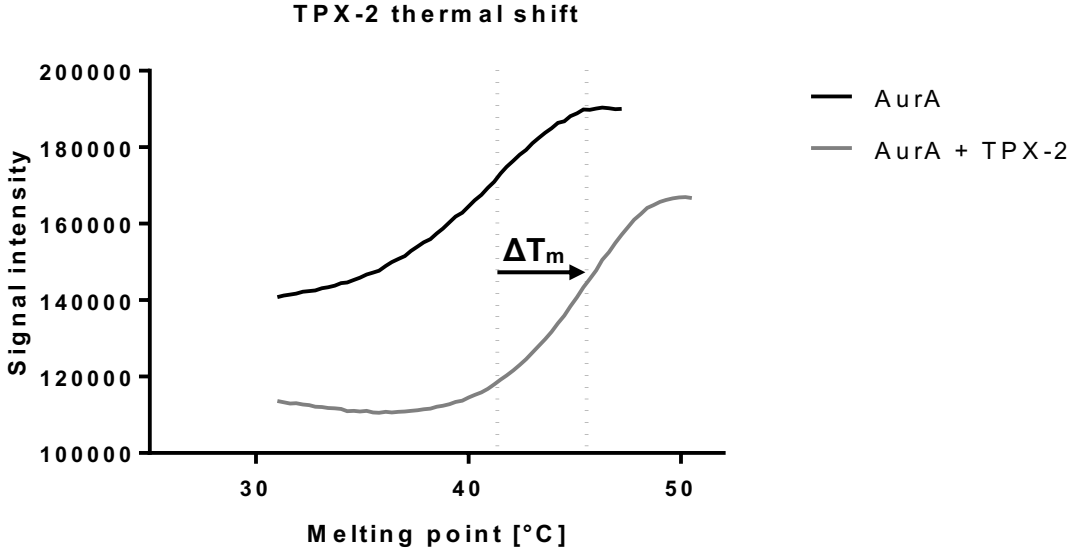

Figure 3.5: Melting curves of AurA and AurA in conformation with 50 µM of TPX2. Result is a melting point shift $\Delta T_m = 4.2$ °C.

After running the cycler, the data was collected and analyzed. Each step of increased temperature is a reading point for fluorescence. During the process of

melting the protein fluorescence increases, while before and after melting fluorescence is steady-state-like with the protein either completely folded or unfolded. The melting point is defined as half the way between beginning and ending of denaturation of the protein. The melting point itself can be easily obtained by treating the melting curve like a mathematical function with the melting point being the inflection point of the curve.

The inflection point can be determined via the first derivative of the curve which can be calculated in GraphPad prism software. The maximum value of the first derivative of the melting curve is the melting point which can in turn be obtained by a set phrase (=MAX({...}) in Microsoft Excel. Melting points of all curves were calculated and duplicates were averaged. If a compound would stabilize the protein, the melting point would be shifted to a higher temperature resulting in a positive ΔT.

3.2.4 Cell viability Assay

To observe the effect of a compound on the viability of cells a 48 h- cell viability assay was performed. For this assay HeLa cells were put in growth medium to grow freely for 24 h resulting in a density of 1.5 x 10^5 cells in 12 ml. This cell solution was spread with 100 µl/well into a 96-well microtiter plate resulting in 1250 cells/ well. The compounds to be tested were diluted in 1 ml cell growth medium to gain final concentrations of 10, 25, and 35 µM. In each well 1 ml growth medium-compound solution was added to the cells. Triplicates of each concentration were made as well as six wells with DMSO and six with growth medium only. Next, 20 µl of the dye CellTiter-Blue were added to each well and incubated for 4 h. Three growth medium-filled wells and three DMSO wells were measured for a 0 h reference value. After this the cells were incubated for 48 h in a CO_2 incubator at 37 °C.

CellTiter-Blue is a dye that indicates redox reactions taking place in viable cells. The chemical resazurin is reduced to resorufin in a NADH dependent reaction changing its color from blue to a fluorescent pink. If a cell is exposed to cytotoxic harm, its metabolism slows down or even stops in case of cell death and no more NADH is produced. The resazurin is not metabolized anymore and

the color stays blue. The assay should be handled with dimmed lights due to the light-sensitivity of CellTiter-Blue.

After 48 h the microtiter plates are measured and fluorescence is detected. The value for growth medium without cells should not have changed between 0 h and 48 h and gives a background signal. The DMSO values should indicate growth between the 0 h and the 48 h measurement. The value for DMSO after 48 h is used as reference of how much the cells could have grown if not inhibited. Calculations are done with Microsoft Excel. Triplicates for each concentration are averaged and divided through the average DMSO value to get a percental value for growth.

3.2.5 Cell cycle assay

The cell cycle assay makes it possible to take a deeper look at the impact of the compounds on the mechanisms of the cell. Cells are kept in culture in 6 cm Petri dishes, treated with either a compound or the control substance Nocodazole and incubated. After rinsing and bringing the cells into solution, the cells are treated with the DNA-intercalating PI-stain (Propidium iodide) to make the DNA fluoresce. The cell solution is aspirated by the flow cytometer and the fluorescence of the PI-stain is measured cell by cell. This way each cell is registered by its amount of DNA and plotted in a diagram.

The control substance Nocodazole is a synthetic Benzimidazole that interferes with the polymerization of the microtubules causing them to destabilize and retard their growth. With a non-functioning cytoskeleton the cell is unable to proceed in cell division and arrests in prometaphase of mitosis. Nocodazole is often used in cell experiments to arrest the cells in G2/M and serves in this experiment as a positive control for a cell cycle arrest.

As in the viability assay, HeLa cells were used. The cells were disseminated in 6cm Petri dishes with a volume of 1ml growth medium each. After one day of growing they reached a density of 2.5 x 10^5 cells per dish. 10 µl of Thymidine were added to each dish except two and incubated for 24 h to synchronize the cell cycle of all cells. After those 24h the Petri dishes were rinsed twice with PBS. Compounds and Nocodazole as control were diluted into 5 ml of growth

medium to reach a final concentration of 25 µM and added to the cells. The cells were incubated with the compounds over night for 16 h.

For harvesting of the cells, the supernatant was withdrawn and retained in one 15 ml falcon tube for each dish to collect the floating cells in G2/M phase also. 1 ml of Trypsin was added and incubated for 5 minutes at 37 °C to loosen the cells from the bottom of the Petri dish. The rest of the cells were harvested and the dishes were rinsed with PBS twice. All supernatant was collected and stored in the 15 ml falcon tubes on ice.

The tubes were centrifuged with 1200/ min at 4 °C for 5 minutes. The supernatant was thrown and the remaining pellet was thoroughly resuspended in 600 µl PBS. 400 µl of this solution was taken into another small tube for western blots.

1ml of cooled Ethanol 70% was added to the remaining 200 µl to fix the cells and incubated for at least 30 minutes at 4 °C. After fixation the tubes were centrifuged with 8000/ min for 30 sec. The supernatant was thrown and the pellet was thoroughly resuspended in 50 µl PBS and transferred to a glass FACS-tube.

Into the FACS-tube 100 µl of RNase A (concentration 1 mg/ml in PBS) and 100 µl of PI-staining solution (Propidium iodide, concentration 100 µg/ml in PBS) were added. This step was performed with dimmed lights since the PI is light-sensitive. The solution was incubated in the dark for 30 min at 37 °C.

Before measuring the tubes were mixed well. The BD FACS-Calibur was used for flow cytometry. Settings for x-axis were FL2 and measurement was taken with slow mode for aspiration.

3.2.6 Western blot

The Western blots were performed with a standard procedure by Dr. Monika Raab, group member of Prof. Klaus Strebhardt. Antibodies used are listed in section 3.1.7.

3.2.7 Thermophoresis

Molecules drift along temperature gradients, an effect called thermophoresis, the Soret effect, or thermodiffusion. This effect applies for all kind of molecules,

from DNA to polystyrene beads to simple peptides and complex proteins. Their thermophoretic motion differs from kind to kind and is influenced by the characteristics of the particular molecule like its hydrophilic properties, its effective charge and its solvation properties. For example, if two binding partners interact, the complex will have a different thermophoretic behavior than the partners alone.

NanoTemper Technology's Monolith NT.115 is used for measuring. For labeling the protein the Monolith NT His-tag labeling kit is used. A collimated infrared laser beam with focus onto a capillary heats the sample in the capillary and generates thermophoretic motion. A 650 nm LED is used to excite fluorescence emitting at 670 nm in the labeled protein and make the depletion or accumulation of the particles detectable. The changing fluorescence signal is visualized by NanoTemper's analyzing software, giving the K_D (dissociation constant) of the two interaction partners.

The protein was labeled according to the NanoTemper protocol for the His-tag labeling dye. It was incubated for 30 minutes at room temperature and then centrifuged with 13x1000 rpm at 4°C.

In general, the interaction partners were dissolved in a dilution buffer (DB) containing 50 mM Tris, 150 mM NaCl, 1 mM DTT and 0.05% Tween20 as detergent. The final protein concentration was kept constant at 50 nM during the experiments. Compounds were prediluted in DMSO to reach a final concentration of 200 µM. A dilution series (1:1,5) of the prediluted compound was prepared in DMSO. 1 µl of the titrated compound was taken and diluted with 9 µl DB (1:10). To the 10 µl of diluted compound were added 10 µl of the labeled protein and mixed well, resulting in a solution with 5% DMSO. The mix is now loaded into the capillaries by dipping the capillaries into the solution and measured by MicroScale Thermophoresis. Nanotemper's premium coated capillaries have been used for the samples. A first run shows the fluorescence in each capillary. 40% of the excitation LED power were used and 20% of the infrared laser. All compounds were tested negative on intrinsic fluorescence and could be tested with this method.

4. Results

The following chapters show the results of experiments and procedures performed to identify and characterize compounds modulating the kinase Aurora A. This principle of early drug discovery was implemented in the composition of this thesis.

The overall steps of the work are presented in Figure 4.1. First, I performed a screening procedure to identify and further characterize compounds that enhance or displace interaction of binding partners AurA/ TPX2. I identified eight compounds that inhibited the interaction between AurA and TPX2. Then, compounds identified in the screening were tested for their effect on the kinase activity of AurA. Here I found that some of the hit-compounds did not affect the activity of Aurora A. Next, I evaluated the effect of the hit-compounds on the thermal stability of AurA. All eight hit-compounds stabilized AurA to some degree, confirming that the compounds bind AurA. To complement the in vitro data, we attempted to obtain the crystal structure of the complex between AurA and the different compounds. Finally, I tested if the hit-compounds would inhibit AurA activity in cells in culture. To this end, we tested their effect of the hit-compound on the viability and cell cycle of cells in culture. All experiments were also performed with well characterized AurA inhibitors, e.g. MLN8237 or VX680, known to bind to the ATP-binding site.

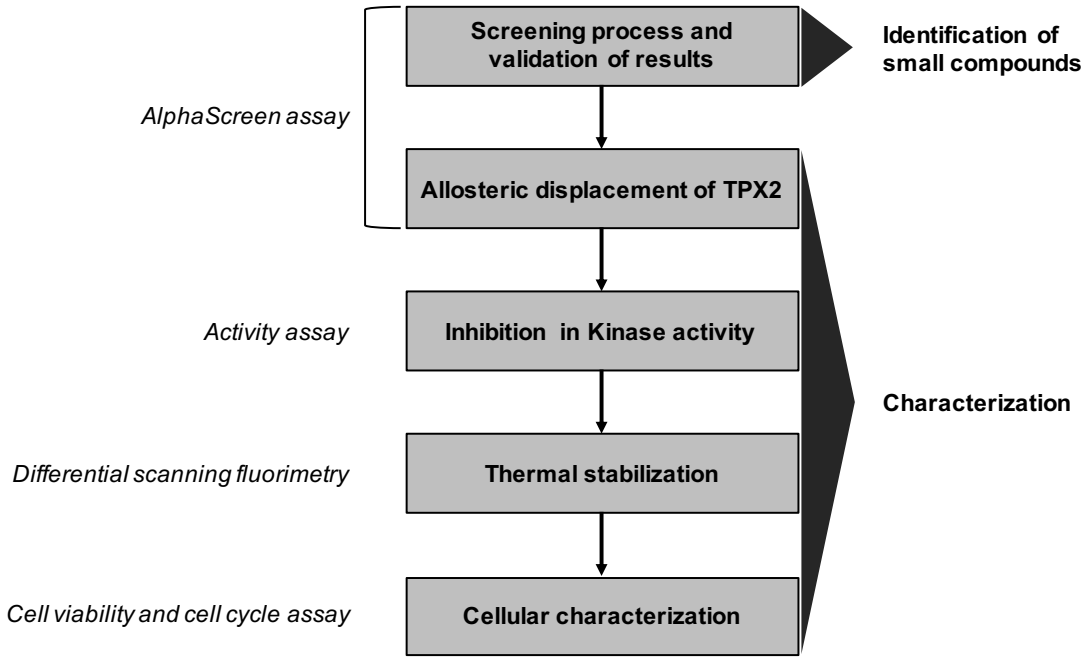

Figure 4.1: Diagrammed order of experiments performed for the identification and characterization of hit-compounds.

4.1 AlphaScreen assay to measure the effect on interaction of AurA/TPX2

The identification process of this thesis is analog to a high-throughput-screening with a target-based setup. Though in this case not fully automated, large numbers of small molecules were tested for displacement of TPX2 from AurA via AlphaScreen. Each hit could be a chemical lead that may be a starting point for developing a new pharmaceutical drug. From the initial screening process further steps were taken to clean and validate the results (Figure 4.2).

We chose the Prestwick's chemical library of 1280 FDA and EMA substances for the screening to identify compounds that affected, inhibited or enhanced, the interaction between TPX2 and AurA. Substances that are already FDA or EMA approved can go on a fast track for clinical trials, if showing effectiveness at low concentrations. Alternatively, the library can be a source of active compounds, that can help to understand the allosteric mechanism of regulation of AurA and as a proof-of-concept.

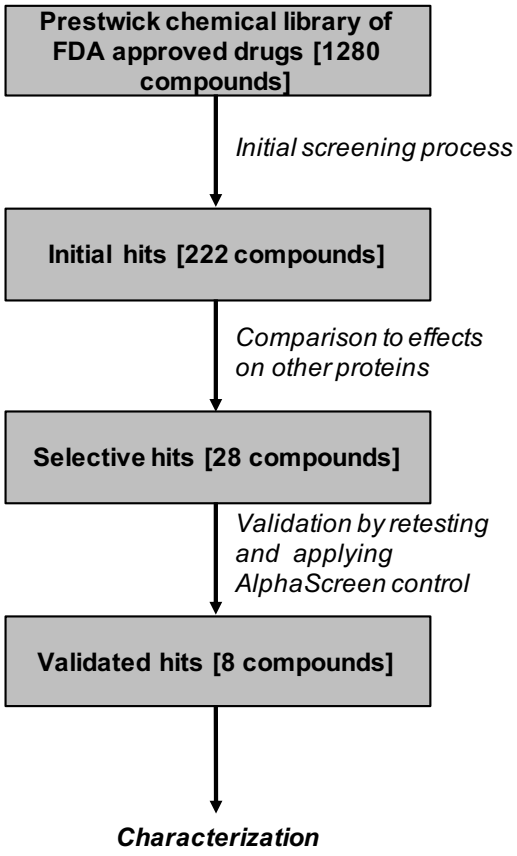

Figure 4.2: Identification process of validating hit compounds for displacement of TPX2 from AurA.

The AlphaScreen interaction assay itself is a simple way to show interference in the binding between AurA and TPX2. Displacement of TPX2 can be achieved by a compound by either competing with TPX2 at its binding site or by binding at a distance from the actual TPX2-binding site, i.e. by binding to the ATP binding site and changing the pocket for TPX2 making use of the bi-directionality of allostery and the "reverse allostery" concept. AlphaScreen shows us, if a compound is displacing TPX-but not in which way. For gaining more information about the interaction, additional assays were performed.

4.1.1 Screening of Prestwick's FDA approved chemical library and identification of initial hits

After determining the right assay conditions in a cross-titration (for details, see Methods), the compounds were screened at a concentration of 50 µM in four 384- well plates in singlicates. The assay was set up as described in the Methods section according to the standard AlphaScreen protocol. The results

give a single value that reflects the binding of AurA to TPX2 in the presence of 50 µM compound. The threshold to rank a compound as inhibiting or activating was set at less than 65 % binding or over 130 %, respectively. The table was analyzed with Microsoft Excel according to those criteria. In this initial screening 222 hits were identified. The raw data of the screening can be seen in the table attached at the end of the thesis.

The initial hits with binding under 65 % or over 130 % were compared to results obtained with other proteins that have been tested in our research group, e.g. p62/ LC3b, PDK-1/ PIFtide or PLK-1/ PoloBoxtide. This way, we could exclude those compounds that were reactive in an unspecific way and identify those hits that are considered selective for Aurora Kinase A. All four plates were processed and analyzed in the same way. In this step the initial 222 hits were reduced to 28 potentially "selective" hits for AurA.

	Initial hits	**Selective hits compared to other proteins**
plate 1	57 hits	10 hits
plate 2	55 hits	3 hits
plate 3	62 hits	9 hits
plate 4	48 hits	6 hits
	222 hits in total	**28 hits in total**

Table 4.1: Identified hits in the initial screening and reduction after comparison to the results of other proteins screened with the Prestwick chemical library.

4.1.2 Validation of the selective hit-compounds

Validation of the screening process and appropriately sorting out unwanted hits is crucial to prevent us working with false positives to keep the list of hits lean. Since there was just one value obtained in the screening per compound, a retesting of the initial hits was done. Therefore, duplicates of each hit compound were tested with AurA/ TPX2 at 50 µM concentration. Additionally, the compounds were tested with 10 nM biotinylated HIS, a control for the AlphaScreen assay itself. Hence, we could eliminate errors due to mistakes in pipetting in the initial screening, fluctuations as well as interference of a

compound with the AlphaScreen method, e.g. interaction with the beads or the oxygen singlet. The results of this validation process are presented in Table 4.2.

	Plate position	Initial Screening	Rescreening (Average of duplicates)	AlphaScreen control biotin-HIS		Name
	4M	**27%**	**42%**	**89%**	**Validated hit**	**Tiratricol**
	5M	59%	78%	102%		
	5O	42%	100%	98%		
	5P	2%	103%	94%		
Inhib.	8J	69%	104%	96%		
	9P	9%	101%	95%		
	17J	49%	77%	110%		
	21P	2%	87%	97%		
	22M	51%	102%	92%		
Activ.	10 O	145%	91%	91%		
	16L	69%	93%	87%		
Inhib.	**22B**	**59%**	**56%**	**93%**	**Validated hit**	**Erlotinib**
Activ.	18H	171%	47%	67%		
	3C	**3%**	**7%**	**83%**	**Validated hit**	**Pranlukast**
	5N	**36%**	**33%**	**80%**	**Validated hit**	**Liothyronine**
	9F	68%	84%	96%		
Inhib.	11N	55%	72%	83%		
	19B	**16%**	**21%**	**90%**	**Validated hit**	**Atractyloside**
	22A	**43%**	**24%**	**88%**	**Validated hit**	**Balsalazide**
	14C	153%	77%	87%		
Activ.	16F	135%	93%	91%		
	16N	140%	110%	90%		
	6K	48%	69%	92%		
	14B	**25%**	**58%**	**88%**	**Validated hit**	**Iopanoic acid**
Inhib.	16G	58%	71%	88%		
	21O	**39%**	**54%**	**97%**	**Validated hit**	**Oxymetholone**
	19I	162%	146%	131%		
Activ.	20B	146%	80%	91%		

Table 4.2: Validation process by testing the selective hits in duplicates; binding of TPX2 to AurA in [%] at 50µM compound concentration, measured in initial screening, rescreening and with AlphaScreen control. Inhibitors and activators are separated by a dotted line.

From the initial 28 hits eight were confirmed in the rescreening to have an effect on displacing TPX2 from AurA. The remaining 20 compounds that did not repeat their effect on displacing TPX2 were not further studied. The hit-compounds that showed enhancement of interaction did not proof to have an impact on AurA. So afterall, we were able to identify inhibitors only in the screening and validation process. When a screening project is performed, the pipetting errors can lead to the selection of potential hits. Here we can estimate that the error was equivalent to 20 errors in 1280 compounds, 1.56%, which is a manageable error rate.

None of the compounds were having any influence on the AlphaScreen control. The eight identified hits we obtained were confirmed to repeatedly displace TPX2 from AurA, did not affect other enzymes we tested and did not interfere with the AlphaScreen assay. They were ordered in a bigger amount for further testing.

4.1.3 Determination of IC50s on displacement of TPX2

To further characterize the compounds identified in the screening I tested concentrations from 200 - 0.03 µM. This way, an IC50 could easily be obtained for each compound. The assays were prepared accordingly to the standard AlphaScreen protocol with the compounds prediluted in DMSO in a 1:3 dilution series. The curves were transformed to a logarithmic scale for better visualization and analyzed with an inhibitory nonlinear regression fit with variable slope. GraphPad Prism software provides parameters from the resulting curve including the IC50 value, the concentration where half of the maximal inhibition is reached. Data points are shown with standard deviation error bars calculated from the duplicates of each concentration in one representative assay. All assays were repeated in order to validate the results.

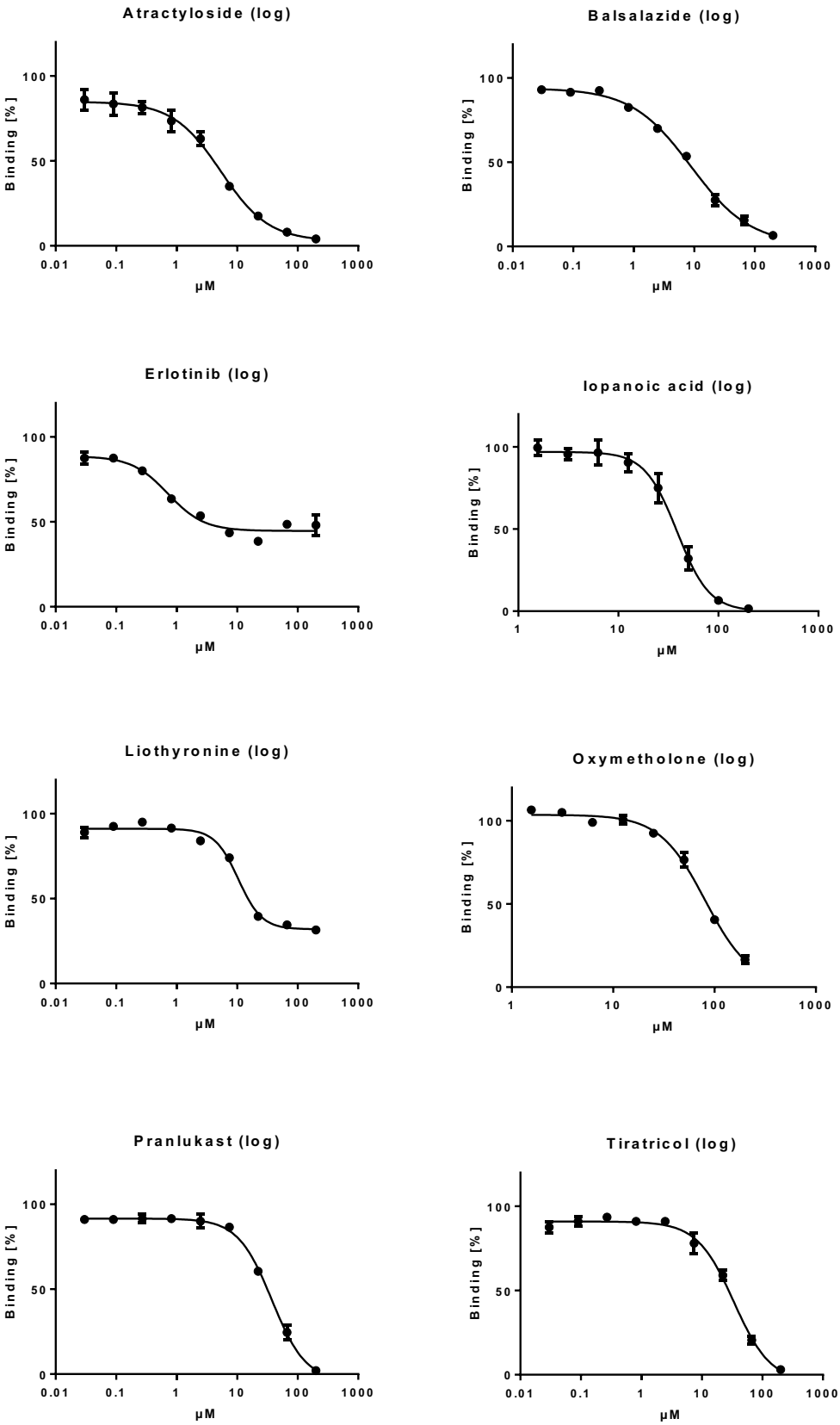

Figure 4.3: Curves for all hit compounds identified and confirmed in screening and rescreening.

	EC50 (without constraint)	IC50 (with Top=100%, Bottom=0%)
Atractyloside	5,4 µM	3,1 µM
Balsalazide	8,8 µM	7,3 µM
Erlotinib	0,7 µM	16,7 µM
Iopanoic acid	38,6 µM	37,2 µM
Liothyronine	10,4 µM	26,0 µM
Oxymetholone	80,9 µM	86,0 µM
Pranlukast	37,4 µM	28,6 µM
Tiratricol	33,7 µM	24,4 µM

Table 4.3: IC50s and EC50s for all validated hit-compounds.

All validated hit-compounds displace TPX2 from AurA more or less potently. Erlotinib and Liothyronine do not reach a full displacement reaching steady state at around 40-50% binding. Observing the behavior of those two compounds during assay preparation a slight precipitation can be noticed.

Therefore the reference point for inhibition has been calculated in two ways: The EC50 gives us the half maximal inhibition directly fitted to the values of the curve ignoring if the curve reaches zero at all. Second, an IC50 has been calculated constraining the top value of the curve to be 100% binding and the bottom value to be 0% giving the true value for 50% displacement. Due to the precipitation, IC50 and EC50 for Erlotinib and Liothyronine become worse by around 15 µM when applying constraints. For the other compounds IC50 and EC50 were similar.

4.2 Effect of FDA compounds on AurA kinase in vitro activity

The next step in characterizing the compounds identified is to determine whether the compounds also have an effect on the activity of AurA kinase. A compound displacing TPX2 doesn't merely tell if a compound is inhibiting the activity of the kinase as well. Three scenarios are possible: The compound is either an allosteric or competitive inhibitor, the compound binds to the TPX2 binding site and displaces it without affecting the conformation of the kinase and

hence not altering activity or the compound binds to the TPX2 binding site and stabilizes the kinase in its active form hence becoming an activator.

AurA is activated twofold by TPX2, as determined by Lisa Eisert in her thesis. Here, the AurA kinase activity assay is performed in the absence of TPX2. Thus, the assay enables to identify enhancers of activity, acting like TPX2, or inhibitors of AurA. After all conditions for the kinase assay were set up, the hit-compounds were tested for their effect on AurA. Concentrations from 200 to 3µM were tested with a DMSO reference. The assay was repeated at least twice.

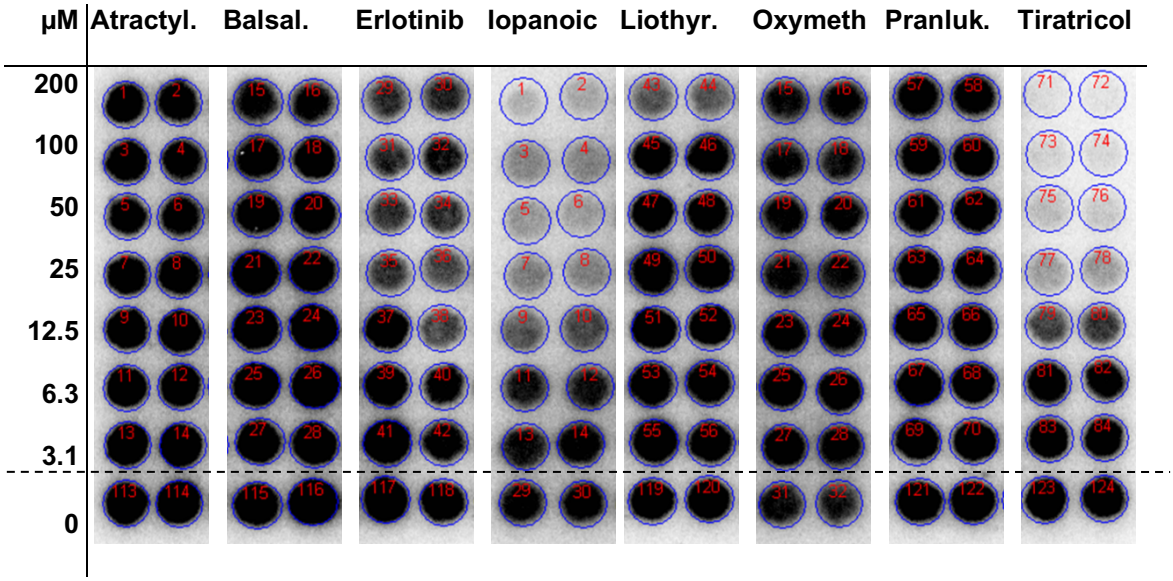

Figure 4.4: Influence of hit-compounds on phosphorylation of substrate Histone H3. Only Iopanoic acid and Tiratricol achieve a visible reduction of substrate turnover and hence inhibition of AurA. The radioactivity associated to each spot was quantified with phosphoimager technology (see Figure 4.5), which measures readioactivity in a linear range over 6 orders of magnitude.

After analysis, the compounds show the following results: Atractyloside inhibits up to 50% and reaches equilibrium afterwards with an EC50 of 4,6 µM. Balsalazide shows only little effect. Erlotinib seems to have inhibitory potential, however the compound is difficult to handle since it is precipitating in all assays and the effect observed could also be due to precipitation. Iopanoic acid inhibits with an IC50 of 18,3 µM. Liothyronine does not show a reproducible inhibitory effect, the curve remains static at around 50% for all concentrations. Oxymetholone shows also only little effect. Pranlukast shows similar to

Atractyloside and inhibit to only about 50%. Tiratricol has a steady inhibitory effect with an IC50 of 14.0 µM.

After these results we decided to drop Erlotinib and Liothyronine and continue experiments without them. On one hand, the concentrations of both drugs that affected the interaction were very high in relation to the concentrations used for the treatment of patients. In addition, the effect of both compounds on the activity of AurA was unclear.

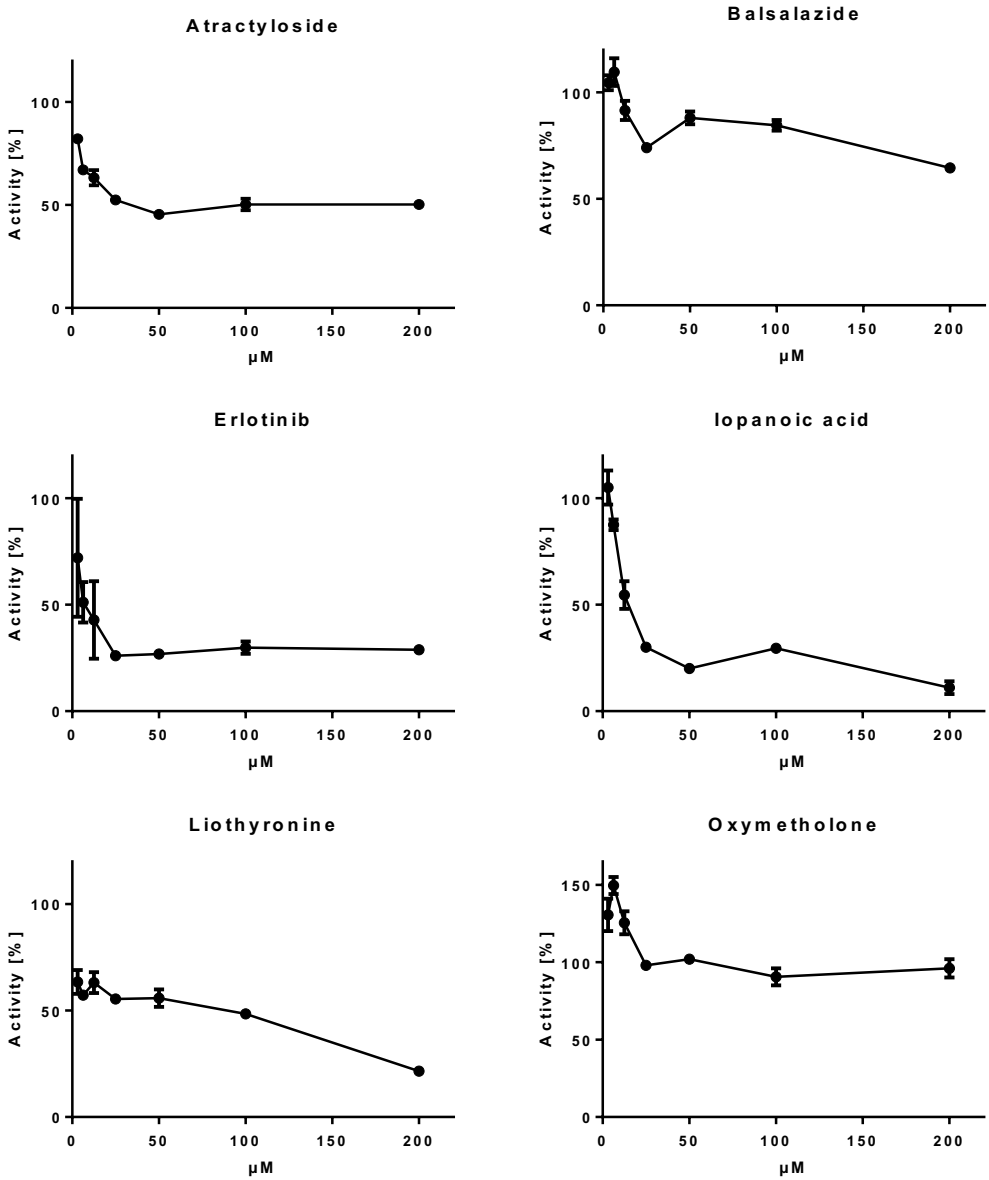

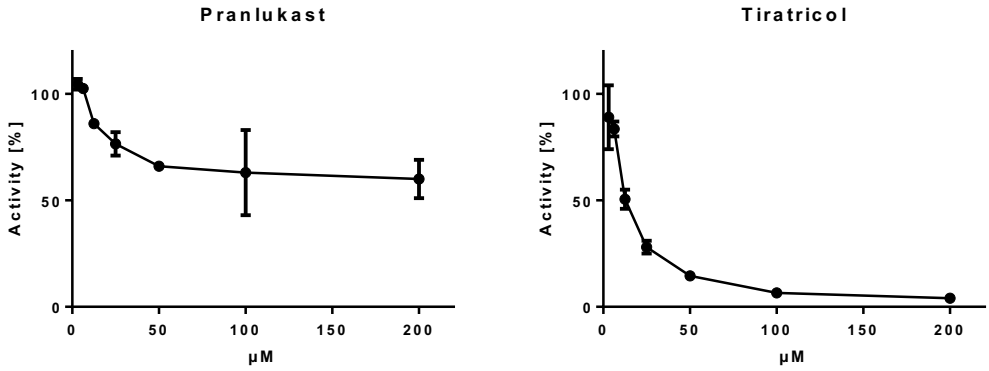

Figure 4.5: Results for hit-compounds tested on the activity of AurA. Only Iopanoic acid and Tiratricol show a clear inhibitory effect.

	EC50 (without constraint)	IC50 (with Top=100%, Bottom=0%)
Atractyloside	4,6 µM	-
Balsalazide	Ambiguous	-
Erlotinib	solubility issues	-
Iopanoic acid	18,3 µM	10 µM
Liothyronine	solubility issues	-
Oxymetholone	little effect	-
Pranlukast	15,2 µM	-
Tiratricol	13,5 µM	14 µM

Table 4.4: EC and IC 50s for all hit-compounds tested in AurA kinase activity assay.

4.3 Influence of the hit-compounds on the thermal stability of Aurora kinase A

Another assay that gives a good lead about the binding and affinity of a compound to a protein is the DSF or thermal stability assay. Whilst heating the protein constantly in a thermocycler the unfolding process can be detected with the help of a dye. The result is a melting curve. If a protein is stabilized by a peptide or compound, the compound delays unfolding until higher temperatures are reached and thus the melting curve shifts. The higher the affinity of a compound to the protein the more the melting point is shifted to higher temperatures. In addition, a stabilization of AurA would further confirm that the compounds indeed bind to AurA.

Experiences with thermal shift assays have shown that drugs developed to bind to the ATP-binding site with high affinity achieve much higher stabilization than allosteric binding partners. The physiological substrate, ATP, on the other hand, binds with micromolar affinity to the kinases, and only stabilizes the kinases around 1 °C.

The compounds we tested achieved a range of different thermal shifts, from less than 1 °C to a big impact with over 10 °C. Most effective were again Iopanoic acid and Tiratricol with shifts of 6.9 and 12.0 °C. Atractyloside and Balsalazide produced shifts of 4.0 and 1.8 °C. Pranlukast and Oxymetholone show shifts varying around 0.4 and 0.5 °C. These results confirmed binding of the compounds to AurA.

Compounds were tested at 50 µM concentration to get a first glance and then twice with duplicates in different concentrations from 100 to 6µM. 1 µM of AurA was used in all assays.

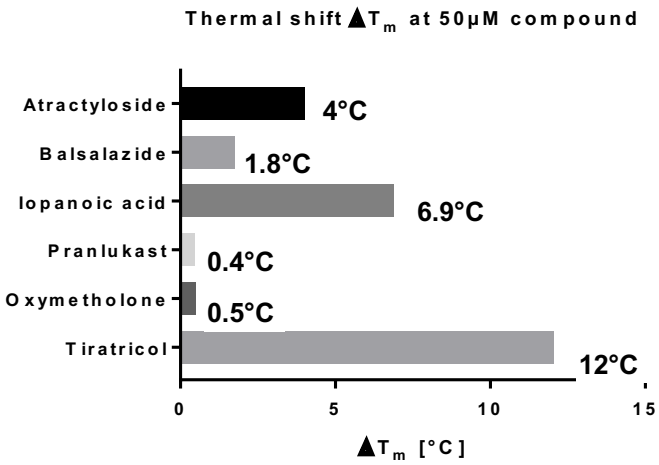

Figure 4.6: Overview of melting point shifts of all hit-compounds at a 50µM concentration.

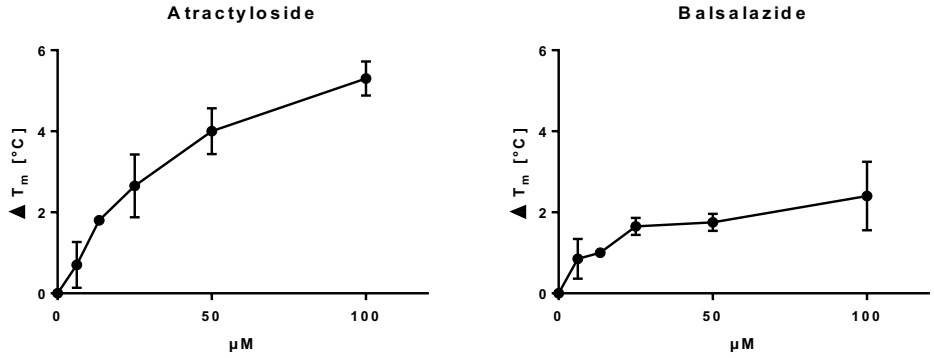

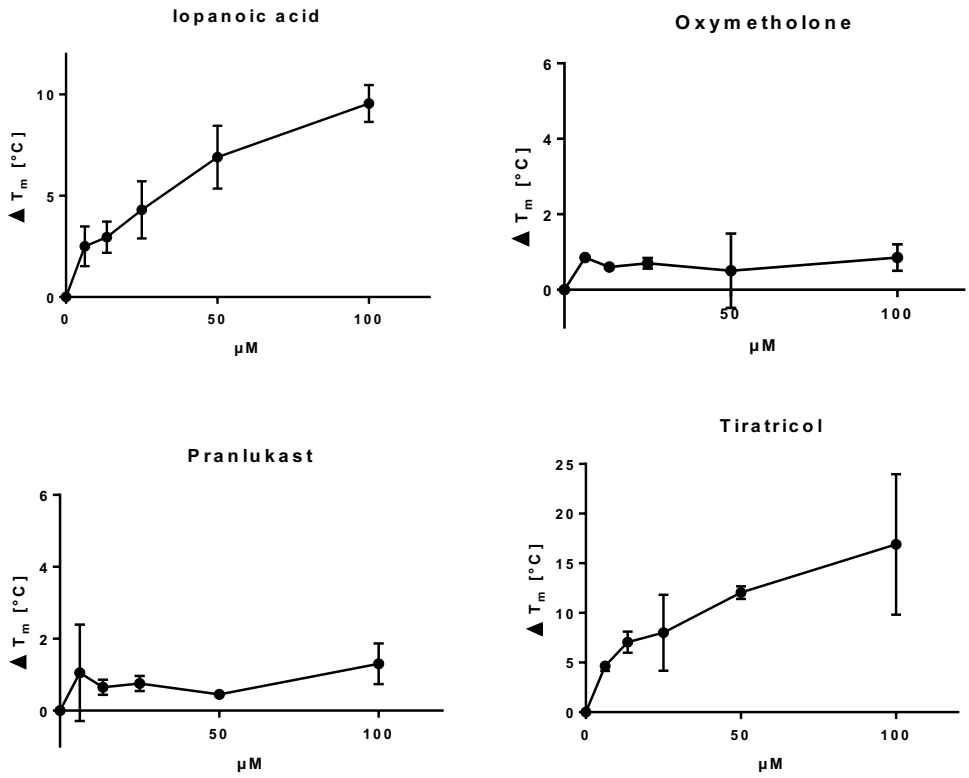

Figure 4.7: Melting point shifts for different concentrations of the compounds.

4.4 Continuation of work on PS 731

The compound PS 731 was identified by Lisa Eisert in another screening with the Maybridge library of small molecules. It was one of the most promising hits for AurA from this screening and the mechanism of binding was not completely solved in the previous work. PS 731 displaces TPX2 in AlphaScreen assay with an IC50 of 5.4 µM and inhibits the activity of AurA in the activity assay with an IC50 of 4.4 µM.

To find out more about the binding mechanisms of PS 731 variants of its chemical structure have been obtained. We hoped that minor changes in the molecule could answer which groups are relevant to the interaction with AurA. AlphaScreen and activity assays were performed twice with these variants and PS 731 in comparison.

Compound	Formula	MW (Da)	Effect
PS 731	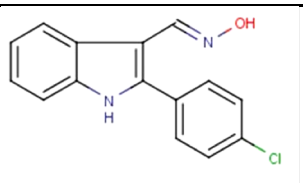	270.06	• AlphaScreen: **displacement** (IC50=5.4 µM) • Activity assay: **inhibition** (IC50=4.4 µM)
PS 876	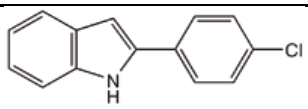	227.05	• AlphaScreen: no effect • Activity assay: no effect
PS 877	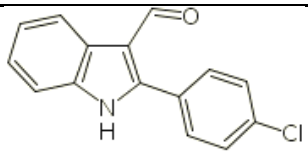	255.05	• AlphaScreen: no effect • Activity assay: no effect
PS 878	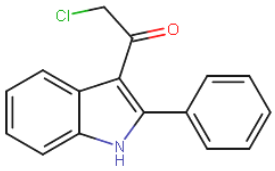	269.06	• AlphaScreen: no effect • Activity assay: **inhibition** (IC50=25.3 µM)
PS 879	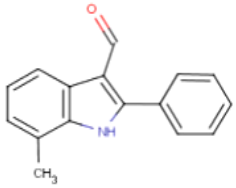	235.1	• AlphaScreen: no effect • Activity assay: **inhibition** (IC50=62.2 µM)
PS 881	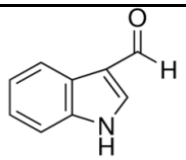	145.16	• AlphaScreen: no effect • Activity assay: no effect
PS 882	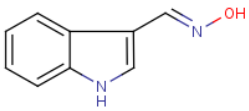	160.17	• AlphaScreen: no effect • Activity assay: **inhibition** (IC50=22.2 µM)

Table 4.5: Variants of PS 731 with their molecular weight and chemical structure tested in AlphaScreen and activity assay for their effect on AurA.

In AlphaScreen none of the variants showed a displacement of TPX2 from AurA. In the activity assay, however, three of the variants inhibited phosphorylation of the substrate by AurA, PS 878, 879 and 882. Most potent in comparison to PS 731- although not as potent as- was the variant PS 882.

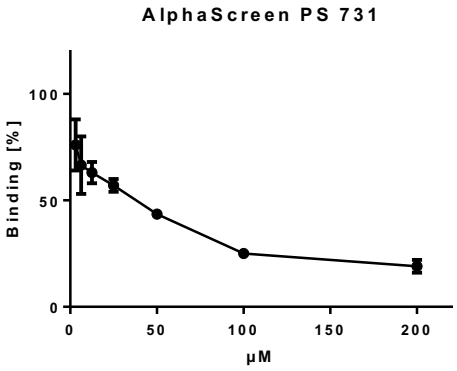
AlphaScreen PS 731
Binding [%]
100
50
0
0
50
100
150
200
µM

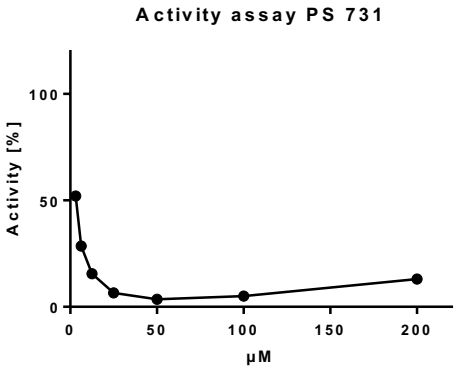
Activity assay PS 731
Activity [%]
100
50
0
0
50
100
150
200
µM

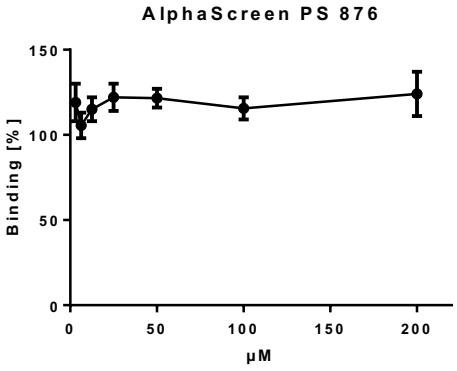
AlphaScreen PS 876
Binding [%]
150
100
50
0
0
50
100
150
200
µM

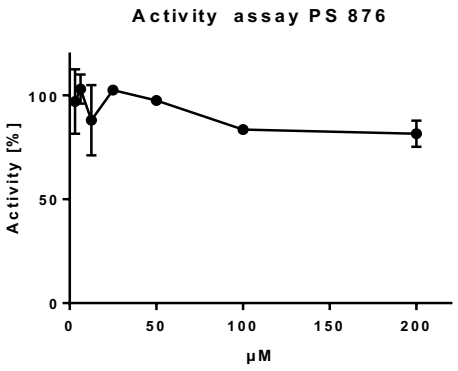
Activity assay PS 876
Activity [%]
100
50
0
0
50
100
150
200
µM

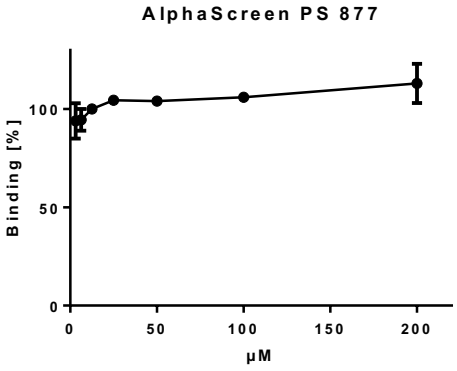
AlphaScreen PS 877
Binding [%]
100
50
0
0
50
100
150
200
µM

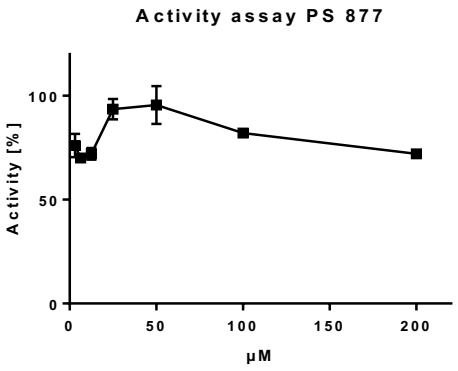
Activity assay PS 877
Activity [%]
100
50
0
0
50
100
150
200
µM

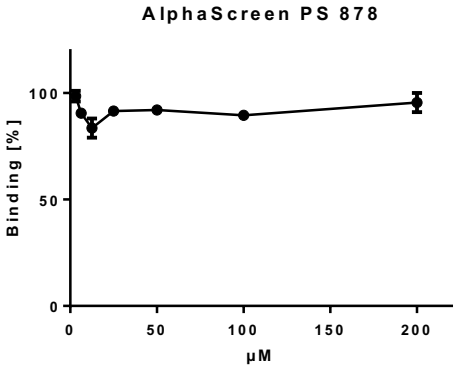
AlphaScreen PS 878
Binding [%]
100
50
0
0
50
100
150
200
µM

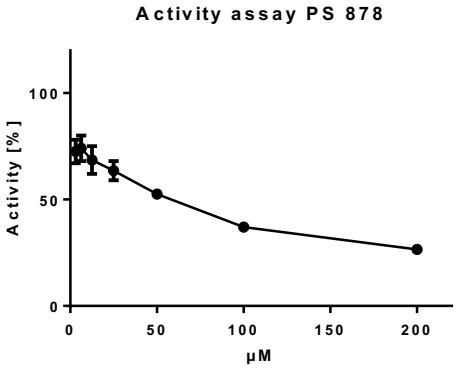
Activity assay PS 878
Activity [%]
100
50
0
0
50
100
150
200
µM

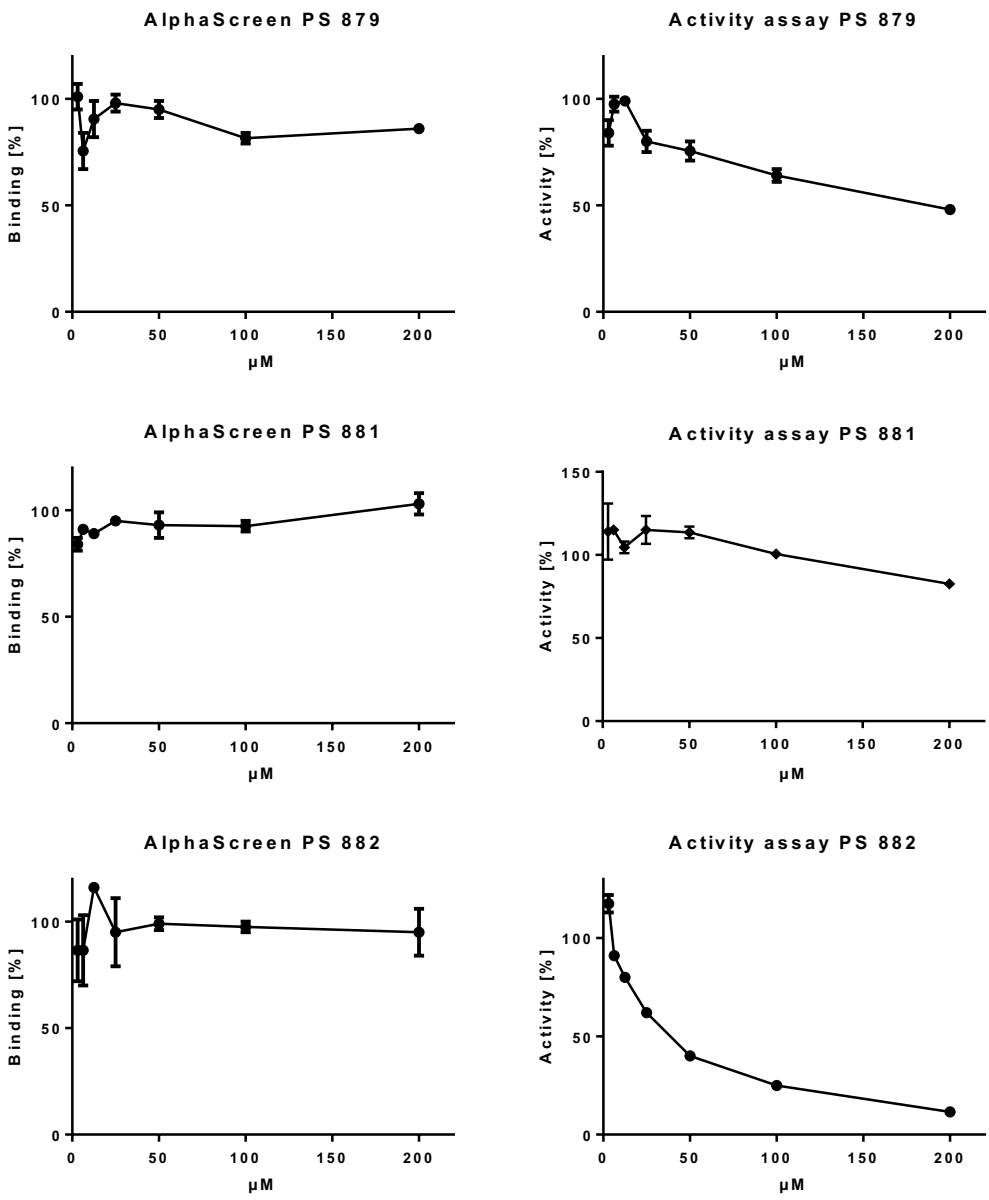

Figure 4.8: Graphs for the variants of PS 731 tested in AlphaScreen and activity assay. No displacement of TPX2 could be observed, although PS 878, 879 and 882 inhibit the activity of AurA.

To explain these effects, the chemical formulas of the compounds need to be considered. PS 882 for example differs from PS 731 only in the missing benzolchloride group. This structure seems to be relevant for the displacement of TPX2 but not for inhibiting activity of the kinase. Further considerations shall be performed in the discussion.

4.5 Comparison of in vitro results to known AurA inhibitors

All assays were performed with control compounds. To have a comparison we used commercially available Aurora kinase inhibitors MLN 8237 (also known as Alisertib) and VX 680, that were in clinical trials already. Also, we used PS 731, whose efficacy on AurA has previously been discovered by our group. This way, we could evaluate the hit-compounds in regard of their potency.

4.5.1 Comparison of AlphaScreen results to other known Aurora A inhibitors

For AlphaScreen assays, VX 680 has been used as a control in our group by Lisa Eisert before. MLN 8237, however, has so far never been tested in AlphaScreen assay. MLN 8237 and VX 680 show IC50s in the low nanomolar range whereas IC50s of PS 731 and the hit compounds range between low and medium micromolar values.

Surprisingly, I found that MLN 8237 displaces TPX2 very potently with an EC50 and IC50 of 0.1 nM (Figure 4.9 a))[44]. However, the compound is known to bind to the ATP-binding site. This means the displacement of TPX2 must be provided allosterically, from a distance.

VX 680 also binds at the ATP-binding site and displaces the interaction with TPX2, although TPX2 remained bound to a high degree even at high micromolar concentrations (see plateau in binding curve, Figure 4.9 b)). Together, our studies unveiled that drugs developed to bind to the ATP-binding site can be very potent inhibitors of the interaction of AurA with TPX2.

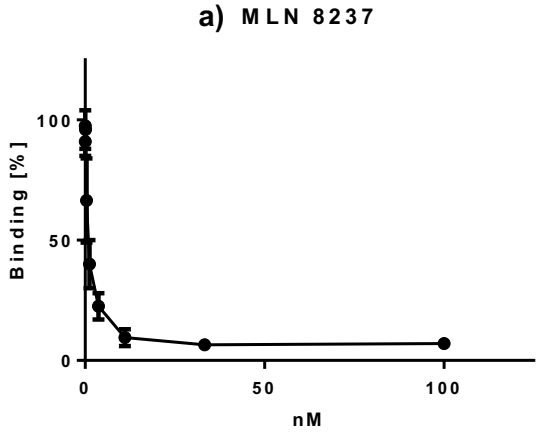

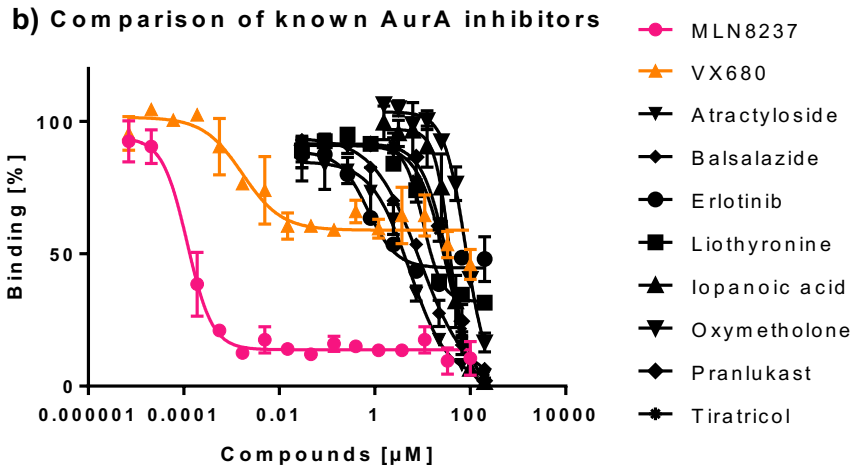

Figure 4.9: Effect of compounds on the interaction between AurA and TPX2 peptide. **a)** Impact of MLN8237 on the binding of TPX2 to AurA. MLN8237 potently displaces TPX2 with an IC50 of 0.1 nM; **b)** Comparison of established AurA inhibitors MLN8237 and VX680 to the hit compounds of the screening.

4.5.2 Comparison of activity assay results to other known Aurora A inhibitors

Comparison of the two most potent inhibitors identified in this screening, Iopanoic acid and Tiratricol, to the AurA inhibitor controls MLN 8237 and VX 680 show again that the hit-compounds are not remotely as potent as the compounds already tested in clinical trials. However, Iopanoic acid and Tiratricol show a similar EC50 as the most promising hit from another screening our group performed, PS 731.

The activity assay is measured at a concentration of 100 µM, while the cellular concentration of ATP can range between 1 and 5 mM. While the MLN 8237 and VX 680 have very low IC50s in our in vitro assay, they require µM concentrations for the inhibition of AurA in cells in culture.

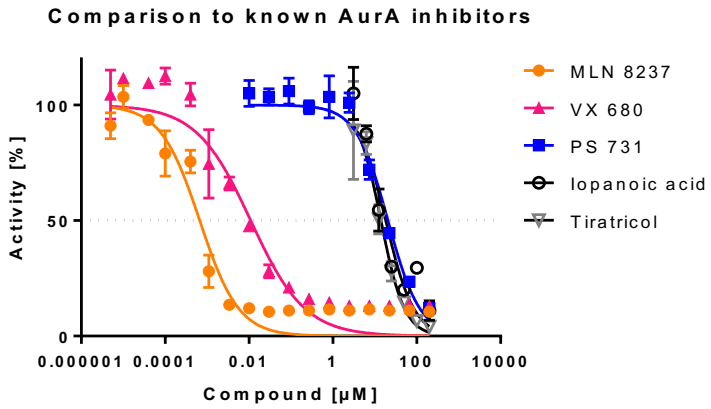

	EC 50 in µM
MLN 8237	0.0007
VX 680	0.012
PS 731	20.63
Iopanoic acid	18.26
Tiratricol	14.03

Figure 4.10 and Table 4.6: Effect of small compounds on the in vitro activity of AurA. EC50 for selected inhibitors from the screening in comparison to known AurA inhibitors that target the ATP-binding site.

4.5.3 Comparison of thermal stability results to other known Aurora A inhibitors

Next to the FDA hits the known AurA inhibitors MLN 8237, VX 680 and the hit from our group PS 731 were tested. MLN 8237 and VX 680 produce a shift of 27 and 23 °C respectively at 50 µM, as expected for potent inhibitors binding to the ATP-binding site. PS 731 is in the range of the other hit-compounds with a large stabilization, reaching 10 °C ΔTm at 50 µM.

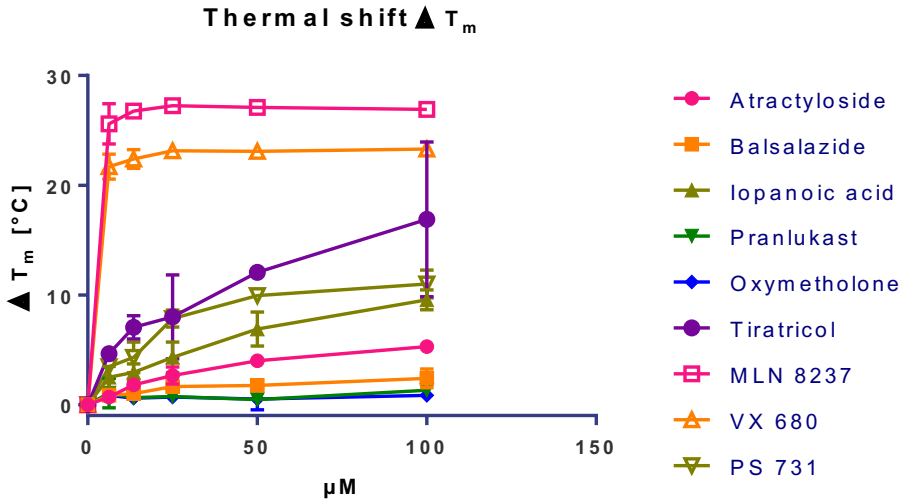

Figure 4.11: Comparison of the produced thermal shift depending on the compound concentration.

4.6 Thermophoresis

With the biophysical method of MicroScale Thermophoresis (MST) the dissociation constant K_D of two ligands can be determined. The K_D describes the affinity of two binding partners towards each other. The value of the K_D can be visualized as half of the binding sites occupied with their binding partner. The lower the K_D is the higher the affinity of the two molecules. For example, Rennie, McIntyre et. al. published a K_D for native TPX2 of 3.54 ± 1.15 µM measured with ITC[130]. In comparison to ITC however, the method of MST requires less amount of protein and compounds. The experiments were performed by me at Institute Pasteur, Paris.

From the FDA hit-compounds Atractyloside, Iopanoic acid, Oxymetholone and Tiratricol were tested and, to gain further information on that compound, PS731. The compounds were tested at concentrations from 500 -1,14 µM with a dilution of 1:1,5 and showed no intrinsic fluorescence in the pretest. FDA hit-compounds Balsalazide and Pranlukast yielded no results with MST.

The results are surprisingly high KDs for PS 731, with IC50s that correspond to 10 times the concentrations that were active in the alphascreen assay using His-AurA. The results may reflect the difficulties of the compounds to bind to the AurA mutant used in this study (AurA D274N). The protein used was a purified AurA mutant protein that is efficient in producing diffracting crystals. It is tempting to speculate that the AurA mutant protein was selected for crystallography for stabilizing the active conformation of the kinase. Compounds that stabilize conformations that are different from the active conformation of the kinase, may struggle to bind to the mutant AurA used in the crystallography studies. This scenario could explain the estimated high KDs of PS731, Atractyloside and Iopanoic acid.

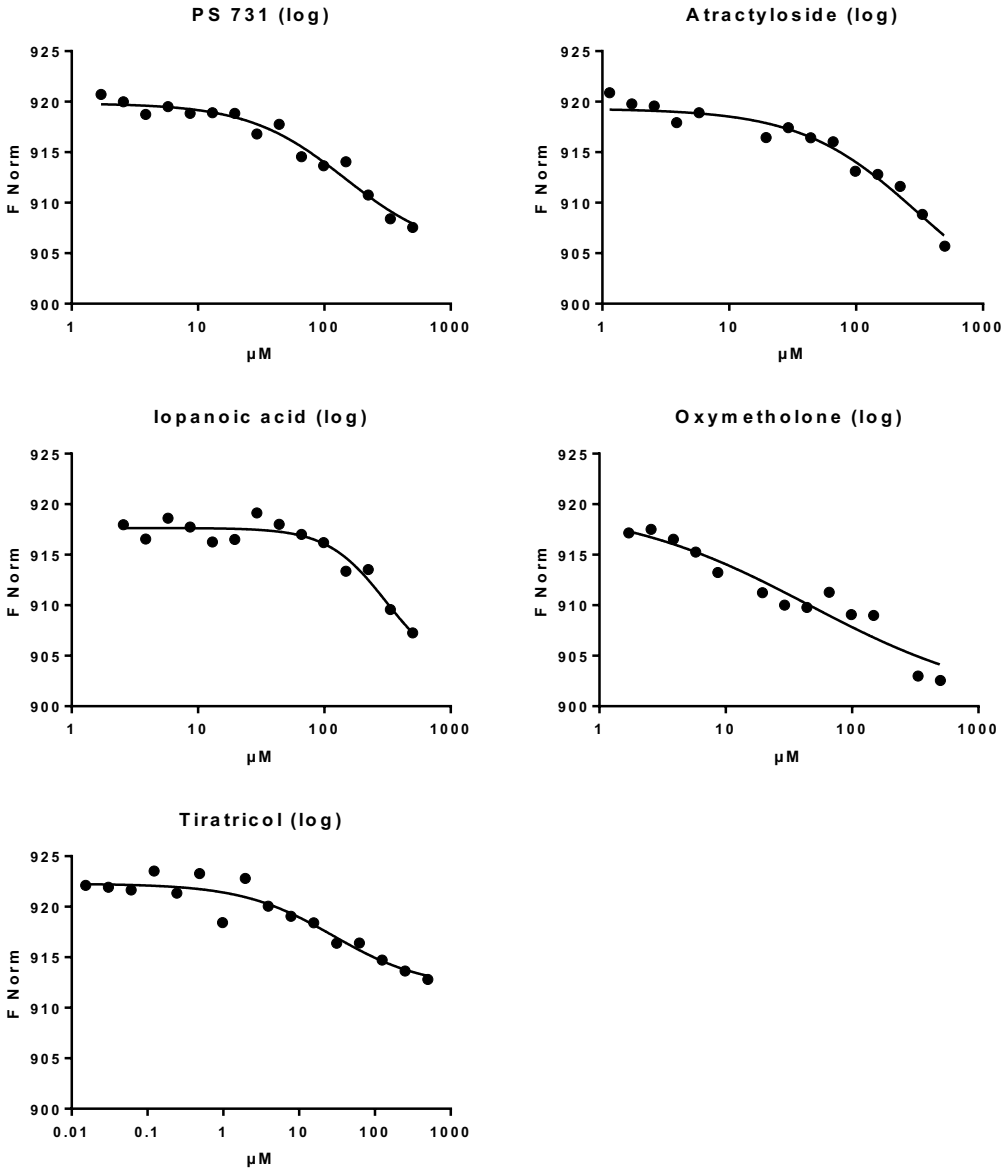

Figure 4.12: Preliminary graphs for the experiments performed with MST.

We obtained the following K_{Ds} for the compounds:

Compound	**K_D**
Atractyloside	299,9 µM (preliminary)
Iopanoic acid	478,2 µM (preliminary)
Oxymetholone	51,7 µM
Tiratricol	36,3 µM
PS 731	126,8 µM

Table 4.7: KDs of the compounds, measured with MST.

4.7 Crystallography of AurA and AurA in complex with hit-compounds

A major remaining question was then to identify the binding site of the identified hit-compounds. The senior crystallographer in our laboratory, Dr. Jörg Schulze, first crystallized two different constructs of mutant forms of AurA that had been previously published. The crystals diffracted poorly, to about 3 Angstrom resolution. The structure of AurA was solved by molecular replacement. The structure of AurA was in overall active conformations. The compounds PS 731, Tiratricol and Iopanoic acid were then soaked into the crystals, and those crystals then solved. Unfortunately, Dr. Schulze could not identify any electron density that could be due to the hit-compounds. In particular, the ATP-binding site was not occupied by our hit-compounds. Dr. Schulze then attempted to mix AurA with PS 731, Tiratricol and Iopanoic acid and screened hundreds of different crystallization conditions. Interestingly, Dr. Schulze identified one crystal form of AurA that was only formed in the presence of PS 731. Unfortunately, again, we were not able to identify a binding site for PS 731 in the AurA crystal. The difficulties in the crystallization of the complexes between the mutant form of AurA and PS731 and Iopanoic acid could be due to the mutant AurA constructs used. Looking back, we notice that those constructs had been previously selected to stabilize the active form of the kinase, to achieve crystals of AurA. However, those constructs may bind more poorly to some of the small compounds identified in the screening, as suggested by the above Thermophoresis experiments.

4.8 Effect of compounds on cellular viability

The inhibition of Aurora A hinders cellular proliferation. As a first approach to check if the identified hit-compounds were active in mammalian cells, we tested the effect of the compounds on the cellular viability assay. Viable cells are able to metabolize the blue resazurin dye in a NADH-dependent redox reaction. Product is the pink and also fluorescent resofurin dye, thus, the more cells are viable, the higher level of pink dye is detectable.

Results are shown in relation to cells treated with DMSO only to have comparable values. All compounds were tested at 10, 25 and 35 µM concentration. As controls MLN 8237, VX 680 and PS 731 were also tested.

Atractyloside shows a concentration-dependent inhibition of growth, with no inhibition at 10 µM but decreasing growth to 74% at 35 µM. Balsalazide shows a slight inhibition in cell growth to around 80% but without correlation to the concentration of the compound. Iopanoic acid shows more inhibition than Balsalazide (lowest 63% at 25 µM) but still without any correlation to the concentration. Oxymetholone shows good inhibition of growth to 46% and also more inhibition with higher concentration of the compound. Pranlukast inhibits to 69% with lowest concentration but with higher concentrations the cells grow better which seems to be indirectly proportional. Tiratricol shows no effect at any concentration.

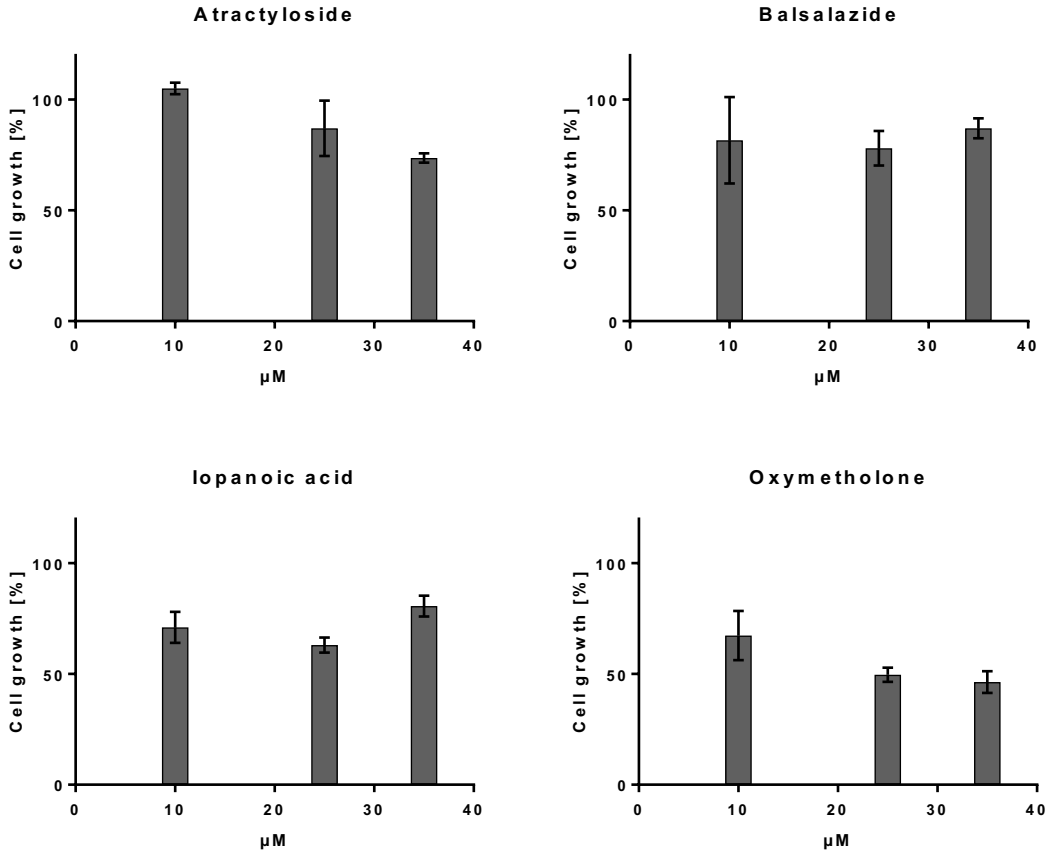

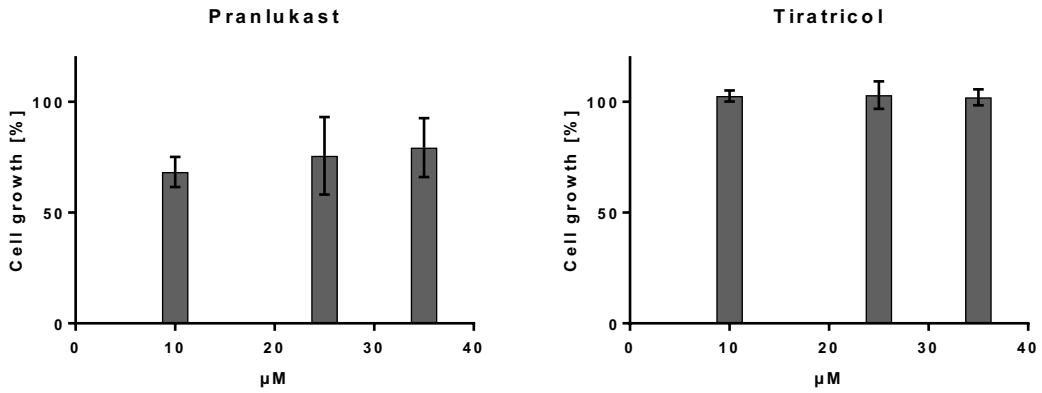

Figure 4.13: Results of MTT-assay for the hit-compounds after 48h incubation, growth in [%] relating to the growth of cells only treated with DMSO.

Based on the results of the study, we conclude that Tiratricol, Pranlukast, Balsalazide and Iopanoic acid do not inhibit the function of Aurora A in cells in culture at the concentrations tested. The reasons for the lack of effect in cells could be various: for Balsalazide and Pranlukast that showed no very potent interaction with AurA in the previous assays, a possible explanation for the lack of effect on the cell viability could be the high ATP concentration in cells. On the other hand, Tiratricol and Iopanoic acid have high hydrophilic properties, which could be problematic in cellular assays.

Atractyloside and Oxymetholone show a small but dose-dependent inhibition of growth. Oxymetholone reaches 54% inhibition which is a higher effect than 10 µM of MLN 8237. Notably, PS 731 is very potent, with similar effects to MLN 8237 and VX 680, decreasing growth to 28% at all concentrations.

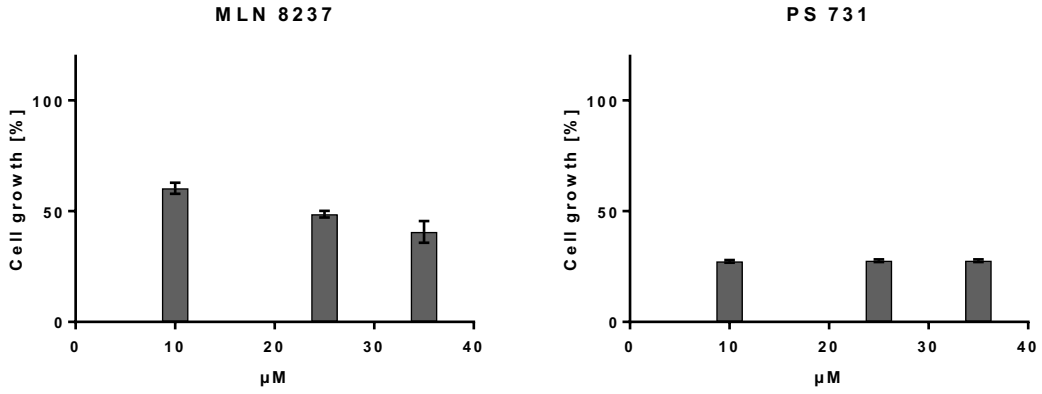

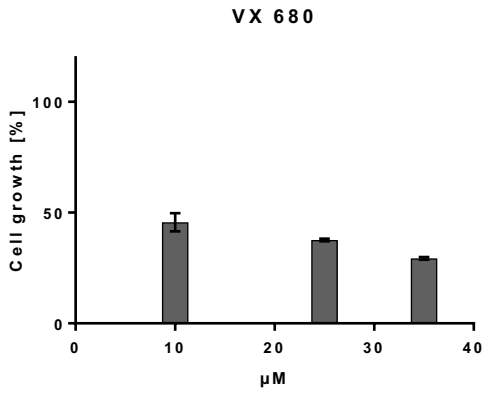

Figure 4.14: Results of MTT-assay for the control compounds and PS 731 after 48h incubation, growth in [%] relating to the growth of cells only treated with DMSO. PS 731 is the most potent inhibitor of growth in this experiment.

4.9 Effect of hit-compounds on the cell cycle

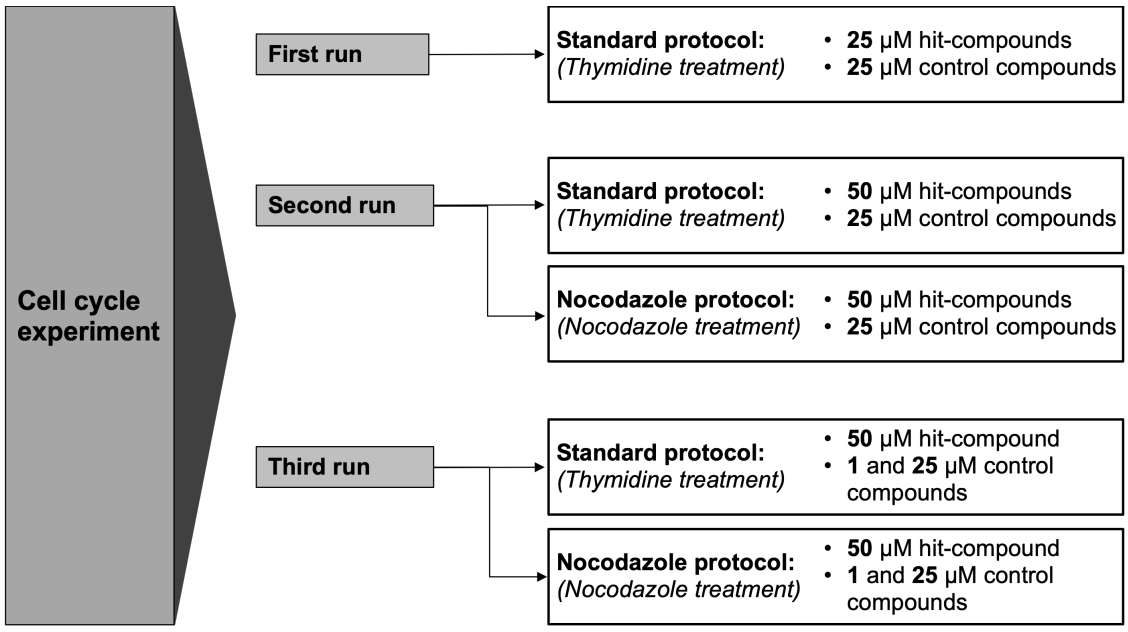

Figure 4.15: Scheme of the cell cycle experiments.

After getting an overview whether the compounds influence the cell growth, the direct impact on the cell cycle was explored. The inhibition of AurA in vivo averts the formation of spindles that are necessary for cell division. Hence in this assay, the inhibition of AurA causes the cells to get caught in G2/M at the spindle assembly checkpoint. For the analysis, the cell cycle was synchronized with a 24h Thymidin treatment and after that incubated for 16h with the

compounds. The flow-cytometer records cells for their amount of genetic material which is stained with the DNA-intercalant PI-stain.

A cell has different amounts of genome during its cell cycle. When in G1 phase, the number of chromosome sets is 2n with n being the number of chromosomes. When it comes to cell division the genome is replicated in the phase of synthesis to supply the daughter cell. After replication the genetic state is 4n. In G2/M phase the cell is split and the genome is distributed onto the two cells and the state becomes 2n again after telophase.

The flow-cytometer detects how much genetic material there is, summing up how many cells are in which state. The scale on x-axis is set in a way that 200 equals 2n and 400 equals 4n.

4.9.1 Flow-cytometry with standard protocol

In the first approach, we tested the hit-compounds and controls MLN 8237, VX 680 and PS 731 for their effect on the cell cycle of HeLa cells. The hit-compound Tiratricol was not tested in the cell cycle assay because it had no effect at all in the 48h- cell viability assay.

The diagram of the untreated cells shows a standard distribution of cells in different states of the cell cycle (Figure 4.16 a)). Around 58% of the cells are in G1 phase with 2n chromosomes (gated with M1), about 19% of the cells are in G2/M (M2) and 22% in synthesis (M3). Cells with less genome than 2n are apoptotic and with more than 4n are polyploid.

Cells treated with Nocodazole show an example for cells arrested in G2/M (Figure 4.16 b)). Cytometry shows 70% of the cells in cell cycle arrest (M2), only 14% remain in G1 (M1).

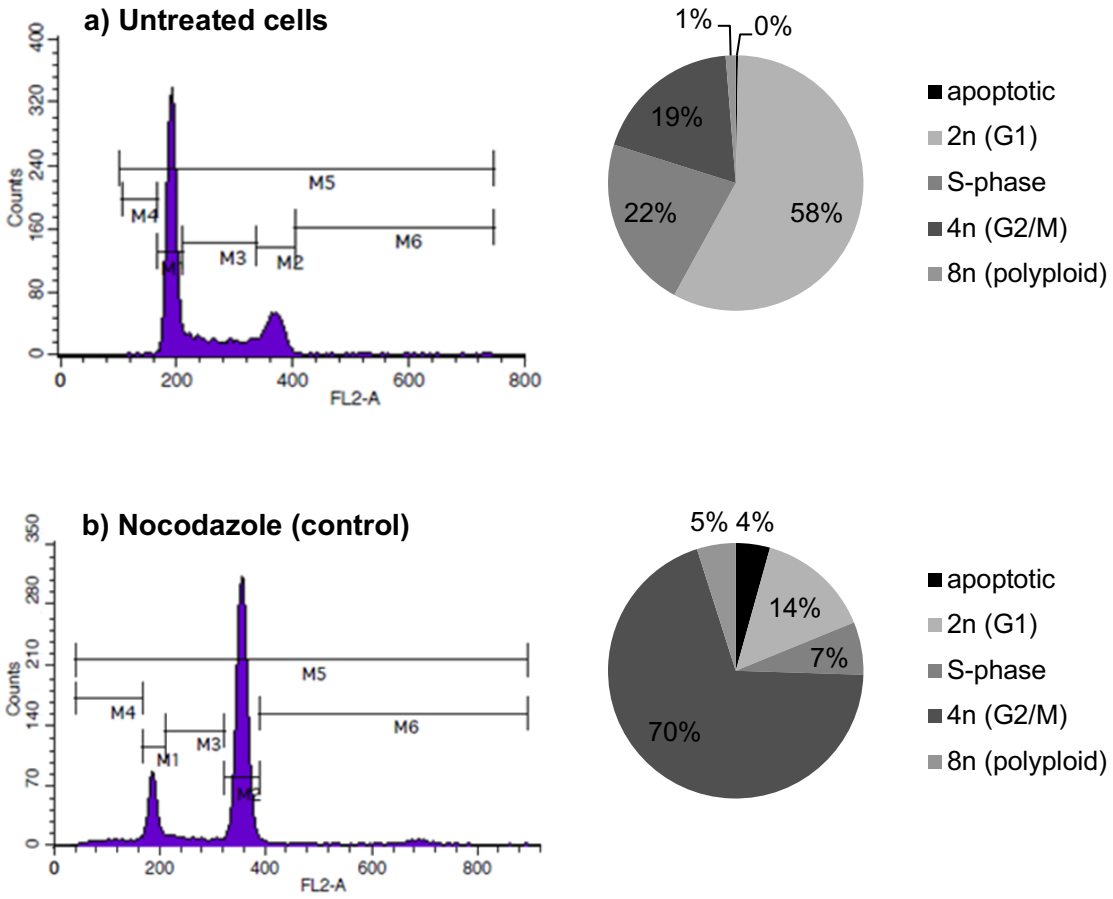

Figure 4.16: Example for **a)** normal distribution of genome of untreated cells and **b)** distribution for cells in cell cycle arrest due to treatment with Nocodazole, a spindle toxin that causes arrest in G2/M.

All other samples have been treated with Thymidin before incubation to synchronize cell cycles. The controls PS 731, MLN 8237 and VX 680 show over 80% a complete cell cycle arrest at 4n as expected.

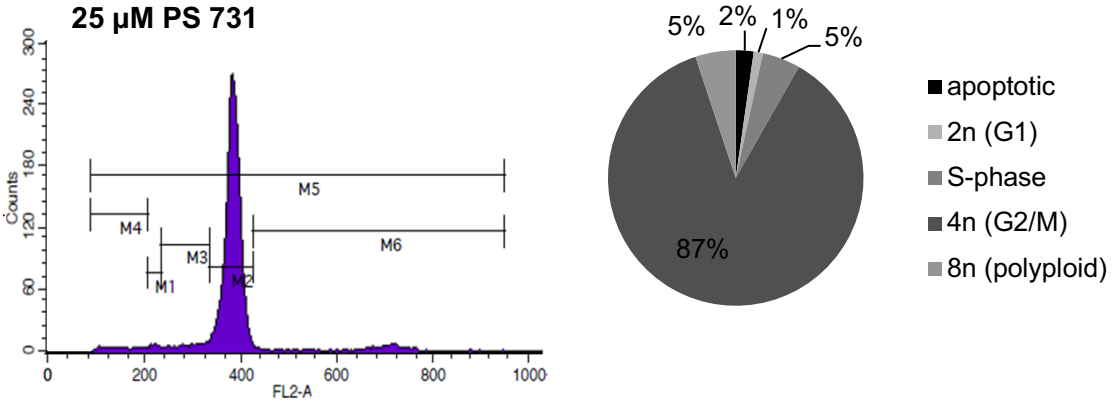

Figure 4.17: Typical Figure of a cell cycle arrest in G2/M caused by PS 731. Cells in G2/M have a chromosome set of 4n. Control compounds MLN 8237 and VX 680 showed the same distribution pattern (see Supplement).

Unfortunately, nearly all of the hit-compounds showed the same distribution pattern as DMSO treated cells meaning that none of them had an effect on the cell cycle and did not produce cell cycle arrest. Repetition of the assay with higher concentrations of 50 µM compound instead of 25 µM did not alter any results. The only exception was Oxymetholone which showed a significant aberration from the control treated with DMSO (Figure 4.18). The high percentage of cells in synthesis is absent, 78% of cells are in G1, only 7% in G2/M and 13% in synthesis. Thus, Oxymetholone arrested cells in G1 phase of the cell cycle.

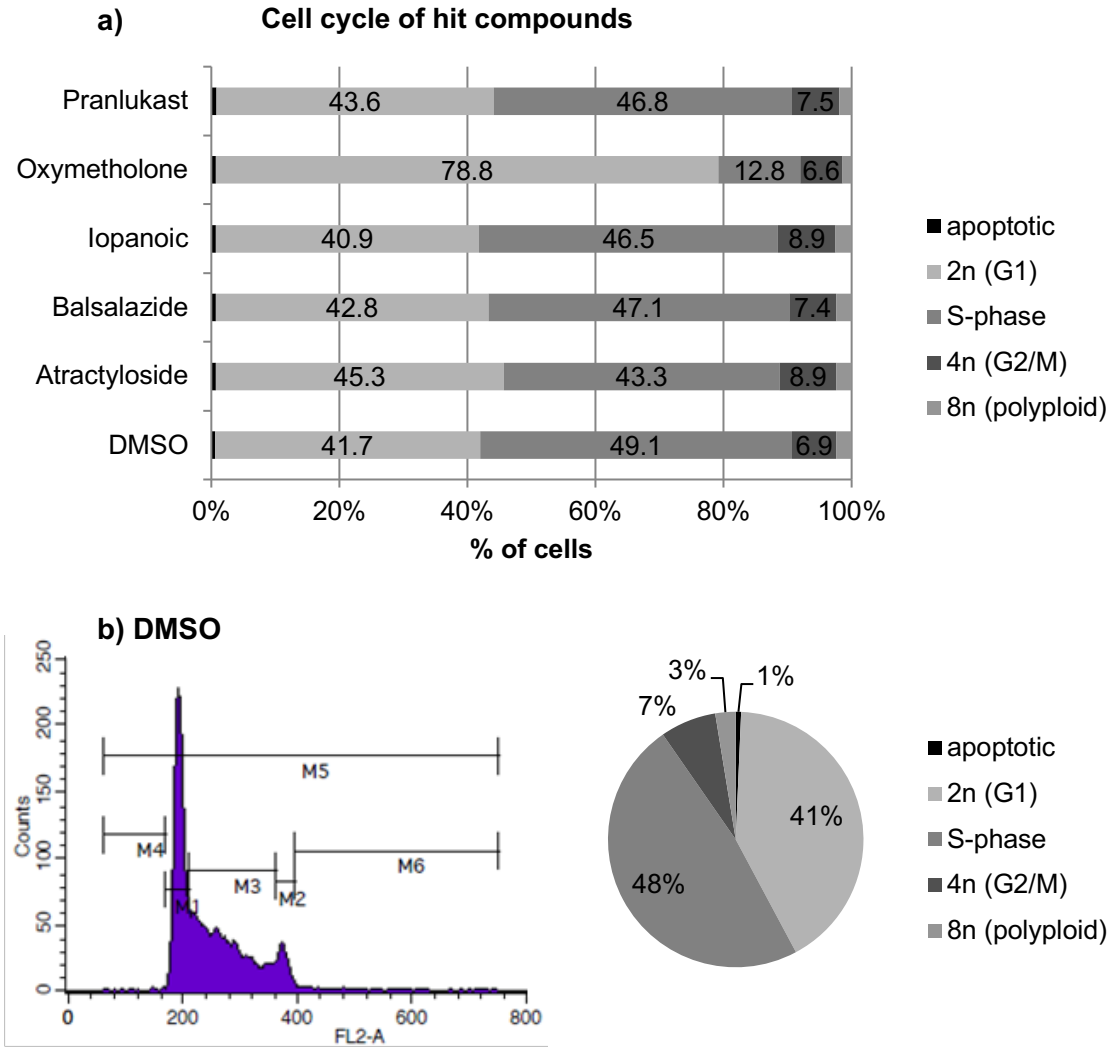

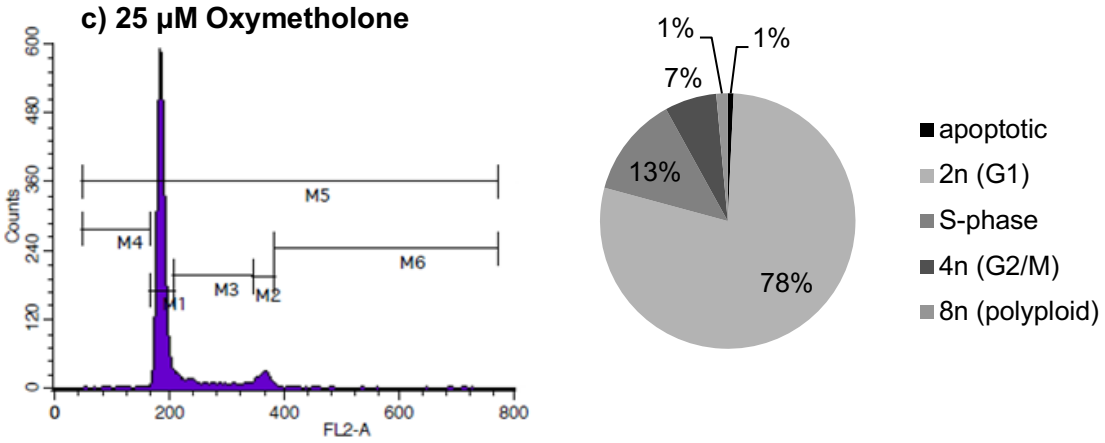

Figure 4.18: a) Cell cycle state of all tested hit-compounds in comparison to DMSO treated cells with nearly half of the cells in G1 phase and half in synthesis. All have the same distribution pattern as DMSO with the exception of Oxymetholone. **b)** Comparison of the FACS analysis of DMSO treated cells and **c)** cells treated with 25 µM Oxymetholone. In the DMSO graph, the shoulder between G1 and G2/M can be explained by the Thymidine treatment for synchronization. This shoulder vanishes in cells treated with Oxymetholone, 78% of the cells remain in G1. A repetition of this assay with 50 µM Oxymetholone showed the same result.

4.9.2 Flow cytometry with additional Nocodazole treatment

In addition, we tested the effect of compounds in another variant of the assay. Instead of the Thymidine treatment, the cells were incubated with the compounds first for 24 h and then treated with Nocodazole for 16 h. This was done mainly to arrest the cells in G2/M and achieve an accumulation of enzymes during this phase of the cell cycle, amongst them AurA. A very similar approach was chosen by Asteriti et al. in their 2017 paper [131]. This way, we hoped to get a clearer view on how especially PS 731 affects AurA and hence more distinct results in the western blots.

For DMSO the flow cytometry showed a peak with 85% in G2/M as expected since Nocodazole arrests the cells and DMSO is not supposed to have any additional effect. The hit-compounds, too, had no effect even with addition of Nocodazole.

Oxymetholone, which before showed an increased number of cells in G1 in comparison to DMSO only, showed no real difference to DMSO when added in combination with Nocodazole. The peak at 4n seems wider for cells treated with

the combination of Oxymetholone and Nocodazole. However, when looked into the numbers only, there is no significant difference.

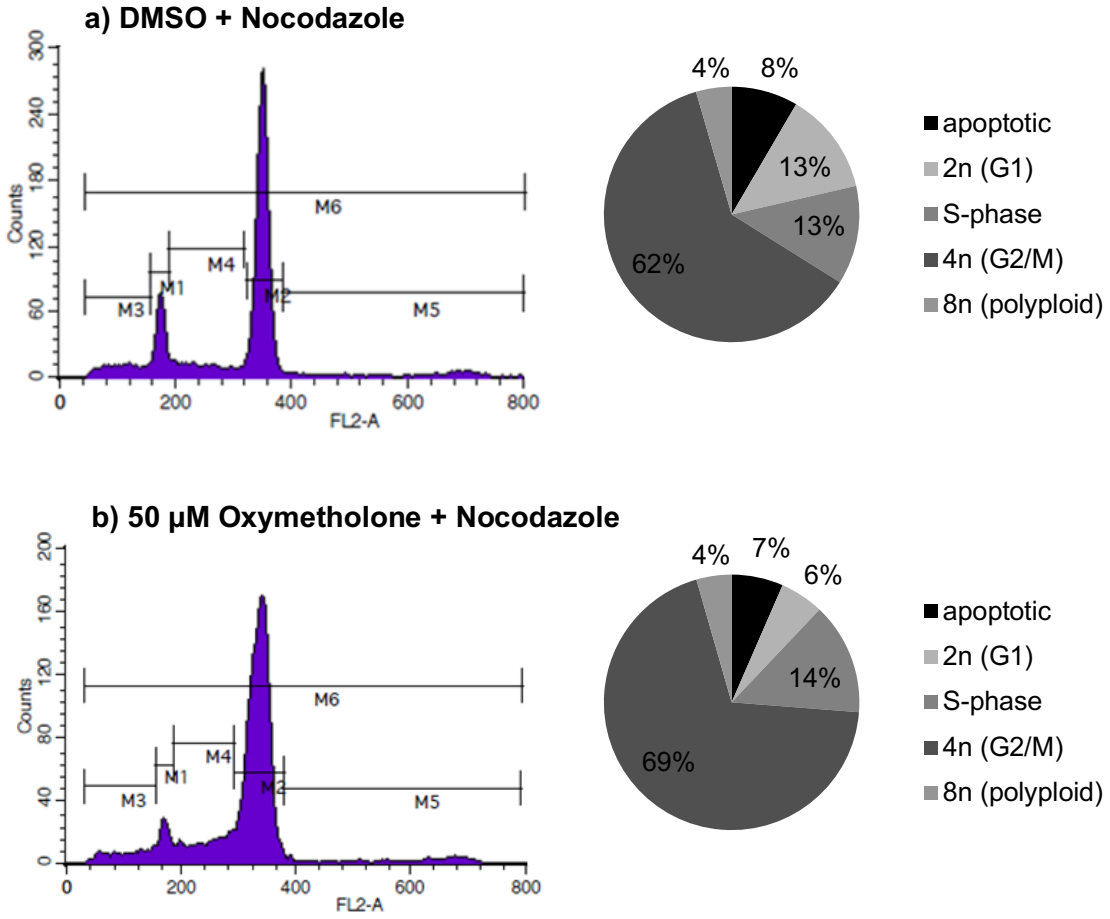

Figure 4.19: a) Cells treated with Nocodazole are arrested in G2/M due to its toxicity to the spindles. **b)** When cells are treated with 50 µM Oxymetholone and Nocodazole, the difference is negligible.

For some of the control compounds, however, we were able to observe mitotic slippage in combination with Nocodazole. In particular, MLN 8237 and AZD 1152 caused a pronounced shift of the genome to 8n. Since this effect is known for combinations of AurB inhibitors and spindle agents it makes sense that AZD 1152, which is an AurB selective inhibitor, and MLN 8237, which targets AurB also at concentrations higher than 1 µM, cause mitotic slippage.

Interestingly, VX 680 that targets Aurora A and B comparably shows no mitotic slippage at 25 µM concentration in combination with Nocodazole. Our compound PS 731 did not produce mitotic slippage. This could be evidence that PS 731 targets AurA selectively.

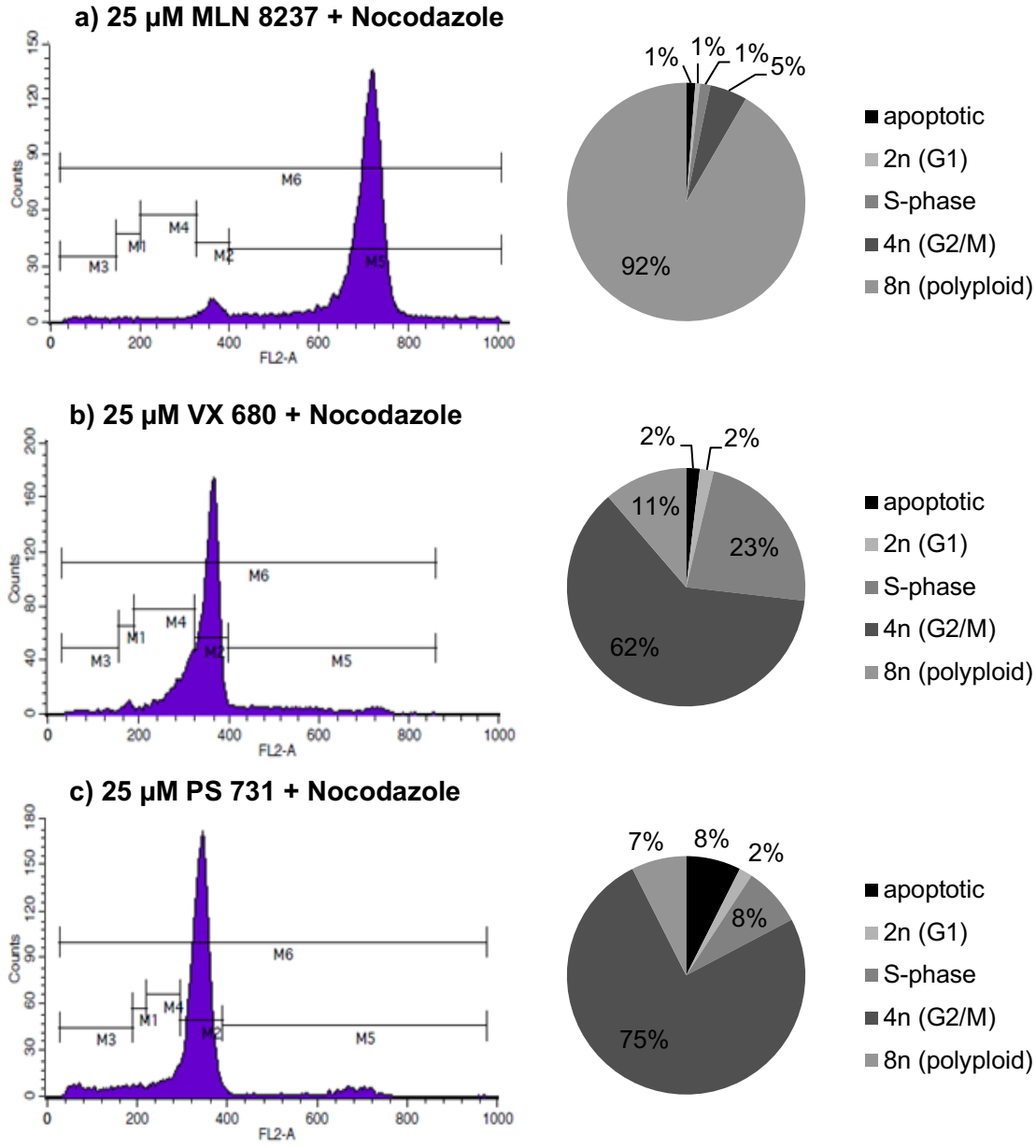

Figure 4.20: Effect of known AurA inhibitors and PS 731 on the cell cycle. 25 µM of **a)** MLN 8237, **b)** VX 680 and **c)** PS 731 with addition of Nocodazole. MLN 8237, which inhibits AurB at concentrations higher than 1 µM, causes mitotic slippage with 92% cells in a polyploid state. Cells treated with VX 680 and Nocodazole remain arrested in G2/M, so are cells treated with PS 731 and Nocodazole.

4.9.3 Effect on downstream signaling (Western blots)

The cells treated for flow cytometry were also examined in western blots. The western blot experiments were performed by Dr. Monika Raab from Prof. Klaus Strebhardt's lab with the cells prepared and harvested according to chapter 3.2.5.

In the western blots, substrates of AurA and marker for cell cycle progression can be traced with specific antibodies. We used antibodies for phosphorylated Aurora Kinase A, B and C as measurement of the kinase activity. Furthermore, we examined the expression of Aurora B and the phosphorylation status of Histone H3 which is a substrate of mainly Aurora B but also Aurora A as marker for entry into mitosis. Additionally, we used an antibody for PLK1 as direct substrate of AurA and a specific antibody for the phosphorylation site of PLK1, Threonin 210 (pT210). Also, the cells were tested for Cyclin B1 which is a regulatory kinase relevant for early mitosis down the AurA-PLK1 pathway.

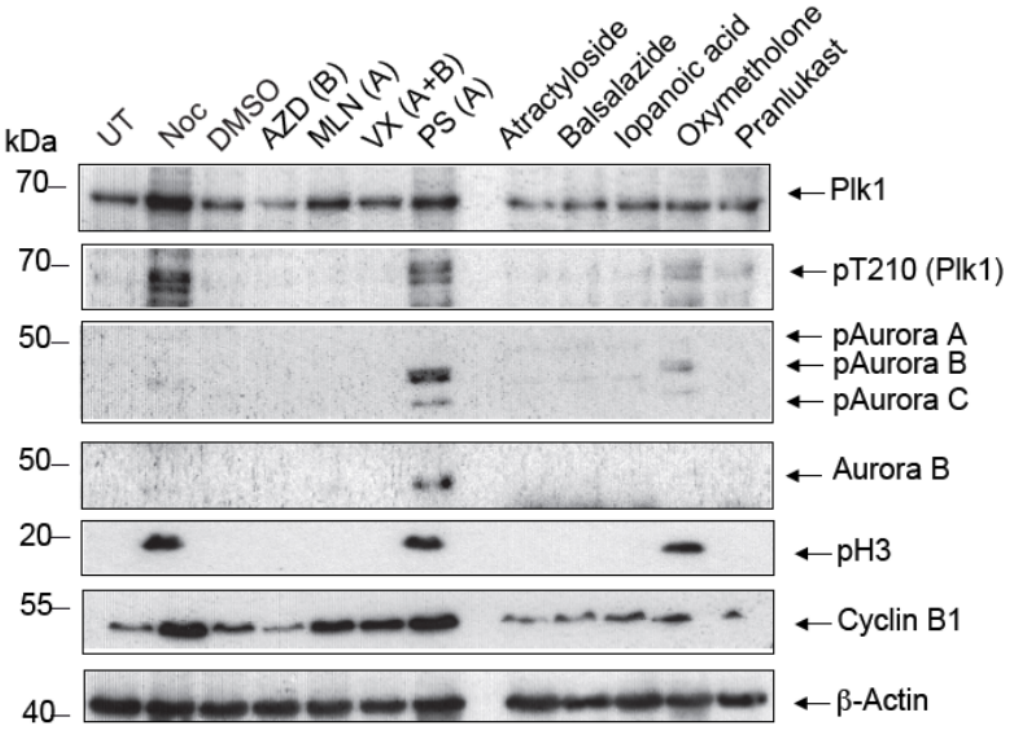

Figure 4.21: Western blot with standard protocol (24h Thymidin, 16h compounds). Antibodies for PLK1 and its phosphorylation site T210, phosphorylated Aurora kinases, amount of Aurora B, its substrate Histone H3 and cell cycle marker Cyclin B1 as well as western blot control β-Actin have been applied. 25 µM of control and hit compounds were used.

Figure 4.21 shows the western blot after synchronization with Thymidin for 24h followed by 16h incubation with the compounds. The first row shows AurA substrate PLK1 which is expressed in every condition tested with higher expression in cells treated with Nocodazole, MLN 8237 and PS 731. Another western blot with two concentrations (1 and 25 µM) of the control compounds

shows that PLK1 expression is dose dependent for PS 731, the more compound the higher the expression (see Supplement). The control drug AZD1152 reduced the levels of PLK1.

A closer look into the active form of PLK1 phosphorylated by AurA in G2 shows an increase in phosphorylation of PLK1 at T210 for Nocodazole, PS 731 and the hit-compound Oxymetholone.

The Aurora kinases A, B and C show a strong (auto)phosphorylation with PS 731. Traces of phosphorylation are visible after Nocodazole and Oxymetholone treatments. Also, Aurora B seems to be only detected in cells treated with PS 731. Correlating with that PS 731 shows a high phosphorylation of Histone H3 (pH3) which is the natural substrate of AurB, but also of AurA. Here PS 731 increases the abundance of pH3. pH3 is well detectable for Nocodazole and Oxymetholone, too (Figure 4.21). This increase in phosphorylation of H3 can be explained by a compensatory increase of AurB [132,133,98]. Because we used concentrations of the control compounds that inhibit AurB as well, we don't observe this effect for MLN8237.

The next row shows Cyclin B1 which functions as a switch for a cell to enter mitosis or not. The hit-compounds show a weak expression of Cyclin B1 correlating with the cells being mostly in G1 phase. Cells treated with MLN 8237, VX 680 and PS 731 express Cyclin B1 in a high amount comparable to Nocodazole with a dose dependence (the more compound, the more Cyclin B1). Only AZD 1152 shows a weaker expression of Cyclin B1, probably due to the fact that more cells have already shifted to 8n and skipped the G2/M phase (Figure 4.21).

The results are consistent with MLN8237, VX680 and AZD1152 inhibiting AurA while PS731 seems not to affect the ability of AurA to phosphorylate Histone H3 and PLK1. Interestingly, Oxymetholone, although having a different chemical structure, produces the same effect as PS731 in the cellular signaling. These compounds affect the signaling but do not inhibit the phosphorylation of all substrates of Aurora kinase. Therefore, we conclude that the cellular effects can be produced without the inhibition of the activity of Aurora kinase A.

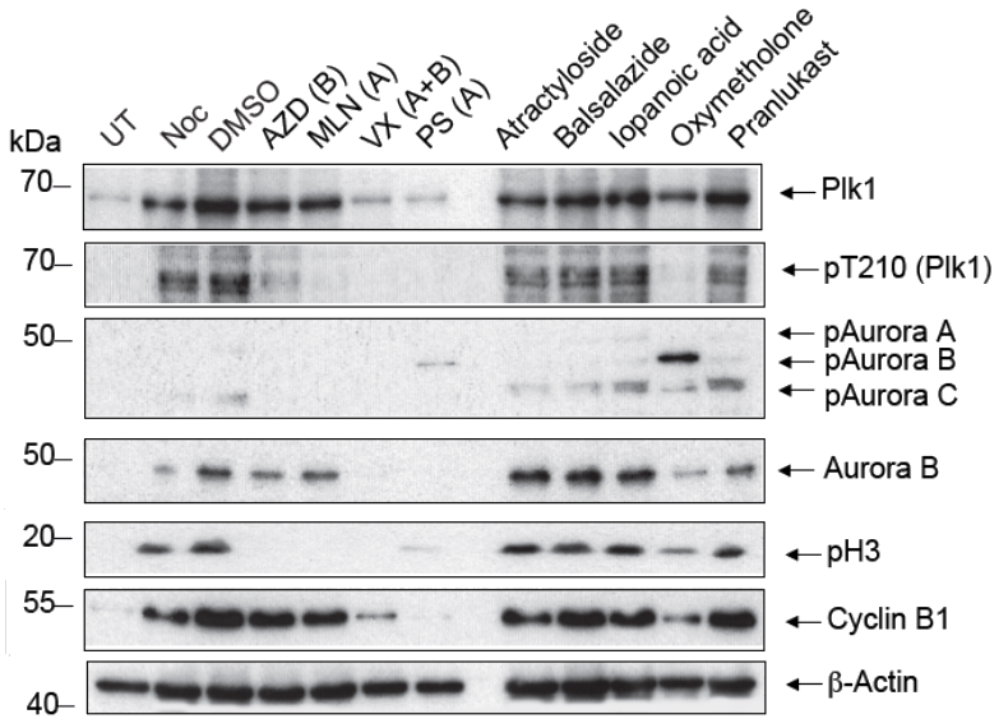

Figure 4.22: Western blot with modified protocol (24h compounds, 16h Nocodazole). Antibodies for PLK1 and its phosphorylation site T210, phosphorylated Aurora kinases, amount of Aurora B, its substrate Histone H3 and cell cycle marker Cyclin B1 as well as western blot control β-Actin have been applied.

The studies were also performed with a modified protocol where the cells were first incubated with the compounds and then treated with Nocodazole to guarantee a cell cycle arrest (Figure 4.22).

With the additional Nocodazole treatment PLK1 accumulates in every cell. Interestingly, PLK1 is not as highly expressed under treatment with VX 680, PS 731 and Oxymetholone. When it comes to its phosphorylation status no phosphorylation is detectable under treatment with MLN 8237, VX 680, PS 731 and also the hit-compound Oxymetholone. This means that the phosphorylation of PLK1 is impaired although AurA enzymatic activity is not inhibited by the compounds.

Under treatment with Nocodazole and the accompanying cell cycle arrest Aurora B is now detectable in almost every probe. Exceptions are VX 680, PS 731 and Oxymetholone where no or less (Oxymetholone) AurB is visible. Correlating with the expression of AurB there is now phosphorylated Histone H3 traceable for the hit-compounds. For the controls AZD 1152, MLN 8237, VX 680

and PS 731 there is almost no pH3 detectable although AurB seems to be expressed. This effect seems to be dose dependent since in a repetition there was still phosphorylation of Histone H3 visible under treatment with 1 µM PS 731 but not anymore with 25 µM. Same applies for AZD 1152 which already is a known AurB inhibitor. Also, Oxymetholone shows less pH3 than DMSO+ Nocodazole or the other hit-compounds, correlating with less expression of AurB in spite of Nocodazole treatment.

Since Cyclin B1 is a marker for mitosis and Nocodazole arrests the cells in G2/M, most of the samples show high expression levels of Cyclin B1, even MLN 8237 and AZD1152 although a high percentage of the cells have slipped to 8n. Exceptions are VX 680, PS 731 and Oxymetholone. Maybe VX 680 and PS 731 inhibit part of a pathway of Aurora A or B that MLN 8237 or AZD 1152 don't touch. This effect is dose dependent since Cyclin B1 is expressed more with lower concentrations of VX 680 and PS 731. Oxymetholone shows less Cyclin B1 than the other hit-compounds.

5. Discussion

The experiments performed for this thesis were started in summer 2014. Until then, little information on allosteric inhibition of Aurora kinase A was available. In the meantime, in 2016 and 2017 before this thesis was written, a few papers with new research data have been published about allosteric modulation of Aurora kinase A and small molecule allosteric inhibitors. Here, the results of this thesis shall be discussed in reference to that new data.

5.1 Summary

This thesis aimed to identify potential inhibitors of Aurora A, which would help us to understand the molecular mechanisms of the regulation of AurA. In addition, by screening a library of FDA-approved drugs, the approach could potentially identify known drugs for fast track into clinical use for a different purpose. Our screening approach was chosen to identify compounds with a novel mode of action, targeting an allosteric interaction of AurA and its binding partner TPX2. In the first part of the thesis I screened a library of 1280 compounds, from where I confirmed and validated six compounds that

specifically interact with AurA and displace the interaction from TPX2 *in vitro*: Atractyloside, Balsalazide, Iopanoic acid, Pranlukast Oxymetholone and Tiratricol. All compounds displaced TPX2 from Aurora A with an IC50 in a low to medium µM range. However, only two compounds, Iopanoic acid and Tiratricol, showed also an impact on the activity of Aurora A, indicating different mechanisms of interaction between the compounds and the protein. Testing the compounds in cell culture was the next step to assess the effectiveness of the compounds on Aurora A *in vivo*. Only Oxymetholone showed a specific effect on the cell cycle. Notably, the effect of Oxymetholone was similar to the effects observed with PS731, a compound that our group had identified in a previous screening.

A very important side-product of our *in vitro* characterizations was the findings about the effects of known ATP-binding site inhibitors on the interaction with TPX2. Indeed, we surprisingly found that MLN8237 is a very potent inhibitor of the interaction between AurA and TPX2. This finding parallels the “reverse allosteric” effects found by our group on the protein kinase PDK1 [44].

This thesis presents two important concepts for AurA drug discovery:

1. Small compounds binding at a site different from the ATP-binding site can be potent functional inhibitors of AurA, even if they don’t inhibit the protein kinase activity of AurA.
2. Drugs binding at the ATP-binding site of AurA can produce strong effects on the formation of multi-protein complexes. The “reverse allosteric” effects are dependent on the chemical structure of the inhibitor.

Therefore, this thesis highlights the importance of the “reverse allosteric” effects along the drug development process directed to the ATP-binding site. Together, our findings are potentially important for the discovery and development of truly allosteric drugs directed to protein kinases.

5.2 Discussion of results

For this thesis, a short discussion of the methodical part is necessary. Additionally, the results of the hit compounds and all other experiments shall be interpreted and the significance evaluated.

5.2.1 Evaluation of the overall approach for the identification and characterization of novel allosteric inhibitors of AurA

In the screening process all compounds of the FDA approved drugs library were tested in singlicates for effect on the binding of TPX2 and AurA. Selected hits were then tested in duplicates afterwards to eliminate false positives und confirm real hits. Any false negatives, however, could not have been identified. This is a minor limitation to our screening approach; however, when performing high-throughput screenings, some limitations have to be accepted to maintain a certain efficiency at a still high sensitivity.

We then followed a path through different *in vitro* characterizations to finally identify a group of compounds that are active *in vivo* by interaction with AurA. The following *in vivo* studies enabled us to conclude that two compounds identified in two screenings performed in our laboratory are indeed active in cell culture, one of them inhibiting AurA function without inhibiting AurA kinase activity in the cellular context. So far, the path chosen for the identification and characterization of hit-compounds was successful.

In contrast, a major drawback of the overall approach was the difficulty to identify the precise binding site of the different compounds. Indeed, the crystallography of proteins in complex with allosteric inhibitors is even more challenging than the crystallography of the protein alone, because the compounds stabilize alternative conformations of the kinase. Without the definite binding site, the interaction mode can hardly be determined accurately. As a consequence, this lack of information hampers the rational-design approach to improve the characteristics of the compounds.

Notably, in spite of the above failure to depict the binding site of the compounds, the recent published work by others provides enough information to conclude that PS 731 binds to the site equivalent to the PIF-pocket in Aurora kinase (see below).

5.2.2 Evaluation of the identified hit-compounds

We have already proven the interaction of the hit-compounds with Aurora A in our screening and the determination of IC50s in displacing TPX2. To further characterize the compounds, a kinase activity assay was done to evaluate the

impact of the compounds on the activity of the kinase. Interestingly, only Iopanoic acid and Tiratricol inhibited the activity of Aurora A. Atractyloside, Balsalazide and Pranlukast inhibited only a little, while Oxymetholone had no effect on the activity.

Having a closer look at Iopanoic acid and Tiratricol, the results for both compounds are significant. Both are similar in their chemical structure in having iodine side chains (for chemical structure, see Supplement) and, additionally to inhibiting AurA activity, both achieve high stabilization in thermal stability assay. Stabilization of a protein in presence of a compound gives a strong hint that the compound indeed binds to the protein and therefore stabilizes it [134]. Iopanoic acid and Tiratricol showed the highest deltas in melting points amongst all other compounds identified by our group. Atractyloside also stabilized, whereas Balsalazide, Pranlukast and Oxymetholone had low but significant stabilization effects on Aurora A. Thus, the assay helped us to confirm that the compounds indeed target Aurora A. An overview of all effects is given in Table 5.1.

Compound	IC50 (with Top=100%, Bottom=0%)	Activity assay	Thermal stablity	MST	48h viability assay	Cell cycle
Atractyloside	3.1 µM	EC50=4.6 µM	4 °C	300 µM	less viable	no effect
Balsalazide	7.3 µM	ambiguous	1.8 °C	-	less viable	no effect
Erlotinib	16.7 µM	solubility issues	-	-	-	-
Iopanoic acid	37.2 µM	EC50=10 µM, IC50=18.3 µM	6.9 °C	478 µM	less viable	no effect
Liothyronine	26.0 µM	solubility issues	-	-	-	-
Oxymetholone	86.0 µM	little effect	0.5 °C	52 µM	less viable	small but significant effect*
Pranlukast	28.6 µM	EC50=15.2 µM	0.4 °C	-	less viable	no effect
Tiratricol	24.4 µM	EC50=13.5 µM, IC50=14.0 µM	12 °C	36 µM	no effect	-
PS731	5.4 µM	4.4 µM	10 °C	126.8 µM	less viable	G2/M arrest

** The effect could have been considered "doubtful" but was validated by having a similar result with PS731.*

Table 5.1: Summary and comparison of all compounds identified in this screening and the control PS731.

In the *in vivo* assays, however, Iopanoic acid and Tiratricol did not produce effects on AurA. That kind of result would be consistent with compounds that bind to the ATP-binding site. The suggestion is that in cells, where the concentration of ATP is physiologically high (1-5 mM), the compounds would have to compete against ATP for the binding site, in consequence requiring higher affinity to achieve effects in cells. Continuing on this thread and applying our results, our compounds could bind to the ATP-binding site and displace TPX2 from its distant site, thus acting by a "reverse allosteric" effect. We showed in this thesis that known Aurora inhibitor MLN8237 works by displacing TPX2 whilst binding to the ATP site.

In the cell cycle assays, Oxymetholone is the only hit-compound that shows some impact. However, it does not cause a cell cycle arrest as expected with inhibition of Aurora A but an arrest in G1, as it seems. In the past, cell cycle arrest in G1 has been described for dihydrotestosterone, of which Oxymetholone is a derivative [135].

Interestingly, in spite of the phenotypic G1 arrest, Oxymetholone shows the same pattern of effects in signaling in the western blots as PS731. Together, these two compounds affect AurA downstream signaling by a mechanism different to the mechanism of action of the traditional inhibitors of AurA.

The results observed in the presence or absence of Nocodazole in the case of PS731 are also different from the other inhibitors of AurA used as control. It is noteworthy that those results are resembled by Oxymetholone. Since both compounds have a very different chemical structure, it is tempting to speculate that the observed effects are due to their targeting of AurA. Of note, PS731 differed from Oxymetholone in that Oxymetholone did not inhibit AurA activity in the kinase activity assay. Since Oxymetholone did not inhibit AurA, it is tempting to speculate that the effects observed by PS731 and Oxymetholone are not due to the direct inhibition of AurA kinase activity but due to their common displacement of TPX2. In line with this, both compounds do not inhibit histone H3 and also show phosphorylation of PLK1 at T210, indicating that, in cells, the compounds do not inhibit the kinase catalytic activity of AurA. Therefore, we speculate that the effect is not due to the direct inhibition of the activity of AurA and must be due to their common effect on the displacement of TPX2 from

AurA. It must be therefore concluded that the inhibition of the physiological function of AurA can be achieved without inhibition of its kinase activity. The sole displacement from its proper location provided by TPX2 must therefore physiologically inactivate the displaced AurA molecules.

It was of major interest to define the binding site of the compounds that we identified to displace the interaction with TPX2. Our laboratory followed the approach to attempt the crystallization of AurA in complex with the different compounds. Our laboratory obtained crystals of AurA in two different crystal packings but unfortunately, we were unable to obtain the structure of the complex with our novel compounds. Based on our own data, we can cannot be certain about the binding site of the different compounds. However, the finding that Oxymetholone does not inhibit the kinase activity of AurA *in vitro* suggests that the binding site of this compound cannot be the ATP-binding site.

5.3 Discussion of the current state of knowledge

During the time that this thesis was written, a number of related papers about allosteric inhibitors of Aurora kinase A were published.

5.3.1 Recent publications on allosteric inhibition of Aurora A

Burgess et al. were the first to publish a paper on allosteric inhibitors of AurA [136]. They discovered a single domain antibody to Aurora's allosteric site, that is equivalent to the PIF pocket in AGC kinases. They confirmed the antibody to bind to Aurora´s allosteric site by obtaining crystal structures and showed inhibition of the kinase in a low micromolar range. However, the antibody is a mere proof that allosteric inhibition of AurA is possible in vitro, but it is no useful tool in cell-based assays because of too low affinity. The findings with a single domain antibody, on the other hand, do not ensure that small compounds could also produce the allosteric inhibition.

Janeček et al. performed a high-throughput screening of 14000 small molecules to find an allosteric inhibitor of the protein-protein interaction of AurA and TPX2[137] (similar to our screening). They identified the compound AurkinA that binds to the PIF-pocket of AurA, or Y-pocket as they named it. They also suggest a general approach to allosteric inhibition for other kinases on the

example of PDK1 as we already stated in our 2015 paper [44]. AurkinA was thus the first small molecule compound to be described in complex with AurA in a crystal structure, proving that it is possible to target AurA allosterically.

Another approach was chosen by Asteriti et al. [131]. They used a virtual screening process to identify allosteric inhibitors of the AurA-TPX2 complex targeting the residues of the binding site 160-200 on AurA (the Y-pocket), where residues 7-11 of TPX2 dock. Results suggested that inhibitors might have a certain chemical structure including two aromatic rings corresponding to Tyrosine residues of TPX2 at position 8 and 10 that fit the Aurora scaffold. Out of the in-silico screening four hits were verified by FastStep Surface Plasmon Resonance (SPR) experiments to affect the binding of Aurora A and TPX2. When tested in cells at a concentration of 10 µM, two of them produced the expected image of AurA inhibition in fluorescence microscopy and also showed reduced AurA activity in western blots. However, only a predicted binding mode is shown, but no crystal structure could be obtained.

In the publication, Asteriti et al. claim that MLN8237 does not affect the binding of TPX2 to the Y-pocket [131]. The statement contradicts the results I obtained with MLN8237. In my hands, MLN8237 clearly displaces TPX2 in AlphaScreen assay[44]. In addition, it is curious that Asteriti et al. found that MLN8237 had Kd of only 40 nM while the affinity of MLN8237 for AurA was estimated by others tobe 1000 times higher (40 pM)[138]. One possible explanation for the discrepancy with Asteriti et al. could be due to the differences in the assays. While I preincubated MLN8237 with AurA (the total incubation time of MLN8237 with AurA was 90 m), Asteriti et al. injected the compound together with GST-TPX2 (1-43) and tested the interaction of TPX2 with AurA during the time of injection into the to a surface-plasmon resonance chip where AurA was coated (up to 200 s). Thus, it is tempting to speculate that MLN8237 may be a tight-binder (and slow-binder) and that MLN8237 did not reach equilibrium with AurA in the experiments by Asteriti et al.

A review on allosteric inhibitors published by Panicker et al. [139] in 2017 highlighted all efforts in drug discoveries on Aurora in the last years. They also suggest high throughput screenings with structure activity relationship (SAR) as probably the best approach to identify suitable agents for the allosteric inhibition

of Aurora kinases. Besides, other approaches on how to identify allosteric inhibitors of AurA are named, e.g. 3D ligand-based Virtual Sreening [140] or a fragment-based approach or SERS= surface enhanced Raman spectroscopy [141].

5.3.2 Our identified compounds in the context of recent publications

So far, PS 731 has been the most promising compound identified in screenings by our group. Derivatives of the compound did not displace TPX2 in AlphaScreen assay, but three of them (PS 878, 870 and 882) inhibited activity in the kinase activity assay, although not as potently as PS 731. However, so far no crystal structures could have been obtained of Aurora A and PS 731, so the definite binding site of the compound remains unknown. Interestingly however, the compound published by Janeček in 2016 called AurkinA[137] has striking similarities with the chemical formula of PS 731. AurkinA has been shown to affect the protein-protein interaction between AurA and TPX2 in a fluorescence anisotropy assay and inhibits AurA with a K_i=3.7 µM, which is in the same range as PS 731. Janeček et al. were able to obtain crystal structures with AurkinA[137], proving that AurkinA binds to the TPX2 binding site or Y-pocket, the equivalent site of the PIF-pocket in AGC kinases, which our group has historically targeted with allosteric compounds [125–127,142].

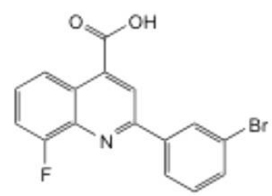	AurkinA	Inhibits AurA and displaces TPX2
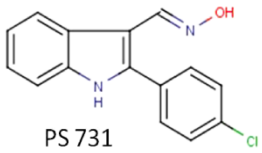 PS 731	PS 731	Inhibits AurA and displaces TPX2
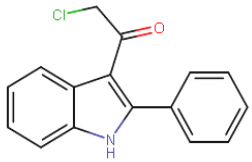	PS 878	Inhibits AurA
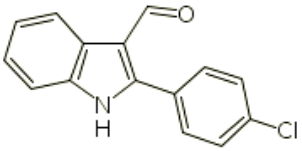	PS 877	No effect
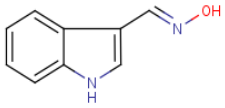	PS 882	Inhibits AurA

Table 5.2: Chemical structures of AurkinA, PS 731 and its derivatives. PS731 has three functional groups, the indole ring, the chlorophenyl group and the side chain, the acetaldehyde oxime. PS876, lacking the oxime group is completely inactive, indicating that this side chaine is a key feature in PS731 to achieve the inhibition of activity and the inhibition of the interaction with TPX2. On the other hand, PS882, lacking the chlorophenyl group, is quite a good inhibitor of AurA activity but lacks the ability to displace the interaction between AurA and TPX2.

The similarities between AurkinA and PS 731 would also suggest that the indole ring of PS 731 and the quinolone ring of AurkinA would occupy a similar site while the chlorophenyl group of PS 731 could occupy the site of the bromobenzene group in AurkinA. The resemblance of PS 731 to AurkinA together with other evidence strongly suggests that PS 731 also binds to the the TPX2 binding site (the PIF-pocket on AurA).

In 2003, Conti, Bayliss et al. claimed in a patent that there are small molecule compounds derived from indoles and indenes that target the Y-pocket of AurA,

but couldn't obtain crystals of their computationally designed compounds[143]. Asteriti et al. suggested in their publication that compounds would need two aromatic rings to fit the Y-pocket[131]. Both demands apply to PS 731 and AurkinA.

Interestingly, AurkinA possesses a carboxylate group, which adds a hydrophilic property to the molecule and is thus expected to reduce the permeability into cells. In this respect, PS 731 appears as a more superior compound for in vivo studies. Indeed, Janeček et al. show complete effect on the mislocalization of AurA from the spindle at 400 µM, at a much higher concentration than in the in vitro assay [137]. For PS 731 we observed a complete cell cycle arrest at a concentration of 25 µM. Thus, while the two compounds appear to have similar IC50s in vitro, our compound appears to be more than ten times more potent in cells.

Considering the chemical formulae of AurkinA, PS 731 and its derivatives, the effect of the different compounds on the inhibition of the AurA-TPX2 interaction and on the inhibition of AurA activity, we can build a simple structure-activity relationship (SAR). It is interesting that the modification of the chlorophenyl group or the side chain produce compounds that do not inhibit the interaction. The data thus shows a very high specific requirements for the inhibition of the interaction.

It is quite possible that PS878, PS879 and PS882 bind with less affinity than PS 731. In the absence of TPX2, as in the activity assay, they would not have to compete with TPX2 for the binding site, producing an allosteric inhibitory effect. We also tested the compounds in the activity assay in presence of TPX2, resulting in a weaker effect on Aurora A. Thus, it is possible that the lack of displacement of TPX2 from AurA by PS878, PS879 and PS882 could just be due to their lower affinities for AurA.

In defiance of all the evidence, PS731 may of course bind to the ATP-binding site and allosterically displace the interaction with TPX2; in such scenarios, PS878, PS879 and PS882 would bind to the ATP-binding site as well, compete with ATP for the site and inhibit the kinase activity, but may not generate the “reverse allosteric” effect.

5.4 Conclusion and outlook

Summa summarum, this thesis confirms theories on allosteric inhibitors to be a valuable target for continuing drug research on Aurora kinase [139]. We have shown with this thesis that no FDA approved drug in our library could directly be used off-label for inhibiting Aurora kinase A or put into fast track drug development. On the other hand, PS 731 remains highly interesting since recent publications have shown a compound with very similar chemical formula bound to the TPX2 binding site (Y-pocket) of AurA in crystal structure [137].

Reviews of current ATP-competitive Aurora inhibitors in clinical trials pointed out rather modest results because of high bone marrow toxicity [144]. Also, outcome on MLN8237 in clinical trials - so far the most potent Aurora A inhibitor in vitro- was not as promising as expected [145,146]. In general, growth rate of solid tumors might be too slow for Aurora kinase inhibitors to really work before adverse effects on hematopoesis become unbearable for patients. In turn, MLN8237 has been shown to support the efficacy of temozolomide and radiation therapy in high grade glioblastoma in vitro [147]. In blood cancers, efficacy was better, possibly because of higher cell turnover rate [148].

Another problem with ATP-competitive Aurora inhibitors is their incomplete specificity. Even MLN8237 affects Aurora B in higher concentrations [73] and has been shown to induce polyploidy overdriving the mitotic cell cycle checkpoint [149]. Mitotic slippage can be a driving factor of tumorigenesis [150] in turn and cause secondary malignancies in patients treated with an unspecific Aurora inhibitor. If that effect applies for allosteric inhibitors as well, is so far unknown. Results presented in this thesis indicate that allosteric inhibitors with a mode of action like PS 731 may not be a cause for aneuploidy in treated cells.

Some Aurora kinase inhibitors were discovered to simultaneously target other oncogenic mutations, for example FLT3 in Acute Myeloid Leukemia [151]. Aurora kinase inhibitors with dual efficacy on Aurora and FLT3, e.g. AZD1152 [14] or CCT137690 [152,153], were shown to have better results regarding outcome and resistance. The next interesting target is therefore PLK1, a downstream Serine/Threonine kinase activated by Aurora A [154]. Selectively inhibiting both the Aurora and PLK1 pathway may result in a more effective cell cycle arrest[155].

Numerous ATP-competitive inhibitors of PLK1 have been developed throughout the years by the pharmaceutical industry [156], while our laboratory has recently described allosteric inhibition of PLK1 [157]. The availability of allosteric inhibitors may be of use in patient therapies due to their higher selectivity and lower side effects, or by their different effects in cells and patients. The availability of more selective inhibitors in the available toolbox of approved drugs may also enable better combination therapies.

Another approach would be the combination of allosteric and ATP-competitive inhibitors to control resistance to the latter. This approach has been proven highly efficient in the example of BCR-ABL1 Tyrosine kinase inhibitor nilotinib, which combined with the new allosteric inhibitor Asciminib (ABL001) could completely control CLL in mice [158].

Besides hematologic malignancies, another possible target for future Aurora A inhibitors would be Neuroblastoma because of Aurora's stabilizing effect on N-myc. Although MLN8237 has not been proven efficient in this area of application, Aurora inhibitor CD532 has shown promising results in the destabilization of N-myc in Neuroblastoma cells [98], leaving the door open for further studies with Aurora A inhibitors in this indication. It is not fully clear if the displacement of TPX2 would also directly affect the stabilization of N-myc. It would be interesting to confirm that CD532 also inhibits the interaction of AurA with TPX2 and investigate if PS 731 also destabilizes N-myc.

In conclusion, the future of Aurora kinase inhibitors and their implementation in standard patient treatment protocols is uncertain. For the past fifteen years it has been subject of countless trials and reviews, but so far, no major breakthrough has been achieved. Therefore the question arises, if Aurora kinase inhibitors continue to exist next to its successful relatives, the Tyrosine kinase inhibitors. Most probable, the future of Aurora kinase inhibitors lies in the development of highly specific drugs, to be employed in combination therapy with other selective kinase inhibitors or inhibitors of oncogenic drivers.

6. References

1. Manning G, Whyte DB, Martinez R, Hunter T, Sudarsanam S. The protein kinase complement of the human genome. *Science*. 2002;298(5600):1912-1934. doi:10.1126/science.1075762.
2. Cheetham GMT, Knegtel RMA, Coll JT, et al. Crystal structure of aurora-2, an oncogenic serine/threonine kinase. *J Biol Chem*. 2002;277(45):42419-42422. doi:10.1074/jbc.C200426200.
3. Kollareddy M, Zheleva D, Dzubak P, Brahmkshatriya PS, Lepsik M, Hajduch M. Aurora kinase inhibitors: progress towards the clinic. *Invest New Drugs*. 2012;30(6):2411-2432. doi:10.1007/s10637-012-9798-6.
4. Wang Y, Ji P, Liu J, Broaddus RR, Xue F, Zhang W. Centrosome-associated regulators of the G(2)/M checkpoint as targets for cancer therapy. *Mol Cancer*. 2009;8:8. doi:10.1186/1476-4598-8-8.
5. Lens SMA, Voest EE, Medema RH. Shared and separate functions of polo-like kinases and aurora kinases in cancer. *Nat Rev Cancer*. 2010;10(12):825-841. doi:10.1038/nrc2964.
6. Asteriti IA, Mattia F de, Guarguaglini G. Cross-Talk between AURKA and Plk1 in Mitotic Entry and Spindle Assembly. *Front Oncol*. 2015;5:283. doi:10.3389/fonc.2015.00283.
7. Barr AR, Gergely F. Aurora-A: the maker and breaker of spindle poles. *J Cell Sci*. 2007;120(Pt 17):2987-2996. doi:10.1242/jcs.013136.
8. Mukherjee S. *The emperor of all maladies: A biography of cancer.* Scribner export ed. New York: Scribner; 2010. http://www.loc.gov/catdir/enhancements/fy1107/2010024114-b.html.
9. Cancer Statistics. https://www.cancer.gov/about-cancer/understanding/statistics. Accessed July 27, 2018.
10. Bray F, Jemal A, Grey N, Ferlay J, Forman D. Global cancer transitions according to the Human Development Index (2008-2030): a population-based study. *Lancet Oncol*. 2012;13(8):790-801. doi:10.1016/S1470-2045(12)70211-5.
11. Saiyed MM, Ong PS, Chew L. Off-label drug use in oncology: A systematic review of literature. *J Clin Pharm Ther*. 2017;42(3):251-258. doi:10.1111/jcpt.12507.

12. Linardopoulos S, Blagg J. Aurora kinase inhibition: A new light in the sky? *J Med Chem*. 2015;58(13):5186-5188. doi:10.1021/acs.jmedchem.5b00918.
13. Frödin M, Antal TL, Dümmler BA, et al. A phosphoserine/threonine-binding pocket in AGC kinases and PDK1 mediates activation by hydrophobic motif phosphorylation. *EMBO J*. 2002;21(20):5396-5407.
14. Bayliss R, Sardon T, Vernos I, Conti E. Structural basis of Aurora-A activation by TPX2 at the mitotic spindle. *Mol Cell*. 2003;12(4):851-862.
15. Biondi RM, Komander D, Thomas CC, et al. High resolution crystal structure of the human PDK1 catalytic domain defines the regulatory phosphopeptide docking site. *EMBO J*. 2002;21(16):4219-4228.
16. Eyers PA, Erikson E, Chen LG, Maller JL. A novel mechanism for activation of the protein kinase Aurora A. *Curr Biol*. 2003;13(8):691-697.
17. Capra M, Nuciforo PG, Confalonieri S, et al. Frequent alterations in the expression of serine/threonine kinases in human cancers. *Cancer Res*. 2006;66(16):8147-8154. doi:10.1158/0008-5472.CAN-05-3489.
18. Bolanos-Garcia VM. Aurora kinases. *Int J Biochem Cell Biol*. 2005;37(8):1572-1577. doi:10.1016/j.biocel.2005.02.021.
19. Castro A, Arlot-Bonnemains Y, Vigneron S, Labbé J-C, Prigent C, Lorca T. APC/Fizzy-Related targets Aurora-A kinase for proteolysis. *EMBO Rep*. 2002;3(5):457-462. doi:10.1093/embo-reports/kvf095.
20. Carmena M, Earnshaw WC. The cellular geography of aurora kinases. *Nat Rev Mol Cell Biol*. 2003;4(11):842-854. doi:10.1038/nrm1245.
21. Marumoto T, Honda S, Hara T, et al. Aurora-A kinase maintains the fidelity of early and late mitotic events in HeLa cells. *J Biol Chem*. 2003;278(51):51786-51795. doi:10.1074/jbc.M306275200.
22. Portier N, Audhya A, Maddox PS, et al. A microtubule-independent role for centrosomes and aurora a in nuclear envelope breakdown. *Developmental Cell*. 2007;12(4):515-529. doi:10.1016/j.devcel.2007.01.019.
23. Ke YW, Dou Z, Zhang J, Yao XB. Function and regulation of Aurora/Ipl1p kinase family in cell division. *Cell Res*. 2003;13(2):69-81. doi:10.1038/sj.cr.7290152.
24. Littlepage LE, Ruderman JV. Identification of a new APC/C recognition domain, the A box, which is required for the Cdh1-dependent destruction of

the kinase Aurora-A during mitotic exit. *Genes Dev*. 2002;16(17):2274-2285. doi:10.1101/gad.1007302.

25. Tavernier N, Panbianco C, Gotta M, Pintard L. Cdk1 plays matchmaker for the Polo-like kinase and its activator SPAT-1/Bora. *Cell Cycle*. 2015;14(15):2394-2398. doi:10.1080/15384101.2015.1053673.
26. Andrews PD. Aurora kinases: shining lights on the therapeutic horizon? *Oncogene*. 2005;24(32):5005-5015. doi:10.1038/sj.onc.1208752.
27. Li X, Sakashita G, Matsuzaki H, et al. Direct association with inner centromere protein (INCENP) activates the novel chromosomal passenger protein, Aurora-C. *J Biol Chem*. 2004;279(45):47201-47211. doi:10.1074/jbc.M403029200.
28. Goto H, Yasui Y, Nigg EA, Inagaki M. Aurora-B phosphorylates Histone H3 at serine28 with regard to the mitotic chromosome condensation. *Genes Cells*. 2002;7(1):11-17.
29. Marumoto T, Zhang D, Saya H. Aurora-A - a guardian of poles. *Nat Rev Cancer*. 2005;5(1):42-50. doi:10.1038/nrc1526.
30. Sasai K, Katayama H, Stenoien DL, et al. Aurora-C kinase is a novel chromosomal passenger protein that can complement Aurora-B kinase function in mitotic cells. *Cell Motil Cytoskeleton*. 2004;59(4):249-263. doi:10.1002/cm.20039.
31. Kimura M, Matsuda Y, Yoshioka T, Okano Y. Cell cycle-dependent expression and centrosome localization of a third human aurora/Ipl1-related protein kinase, AIK3. *J Biol Chem*. 1999;274(11):7334-7340.
32. Littlepage LE, Wu H, Andresson T, Deanehan JK, Amundadottir LT, Ruderman JV. Identification of phosphorylated residues that affect the activity of the mitotic kinase Aurora-A. *Proc Natl Acad Sci U S A*. 2002;99(24):15440-15445. doi:10.1073/pnas.202606599.
33. van Horn RD, Chu S, Fan L, et al. Cdk1 activity is required for mitotic activation of aurora A during G2/M transition of human cells. *J Biol Chem*. 2010;285(28):21849-21857. doi:10.1074/jbc.M110.141010.
34. Terada Y, Uetake Y, Kuriyama R. Interaction of Aurora-A and centrosomin at the microtubule-nucleating site in Drosophila and mammalian cells. *J Cell Biol*. 2003;162(5):757-763. doi:10.1083/jcb.200305048.

35. Heidebrecht HJ, Buck F, Steinmann J, Sprenger R, Wacker HH, Parwaresch R. p100: A novel proliferation-associated nuclear protein specifically restricted to cell cycle phases S, G2, and M. *Blood*. 1997;90(1):226-233.
36. Neumayer G, Belzil C, Gruss OJ, Nguyen MD. TPX2: of spindle assembly, DNA damage response, and cancer. *Cell Mol Life Sci*. 2014;71(16):3027-3047. doi:10.1007/s00018-014-1582-7.
37. Heidebrecht H-J, Adam-Klages S, Szczepanowski M, et al. repp86: A human protein associated in the progression of mitosis. *Mol Cancer Res*. 2003;1(4):271-279.
38. Punta M, Coggill PC, Eberhardt RY, et al. The Pfam protein families database. *Nucleic Acids Res*. 2012;40(Database issue):D290-301. doi:10.1093/nar/gkr1065.
39. Schatz CA, Santarella R, Hoenger A, et al. Importin alpha-regulated nucleation of microtubules by TPX2. *EMBO J*. 2003;22(9):2060-2070. doi:10.1093/emboj/cdg195.
40. Gruss OJ, Vernos I. The mechanism of spindle assembly: functions of Ran and its target TPX2. *J Cell Biol*. 2004;166(7):949-955. doi:10.1083/jcb.200312112.
41. Kufer TA, Sillje HHW, Korner R, Gruss OJ, Meraldi P, Nigg EA. Human TPX2 is required for targeting Aurora-A kinase to the spindle. *J Cell Biol*. 2002;158(4):617-623. doi:10.1083/jcb.200204155.
42. Dodson CA, Bayliss R. Activation of Aurora-A kinase by protein partner binding and phosphorylation are independent and synergistic. *J Biol Chem*. 2012;287(2):1150-1157. doi:10.1074/jbc.M111.312090.
43. Anderson K, Yang J, Koretke K, et al. Binding of TPX2 to Aurora A alters substrate and inhibitor interactions. *Biochemistry*. 2007;46(36):10287-10295. doi:10.1021/bi7011355.
44. Schulze JO, Saladino G, Busschots K, et al. Bidirectional Allosteric Communication between the ATP-Binding Site and the Regulatory PIF Pocket in PDK1 Protein Kinase. *Cell Chem Biol*. 2016;23(10):1193-1205. doi:10.1016/j.chembiol.2016.06.017.
45. Bayliss R, Burgess SG, McIntyre PJ. Switching Aurora-A kinase on and off at an allosteric site. *FEBS J*. 2017;284(18):2947-2954. doi:10.1111/febs.14069.

46. David R. Cell cycle: Dissecting mitosis. *Nat Rev Mol Cell Biol*. 2010;11(5):310. doi:10.1038/nrm2892.
47. Dodson CA, Haq T, Yeoh S, Fry AM, Bayliss R. The structural mechanisms that underpin mitotic kinase activation. *Biochem Soc Trans*. 2013;41(4):1037-1041. doi:10.1042/BST20130066.
48. Nicklas RB. How cells get the right chromosomes. *Science*. 1997;275(5300):632-637.
49. Bartek J, Lukas J. Mammalian G1- and S-phase checkpoints in response to DNA damage. *Current Opinion in Cell Biology*. 2001;13(6):738-747. doi:10.1016/S0955-0674(00)00280-5.
50. Takizawa CG, Morgan DO. Control of mitosis by changes in the subcellular location of cyclin-B1-Cdk1 and Cdc25C. *Current Opinion in Cell Biology*. 2000;12(6):658-665.
51. McIntosh JR. Structural and mechanical control of mitotic progression. *Cold Spring Harb Symp Quant Biol*. 1991;56:613-619.
52. Peters J-M. SCF and APC: The Yin and Yang of cell cycle regulated proteolysis. *Current Opinion in Cell Biology*. 1998;10(6):759-768. doi:10.1016/S0955-0674(98)80119-1.
53. Hutterer A, Berdnik D, Wirtz-Peitz F, Žigman M, Schleiffer A, Knoblich JA. Mitotic Activation of the Kinase Aurora-A Requires Its Binding Partner Bora. *Developmental Cell*. 2006;11(2):147-157. doi:10.1016/j.devcel.2006.06.002.
54. Murray AW. Recycling the cell cycle: cyclins revisited. *Cell*. 2004;116(2):221-234.
55. Seki A, Coppinger JA, Jang C-Y, Yates JR, Fang G. Bora and the kinase Aurora a cooperatively activate the kinase Plk1 and control mitotic entry. *Science*. 2008;320(5883):1655-1658. doi:10.1126/science.1157425.
56. Kramer A, Mailand N, Lukas C, et al. Centrosome-associated Chk1 prevents premature activation of cyclin-B-Cdk1 kinase. *Nat Cell Biol*. 2004;6(9):884-891. doi:10.1038/ncb1165.
57. Harvey SL, Charlet A, Haas W, Gygi SP, Kellogg DR. Cdk1-dependent regulation of the mitotic inhibitor Wee1. *Cell*. 2005;122(3):407-420. doi:10.1016/j.cell.2005.05.029.
58. Hermeking H, Lengauer C, Polyak K, et al. 14-3-3sigma is a p53-regulated inhibitor of G2/M progression. *Mol Cell*. 1997;1(1):3-11.

59. Chan EHY, Santamaria A, Silljé HHW, Nigg EA. Plk1 regulates mitotic Aurora A function through betaTrCP-dependent degradation of hBora. *Chromosoma*. 2008;117(5):457-469. doi:10.1007/s00412-008-0165-5.
60. Feine O, Hukasova E, Bruinsma W, et al. Phosphorylation-mediated stabilization of Bora in mitosis coordinates Plx1/Plk1 and Cdk1 oscillations. *Cell Cycle*. 2014;13(11):1727-1736. doi:10.4161/cc.28630.
61. Gomez-Ferreria MA, Rath U, Buster DW, et al. Human Cep192 is required for mitotic centrosome and spindle assembly. *Curr Biol*. 2007;17(22):1960-1966. doi:10.1016/j.cub.2007.10.019.
62. Bird AW, Hyman AA. Building a spindle of the correct length in human cells requires the interaction between TPX2 and Aurora A. *J Cell Biol*. 2008;182(2):289-300. doi:10.1083/jcb.200802005.
63. Joukov V, Walter JC, Nicolo A de. The Cep192-organized aurora A-Plk1 cascade is essential for centrosome cycle and bipolar spindle assembly. *Mol Cell*. 2014;55(4):578-591. doi:10.1016/j.molcel.2014.06.016.
64. Ma N, Titus J, Gable A, Ross JL, Wadsworth P. TPX2 regulates the localization and activity of Eg5 in the mammalian mitotic spindle. *J Cell Biol*. 2011;195(1):87-98. doi:10.1083/jcb.201106149.
65. Lioutas A, Vernos I. Aurora A kinase and its substrate TACC3 are required for central spindle assembly. *EMBO Rep*. 2013;14(9):829-836. doi:10.1038/embor.2013.109.
66. Mayer TU, Kapoor TM, Haggarty SJ, King RW, Schreiber SL, Mitchison TJ. Small molecule inhibitor of mitotic spindle bipolarity identified in a phenotype-based screen. *Science*. 1999;286(5441):971-974.
67. Hoar K, Chakravarty A, Rabino C, et al. MLN8054, a small-molecule inhibitor of Aurora A, causes spindle pole and chromosome congression defects leading to aneuploidy. *Mol Cell Biol*. 2007;27(12):4513-4525. doi:10.1128/MCB.02364-06.
68. Bharadwaj R, Yu H. The spindle checkpoint, aneuploidy, and cancer. *Oncogene*. 2004;23(11):2016-2027. doi:10.1038/sj.onc.1207374.
69. Tao W, South VJ, Zhang Y, et al. Induction of apoptosis by an inhibitor of the mitotic kinesin KSP requires both activation of the spindle assembly checkpoint and mitotic slippage. *Cancer Cell*. 2005;8(1):49-59. doi:10.1016/j.ccr.2005.06.003.

70. Minn AJ, Boise LH, Thompson CB. Expression of Bcl-xL and loss of p53 can cooperate to overcome a cell cycle checkpoint induced by mitotic spindle damage. *Genes Dev*. 1996;10(20):2621-2631.
71. Brito DA, Rieder CL. Mitotic checkpoint slippage in humans occurs via cyclin B destruction in the presence of an active checkpoint. *Curr Biol*. 2006;16(12):1194-1200. doi:10.1016/j.cub.2006.04.043.
72. Keen N, Taylor S. Aurora-kinase inhibitors as anticancer agents. *Nat Rev Cancer*. 2004;4(12):927-936. doi:10.1038/nrc1502.
73. Marxer M, Ma HT, Man WY, Poon RYC. p53 deficiency enhances mitotic arrest and slippage induced by pharmacological inhibition of Aurora kinases. *Oncogene*. 2014;33(27):3550-3560. doi:10.1038/onc.2013.325.
74. Landen CN, Lin YG, Immaneni A, et al. Overexpression of the centrosomal protein Aurora-A kinase is associated with poor prognosis in epithelial ovarian cancer patients. *Clin Cancer Res*. 2007;13(14):4098-4104. doi:10.1158/1078-0432.CCR-07-0431.
75. Schneider MA, Christopoulos P, Muley T, et al. AURKA, DLGAP5, TPX2, KIF11 and CKAP5: Five specific mitosis-associated genes correlate with poor prognosis for non-small cell lung cancer patients. *Int J Oncol*. 2017;50(2):365-372. doi:10.3892/ijo.2017.3834.
76. Koh HM, Jang BG, Hyun CL, et al. Aurora Kinase A Is a Prognostic Marker in Colorectal Adenocarcinoma. *J Pathol Transl Med*. 2017;51(1):32-39. doi:10.4132/jptm.2016.10.17.
77. Zhou H, Kuang J, Zhong L, et al. Tumour amplified kinase STK15/BTAK induces centrosome amplification, aneuploidy and transformation. *Nat Genet*. 1998;20(2):189-193. doi:10.1038/2496.
78. Kitajima S, Kudo Y, Ogawa I, et al. Constitutive phosphorylation of aurora-a on ser51 induces its stabilization and consequent overexpression in cancer. *PLoS ONE*. 2007;2(9):e944. doi:10.1371/journal.pone.0000944.
79. Schvartzman J-M, Sotillo R, Benezra R. Mitotic chromosomal instability and cancer: mouse modelling of the human disease. *Nat Rev Cancer*. 2010;10(2):102-115. doi:10.1038/nrc2781.
80. Sen S, Zhou H, White RA. A putative serine/threonine kinase encoding gene BTAK on chromosome 20q13 is amplified and overexpressed in human

breast cancer cell lines. *Oncogene*. 1997;14(18):2195-2200. doi:10.1038/sj.onc.1201065.

81. Bischoff JR, Anderson L, Zhu Y, et al. A homologue of Drosophila aurora kinase is oncogenic and amplified in human colorectal cancers. *EMBO J*. 1998;17(11):3052-3065. doi:10.1093/emboj/17.11.3052.
82. Reznikoff CA, Belair CD, Yeager TR, et al. A molecular genetic model of human bladder cancer pathogenesis. *Semin Oncol*. 1996;23(5):571-584.
83. Iwabuchi H, Sakamoto M, Sakunaga H, et al. Genetic analysis of benign, low-grade, and high-grade ovarian tumors. *Cancer Res*. 1995;55(24):6172-6180.
84. He Y, Jiang W, Qian X, Liu F, Zhang Q, You C. Role of Aurora-A in Ovarian Cancer: A Meta-Analysis. *Oncol Res Treat*. 2015;38(9):442-447. doi:10.1159/000439194.
85. World Health Organization. Cancer. http://www.who.int/mediacentre/factsheets/fs297/en/. Updated July 19, 2017. Accessed July 24, 2017.
86. Reiter R, Gais P, Jütting U, et al. Aurora kinase A messenger RNA overexpression is correlated with tumor progression and shortened survival in head and neck squamous cell carcinoma. *Clin Cancer Res*. 2006;12(17):5136-5141. doi:10.1158/1078-0432.CCR-05-1650.
87. Meraldi P. Aurora-A overexpression reveals tetraploidization as a major route to centrosome amplification in p53-/- cells. *EMBO J*. 2002;21(4):483-492. doi:10.1093/emboj/21.4.483.
88. Katayama H, Sasai K, Kawai H, et al. Phosphorylation by aurora kinase A induces Mdm2-mediated destabilization and inhibition of p53. *Nat Genet*. 2004;36(1):55-62. doi:10.1038/ng1279.
89. Yang G, Chang B, Yang F, et al. Aurora kinase A promotes ovarian tumorigenesis through dysregulation of the cell cycle and suppression of BRCA2. *Clin Cancer Res*. 2010;16(12):3171-3181. doi:10.1158/1078-0432.CCR-09-3171.
90. Zhang D, Hirota T, Marumoto T, et al. Cre-loxP-controlled periodic Aurora-A overexpression induces mitotic abnormalities and hyperplasia in mammary glands of mouse models. *Oncogene*. 2004;23(54):8720-8730. doi:10.1038/sj.onc.1208153.

91. Zhang D, Shimizu T, Araki N, et al. Aurora A overexpression induces cellular senescence in mammary gland hyperplastic tumors developed in p53-deficient mice. *Oncogene*. 2008;27(31):4305-4314. doi:10.1038/onc.2008.76.
92. Wang X, Zhou Y-X, Qiao W, et al. Overexpression of aurora kinase A in mouse mammary epithelium induces genetic instability preceding mammary tumor formation. *Oncogene*. 2006;25(54):7148-7158. doi:10.1038/sj.onc.1209707.
93. Gustafson WC, Weiss WA. Myc proteins as therapeutic targets. *Oncogene*. 2010;29(9):1249-1259. doi:10.1038/onc.2009.512.
94. Brodeur G, Seeger R, Schwab M, Varmus H, Bishop J. Amplification of N-myc in untreated human neuroblastomas correlates with advanced disease stage. *Science*. 1984;224(4653):1121-1124. doi:10.1126/science.6719137.
95. Prochownik EV, Vogt PK. Therapeutic Targeting of Myc. *Genes Cancer*. 2010;1(6):650-659. doi:10.1177/1947601910377494.
96. Otto T, Horn S, Brockmann M, et al. Stabilization of N-Myc is a critical function of Aurora A in human neuroblastoma. *Cancer Cell*. 2009;15(1):67-78. doi:10.1016/j.ccr.2008.12.005.
97. Shang X, Burlingame SM, Okcu MF, et al. Aurora A is a negative prognostic factor and a new therapeutic target in human neuroblastoma. *Mol Cancer Ther*. 2009;8(8):2461-2469. doi:10.1158/1535-7163.MCT-08-0857.
98. Gustafson WC, Meyerowitz JG, Nekritz EA, et al. Drugging MYCN through an allosteric transition in Aurora kinase A. *Cancer Cell*. 2014;26(3):414-427. doi:10.1016/j.ccr.2014.07.015.
99. Brockmann M, Poon E, Berry T, et al. Small molecule inhibitors of aurora-a induce proteasomal degradation of N-myc in childhood neuroblastoma. *Cancer Cell*. 2013;24(1):75-89. doi:10.1016/j.ccr.2013.05.005.
100. Richards MW, Burgess SG, Poon E, et al. Structural basis of N-Myc binding by Aurora-A and its destabilization by kinase inhibitors. *Proc Natl Acad Sci U S A*. 2016;113(48):13726-13731. doi:10.1073/pnas.1610626113.
101. Wang Z. ErbB Receptors and Cancer. *Methods Mol Biol*. 2017;1652:3-35. doi:10.1007/978-1-4939-7219-7_1.

102. Ross JS, Fletcher JA. The HER-2/neu oncogene in breast cancer: Prognostic factor, predictive factor, and target for therapy. *Stem Cells*. 1998;16(6):413-428. doi:10.1002/stem.160413.

103. Ziemska J, Solecka J. Tyrosine kinase, aurora kinase and leucine aminopeptidase as attractive drug targets in anticancer therapy - characterisation of their inhibitors. *Rocz Panstw Zakl Hig*. 2016;67(4):329-342.

104. Yan M, Wang C, He B, et al. Aurora-A Kinase: A Potent Oncogene and Target for Cancer Therapy. *Med Res Rev*. 2016;36(6):1036-1079. doi:10.1002/med.21399.

105. Lapenna S, Giordano A. Cell cycle kinases as therapeutic targets for cancer. *Nat Rev Drug Discov*. 2009;8(7):547-566. doi:10.1038/nrd2907.

106. Falchook GS, Bastida CC, Kurzrock R. Aurora Kinase Inhibitors in Oncology Clinical Trials: Current State of the Progress. *Semin Oncol*. 2015;42(6):832-848. doi:10.1053/j.seminoncol.2015.09.022.

107. Cheung CHA, Coumar MS, Hsieh H-P, Chang J-Y. Aurora kinase inhibitors in preclinical and clinical testing. *Expert Opin Investig Drugs*. 2009;18(4):379-398. doi:10.1517/13543780902806392.

108. Soncini C, Carpinelli P, Gianellini L, et al. PHA-680632, a novel Aurora kinase inhibitor with potent antitumoral activity. *Clin Cancer Res*. 2006;12(13):4080-4089. doi:10.1158/1078-0432.CCR-05-1964.

109. Fletcher GC, Brokx RD, Denny TA, et al. ENMD-2076 is an orally active kinase inhibitor with antiangiogenic and antiproliferative mechanisms of action. *Mol Cancer Ther*. 2011;10(1):126-137. doi:10.1158/1535-7163.MCT-10-0574.

110. Cohen RB, Jones SF, Aggarwal C, et al. A phase I dose-escalation study of danusertib (PHA-739358) administered as a 24-hour infusion with and without granulocyte colony-stimulating factor in a 14-day cycle in patients with advanced solid tumors. *Clin Cancer Res*. 2009;15(21):6694-6701. doi:10.1158/1078-0432.CCR-09-1445.

111. Boss DS, Witteveen PO, van der Sar J, et al. Clinical evaluation of AZD1152, an i.v. inhibitor of Aurora B kinase, in patients with solid malignant tumors. *Ann Oncol*. 2011;22(2):431-437. doi:10.1093/annonc/mdq344.

112. Gontarewicz A, Brümmendorf TH. Danusertib (formerly PHA-739358)--a novel combined pan-Aurora kinases and third generation Bcr-Abl tyrosine kinase inhibitor. *Recent Results Cancer Res*. 2010;184:199-214. doi:10.1007/978-3-642-01222-8_14.

113. Diamond JR, Bastos BR, Hansen RJ, et al. Phase I safety, pharmacokinetic, and pharmacodynamic study of ENMD-2076, a novel angiogenic and Aurora kinase inhibitor, in patients with advanced solid tumors. *Clin Cancer Res*. 2011;17(4):849-860. doi:10.1158/1078-0432.CCR-10-2144.

114. Anand S, Penrhyn-Lowe S, Venkitaraman AR. AURORA-A amplification overrides the mitotic spindle assembly checkpoint, inducing resistance to Taxol. *Cancer Cell*. 2003;3(1):51-62. doi:10.1016/S1535-6108(02)00235-0.

115. Harrington EA, Bebbington D, Moore J, et al. VX-680, a potent and selective small-molecule inhibitor of the Aurora kinases, suppresses tumor growth in vivo. *Nat Med*. 2004;10(3):262-267. doi:10.1038/nm1003.

116. Zhao B, Smallwood A, Lai Z. *Crystal structure of Aurora A in complex with VX-680 and TPX2*; 2008.

117. Sells TB, Chau R, Ecsedy JA, et al. MLN8054 and Alisertib (MLN8237): Discovery of Selective Oral Aurora A Inhibitors. *ACS Med Chem Lett*. 2015;6(6):630-634. doi:10.1021/ml500409n.

118. SHESKIN J. THALIDOMIDE IN THE TREATMENT OF LEPRA REACTIONS. *Clin Pharmacol Ther*. 1965;6:303-306.

119. Jacobson JM, Greenspan JS, Spritzler J, et al. Thalidomide for the treatment of oral aphthous ulcers in patients with human immunodeficiency virus infection. National Institute of Allergy and Infectious Diseases AIDS Clinical Trials Group. *N Engl J Med*. 1997;336(21):1487-1493. doi:10.1056/NEJM199705223362103.

120. Singhal S, Mehta J, Desikan R, et al. Antitumor activity of thalidomide in refractory multiple myeloma. *N Engl J Med*. 1999;341(21):1565-1571. doi:10.1056/NEJM199911183412102.

121. Rajkumar SV. Thalidomide: Tragic Past and Promising Future. *Mayo Clinic Proceedings*. 2004;79(7):899-903. doi:10.4065/79.7.899.

122. Shah SR, Tran TM. Lenalidomide in myelodysplastic syndrome and multiple myeloma. *Drugs*. 2007;67(13):1869-1881.

123. Fenton AW. Allostery: an illustrated definition for the 'second secret of life'. *Trends Biochem Sci*. 2008;33(9):420-425. doi:10.1016/j.tibs.2008.05.009.

124. Changeux J-P, Edelstein SJ. Allosteric mechanisms of signal transduction. *Science*. 2005;308(5727):1424-1428. doi:10.1126/science.1108595.

125. Engel M, Hindie V, Lopez-Garcia LA, et al. Allosteric activation of the protein kinase PDK1 with low molecular weight compounds. *EMBO J*. 2006;25(23):5469-5480. doi:10.1038/sj.emboj.7601416.

126. Hindie V, Stroba A, Zhang H, et al. Structure and allosteric effects of low-molecular-weight activators on the protein kinase PDK1. *Nat Chem Biol*. 2009;5(10):758-764. doi:10.1038/nchembio.208.

127. Busschots K, Lopez-Garcia LA, Lammi C, et al. Substrate-selective inhibition of protein kinase PDK1 by small compounds that bind to the PIF-pocket allosteric docking site. *Chem Biol*. 2012;19(9):1152-1163. doi:10.1016/j.chembiol.2012.07.017.

128. Rettenmaier TJ, Sadowsky JD, Thomsen ND, et al. A small-molecule mimic of a peptide docking motif inhibits the protein kinase PDK1. *Proc Natl Acad Sci U S A*. 2014;111(52):18590-18595. doi:10.1073/pnas.1415365112.

129. Sells T, Ecsedy J, Stroud S, et al. MLN8237: An orally active small molecule inhibitor of Aurora A kinase in phase I clinical trials. *Cancer Res*. 2008;68(9 Supplement):237.

130. Rennie YK, McIntyre PJ, Akindele T, Bayliss R, Jamieson AG. A TPX2 Proteomimetic Has Enhanced Affinity for Aurora-A Due to Hydrocarbon Stapling of a Helix. *ACS Chem Biol*. 2016;11(12):3383-3390. doi:10.1021/acschembio.6b00727.

131. Asteriti IA, Daidone F, Colotti G, et al. Identification of small molecule inhibitors of the Aurora-A/TPX2 complex. *Oncotarget*. 2017;8(19):32117-32133. doi:10.18632/oncotarget.16738.

132. Görgün G, Calabrese E, Hideshima T, et al. A novel Aurora-A kinase inhibitor MLN8237 induces cytotoxicity and cell-cycle arrest in multiple myeloma. *Blood*. 2010;115(25):5202-5213. doi:10.1182/blood-2009-12-259523.

133. Wen Q, Goldenson B, Silver SJ, et al. Identification of regulators of polyploidization presents therapeutic targets for treatment of AMKL. *Cell*. 2012;150(3):575-589. doi:10.1016/j.cell.2012.06.032.

134. Waldron TT, Murphy KP. Stabilization of proteins by ligand binding: Application to drug screening and determination of unfolding energetics. *Biochemistry*. 2003;42(17):5058-5064. doi:10.1021/bi034212v.

135. Heisler LE, Evangelou A, Lew AM, Trachtenberg J, Elsholtz HP, Brown TJ. Androgen-dependent cell cycle arrest and apoptotic death in PC-3 prostatic cell cultures expressing a full-length human androgen receptor. *Mol Cell Endocrinol*. 1997;126(1):59-73.

136. Burgess SG, Oleksy A, Cavazza T, et al. Allosteric inhibition of Aurora-A kinase by a synthetic vNAR domain. *Open Biol*. 2016;6(7). doi:10.1098/rsob.160089.

137. Janeček M, Rossmann M, Sharma P, et al. Allosteric modulation of AURKA kinase activity by a small-molecule inhibitor of its protein-protein interaction with TPX2. *Sci Rep*. 2016;6:28528. doi:10.1038/srep28528.

138. Groot CO de, Hsia JE, Anzola JV, et al. A Cell Biologist's Field Guide to Aurora Kinase Inhibitors. *Front Oncol*. 2015;5:285. doi:10.3389/fonc.2015.00285.

139. Panicker RC, Coyne AG, Srinivasan R. Allosteric Targeting of Aurora A Kinase Using Small Molecules: A Step Forward Towards Next Generation Medicines? *Curr Med Chem*. 2017. doi:10.2174/0929867324666170727120315.

140. Kilchmann F, Marcaida MJ, Kotak S, et al. Discovery of a Selective Aurora A Kinase Inhibitor by Virtual Screening. *J Med Chem*. 2016;59(15):7188-7211. doi:10.1021/acs.jmedchem.6b00709.

141. Karthigeyan D, Siddhanta S, Kishore AH, et al. SERS and MD simulation studies of a kinase inhibitor demonstrate the emergence of a potential drug discovery tool. *Proc Natl Acad Sci U S A*. 2014;111(29):10416-10421. doi:10.1073/pnas.1402695111.

142. Zhang H, Neimanis S, Lopez-Garcia LA, et al. Molecular mechanism of regulation of the atypical protein kinase C by N-terminal domains and an allosteric small compound. *Chem Biol*. 2014;21(6):754-765. doi:10.1016/j.chembiol.2014.04.007.

143. US20080051327A1 - Crystals of an Aurora-A Tpx2 Complex, Tpx2 Binding Site of Aurora-A, Aurora-A Ligands and Their Use - Google Patents. https://patents.google.com/patent/US20080051327A1/en#patentCitations. Updated October 11, 2004. Accessed July 27, 2018.

144. Bavetsias V, Linardopoulos S. Aurora Kinase Inhibitors: Current Status and Outlook. *Front Oncol*. 2015;5:278. doi:10.3389/fonc.2015.00278.

145. Matulonis UA, Sharma S, Ghamande S, et al. Phase II study of MLN8237 (alisertib), an investigational Aurora A kinase inhibitor, in patients with platinum-resistant or -refractory epithelial ovarian, fallopian tube, or primary peritoneal carcinoma. *Gynecol Oncol*. 2012;127(1):63-69. doi:10.1016/j.ygyno.2012.06.040.

146. Tayyar Y, Jubair L, Fallaha S, McMillan NAJ. Critical risk-benefit assessment of the novel anti-cancer aurora a kinase inhibitor alisertib (MLN8237): A comprehensive review of the clinical data. *Crit Rev Oncol Hematol*. 2017;119:59-65. doi:10.1016/j.critrevonc.2017.09.006.

147. Hong X, O'Donnell JP, Salazar CR, et al. The selective Aurora-A kinase inhibitor MLN8237 (alisertib) potently inhibits proliferation of glioblastoma neurosphere tumor stem-like cells and potentiates the effects of temozolomide and ionizing radiation. *Cancer Chemother Pharmacol*. 2014;73(5):983-990. doi:10.1007/s00280-014-2430-z.

148. Goldberg SL, Fenaux P, Craig MD, et al. An exploratory phase 2 study of investigational Aurora A kinase inhibitor alisertib (MLN8237) in acute myelogenous leukemia and myelodysplastic syndromes. *Leuk Res Rep*. 2014;3(2):58-61. doi:10.1016/j.lrr.2014.06.003.

149. Asteriti IA, Di Cesare E, Mattia F de, et al. The Aurora-A inhibitor MLN8237 affects multiple mitotic processes and induces dose-dependent mitotic abnormalities and aneuploidy. *Oncotarget*. 2014;5(15):6229-6242. doi:10.18632/oncotarget.2190.

150. Fang X, Zhang P. Aneuploidy and tumorigenesis. *Semin Cell Dev Biol*. 2011;22(6):595-601. doi:10.1016/j.semcdb.2011.03.002.

151. Levis MJ. Will newer tyrosine kinase inhibitors have an impact in AML? *Best Pract Res Clin Haematol*. 2010;23(4):489-494. doi:10.1016/j.beha.2010.09.008.

152. Grundy M, Seedhouse C, Shang S, Richardson J, Russell N, Pallis M. The FLT3 internal tandem duplication mutation is a secondary target of the aurora B kinase inhibitor AZD1152-HQPA in acute myelogenous leukemia cells. *Mol Cancer Ther*. 2010;9(3):661-672. doi:10.1158/1535-7163.MCT-09-1144.

153. Moore AS, Faisal A, Gonzalez de Castro D, et al. Selective FLT3 inhibition of FLT3-ITD+ acute myeloid leukaemia resulting in secondary D835Y mutation: A model for emerging clinical resistance patterns. *Leukemia*. 2012;26(7):1462-1470. doi:10.1038/leu.2012.52.

154. Macůrek L, Lindqvist A, Lim D, et al. Polo-like kinase-1 is activated by aurora A to promote checkpoint recovery. *Nature*. 2008;455(7209):119-123. doi:10.1038/nature07185.

155. Warner SL, Gray PJ, Hoff DD von. Tubulin-associated drug targets: Aurora kinases, Polo-like kinases, and others. *Semin Oncol*. 2006;33(4):436-448. doi:10.1053/j.seminoncol.2006.04.007.

156. Gutteridge REA, Ndiaye MA, Liu X, Ahmad N. Plk1 Inhibitors in Cancer Therapy: From Laboratory to Clinics. *Mol Cancer Ther*. 2016;15(7):1427-1435. doi:10.1158/1535-7163.MCT-15-0897.

157. Raab M, Sanhaji M, Pietsch L, et al. Modulation of the Allosteric Communication between the Polo-Box Domain and the Catalytic Domain in Plk1 by Small Compounds. *ACS Chem Biol*. 2018. doi:10.1021/acschembio.7b01078.

158. Wylie AA, Schoepfer J, Jahnke W, et al. The allosteric inhibitor ABL001 enables dual targeting of BCR-ABL1. *Nature*. 2017;543(7647):733-737. doi:10.1038/nature21702.

7. Supplement

7.1 Hit compounds and their properties

	Hit	Name	Library name	Usage	Function	Side effects
plate 1	4M	**Tiratricol, 3,3',5-triiodothyroacetic acid**	Prestw-202	TSH-suppression	Thyroid hormone analogue	Hyper-thyreodic
plate 2	22B	**Erlotinib**	Prestw-1242	Antineoplastic	Tyrosine kinase inhibitor	Severe allergic reactions
plate 3	3C	**Pranlukast**	Prestw-1317	Antiasthmatic	Leukotriene receptor-1 antagonist	
	5N	**Liothyronine**	Prestw-853	Thyroidic drug	Thyroid hormone	Hyper-thyreodic
	19B	**Atractyloside potassium salt**	Prestw-737	Anticancer	Nucleotide transport inhibitor	Toxic
	22A	**Balsalazide Sodium**	Prestw-730	Anti-inflammatory		Nausea
plate 4	14B	**Iopanoic acid**	Prestw-1052	Contrastant		Nausea, Hyper-thyreosis
	21O	**Oxymetholone**	Prestw-1780	Anabolic	Testosterone-derivative	Nausea

Table S1: Overview of all hit-compounds with their Prestwick library name, pharmacological usage, biochemical function and side-effects.

Atractyloside	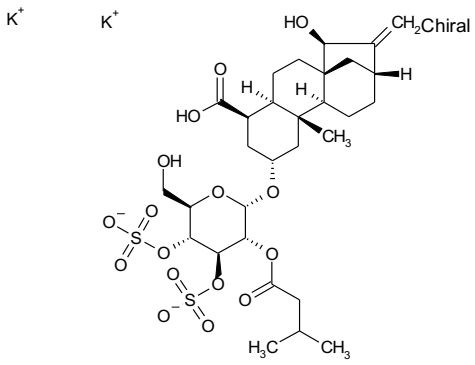
Balsalazide	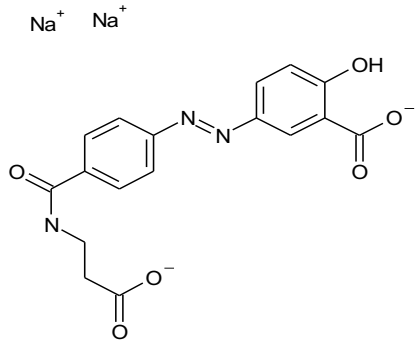
Erlotinib	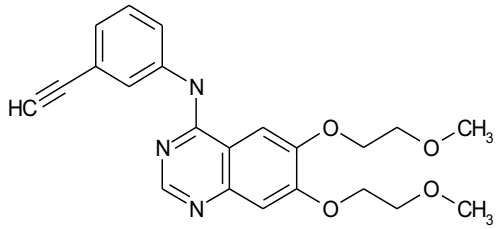
Liothyronine	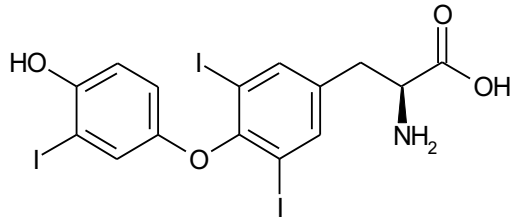
Iopanoic acid	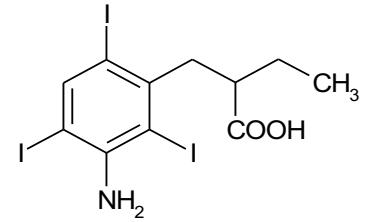
Oxymetholone	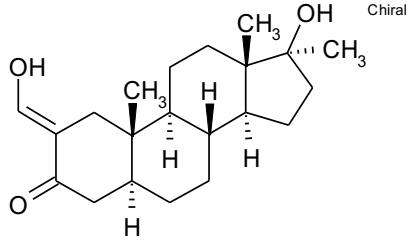

Pranlukast	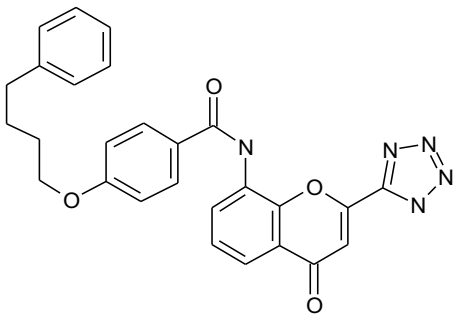
Tiratricol	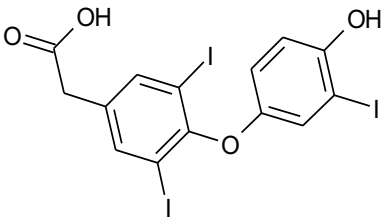

Table S2: Chemical structures of hit-compounds.

7.1 Occurrence of reactive oxygen species

The influence of the hit-compounds on the occurrence of reactive oxygen species was tested by Daniel Pastor-Flores at DKFZ in Heidelberg, a former group member who kindly tested the compounds in this assay that is not established in our lab.

The assay observes the growth per time of Saccharomyces cerevisiae cells and the oxidation state of the cell. For further examination, PS 731 has also been tested since there has been no data for this experiment on PS 731 before. Only graphs with a visible effect are shown.

PS 731 stops the growth of yeast and induces high oxidative stress from the moment of addition, reaching its maximum after approximately 4h.

From the hit-compounds only Erlotinib, Pranlukast and Tiratricol show some effect. The compounds were tested at a 125 µM concentration. Erlotinib slows down the growth of the yeast cells and after 24h they still don't reach the level of untreated yeast. Also, the cells show a risen level of oxidative stress. Pranlukast was tested at two concentrations. At 125 µM the yeast first shows a decelerated growth, but after approximately 16h they reach level with the untreated cells and even pass by a small bit. However, in presence of 250 µM Pranlukast the yeast stops growing and stays level. Addition of Pranlukast

induces reactive oxygen species with a delay of approximately 4h but then it has higher effect than Erlotinib. Tiratricol slows down the growth of yeast cells less than Erlotinib with only a small deceleration visible after addition of the compound, but nevertheless induces production of reactive oxygen species.

These experiments on yeast are important in view of a possible use of Aurora inhibitors for treating infections with parasites. Systemic infections with Candida albicans and other pathogenic yeast strains are a common but dangerous threat to immunocompromised patients, e.g. cancer patients, patients on intensive care units or after an organ transplant. Because Aurora is a highly preserved kinase, it would be an attractive target for drugging infections with Candida albicans. In times of growing resistance to available antibiotics and antimycotics new targets are urgently needed.

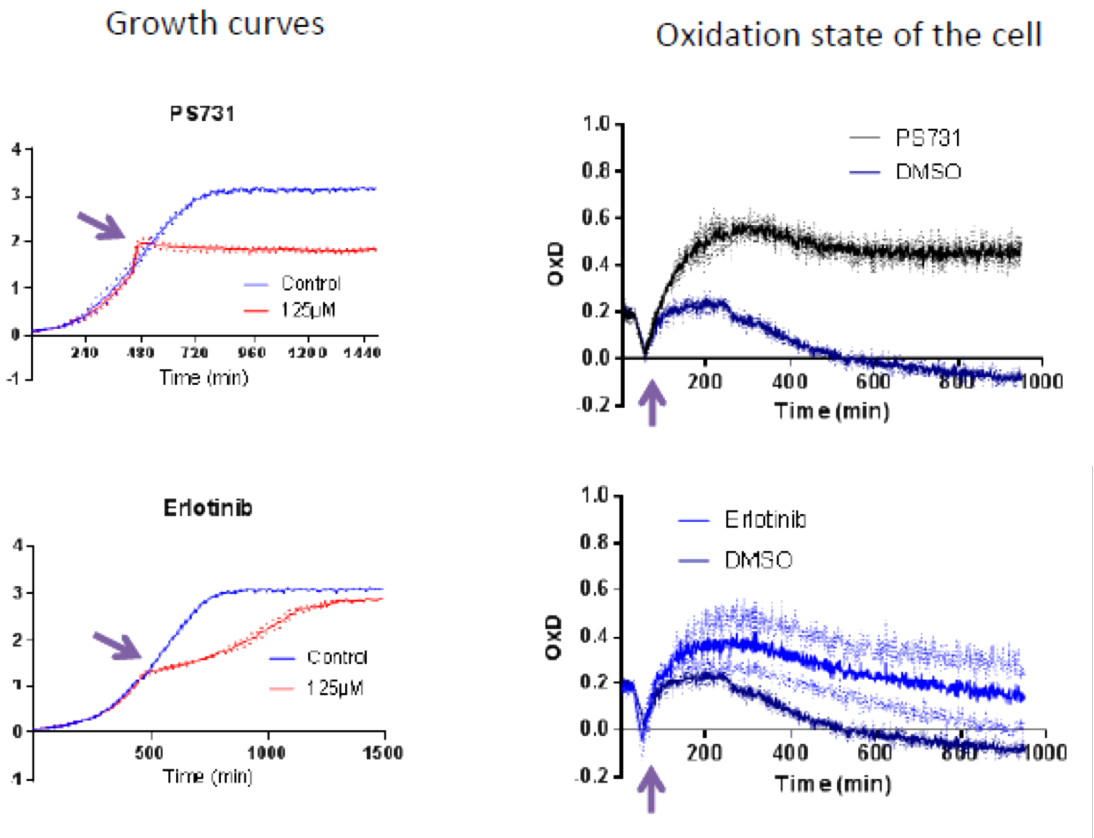

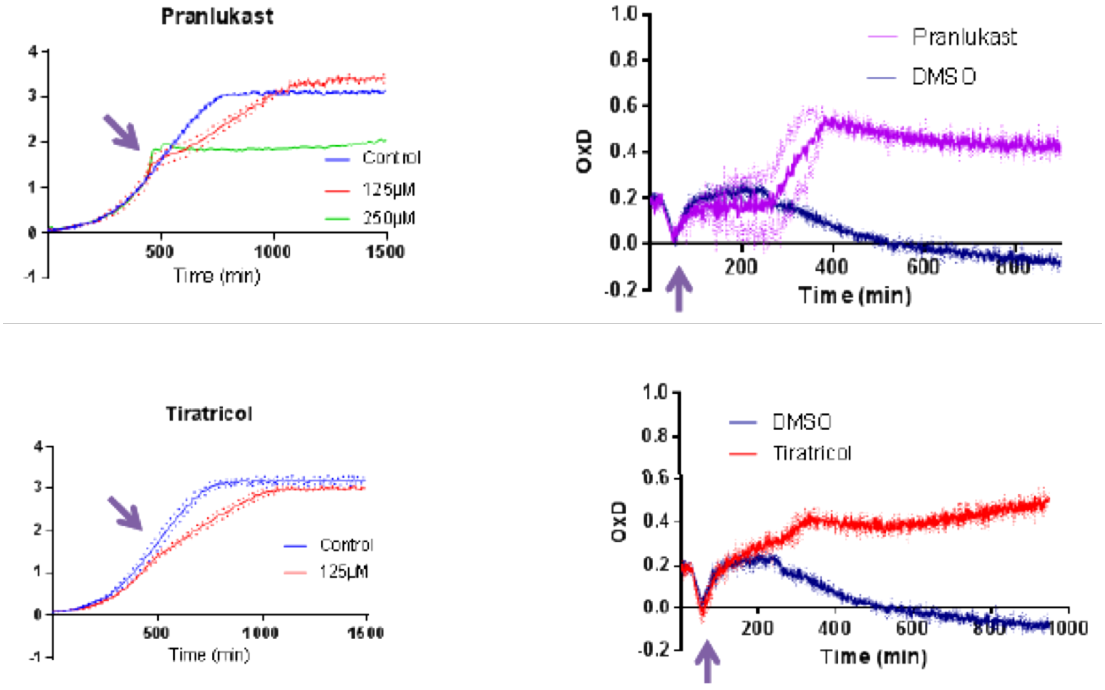

Figure S1: Growth curves and oxidation state of the cell of PS 731, Erlotinib, Pranlukast and Tiratricol with OxD being the degree of sensor oxidation in comparison with cells only treated with DMSO. Arrow indicates addition of compound.

7.3 Supplement for cell cycle experiments

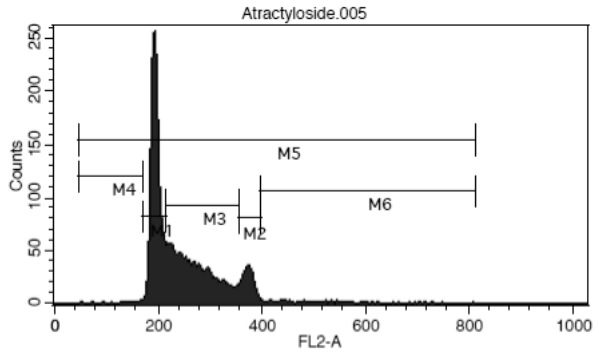

Histogram Statistics

File: Atractyloside.005 Log Data Units: Linear Values
Acquisition Date: 28-Jan-15 Gate: G1
Gated Events: 9990 Total Events: 10756
X Parameter: FL2-A (Linear)

Marker	Left, Right	Events	% Gated	% Total	Mean	Geo Mean
All	0, 1023	9990	100.00	92.88	250.12	240.55
M1	169, 215	4526	45.31	42.08	194.33	194.15
M2	353, 396	890	8.91	8.27	370.46	370.34
M3	215, 353	4326	43.30	40.22	268.42	265.86
M4	44, 170	67	0.67	0.62	125.07	118.24
M5	44, 809	9981	99.91	92.79	249.53	240.27
M6	396, 810	240	2.40	2.23	533.09	522.95

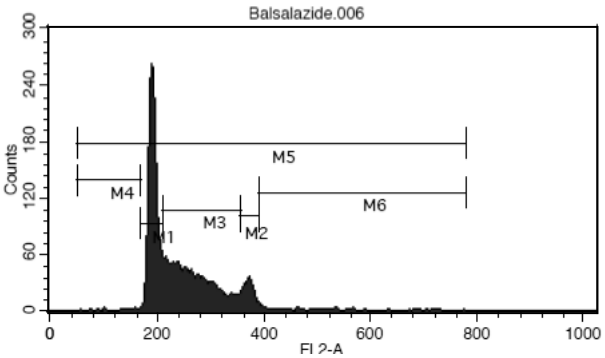

Histogram Statistics

File: Balsalazide.006 Log Data Units: Linear Values
Acquisition Date: 28-Jan-15 Gate: G1
Gated Events: 9995 Total Events: 10632
X Parameter: FL2-A (Linear)

Marker	Left, Right	Events	% Gated	% Total	Mean	Geo Mean
All	0, 1023	9995	100.00	94.01	250.49	241.47
M1	171, 213	4274	42.76	40.20	194.40	194.26
M2	358, 391	742	7.42	6.98	372.37	372.29
M3	213, 357	4712	47.14	44.32	269.58	266.82
M4	51, 171	72	0.72	0.68	127.24	121.63
M5	52, 779	9988	99.93	93.94	250.13	241.32
M6	391, 779	238	2.38	2.24	516.14	505.53

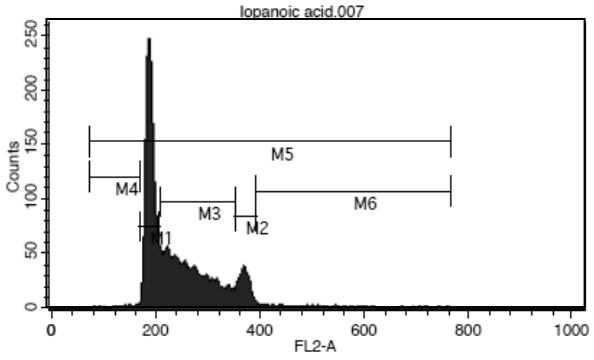

Histogram Statistics

File: Iopanoic acid.007 Log Data Units: Linear Values
Acquisition Date: 28-Jan-15 Gate: G1
Gated Events: 9987 Total Events: 10373
X Parameter: FL2-A (Linear)

Marker	Left, Right	Events	% Gated	% Total	Mean	Geo Mean
All	0, 1023	9987	100.00	96.28	250.14	240.40
M1	171, 207	4087	40.92	39.40	190.69	190.57
M2	353, 393	891	8.92	8.59	370.07	369.96
M3	209, 353	4642	46.48	44.75	266.24	263.38
M4	76, 171	69	0.69	0.67	138.59	135.95
M5	76, 767	9973	99.86	96.14	249.59	240.23
M6	393, 767	249	2.49	2.40	521.83	512.07

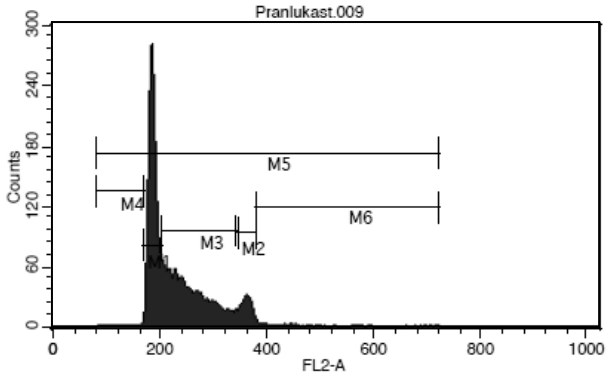

Histogram Statistics

File: Pranlukast.009 Log Data Units: Linear Values
Acquisition Date: 28-Jan-15 Gate: G1
Gated Events: 9985 Total Events: 10644
X Parameter: FL2-A (Linear)

Marker	Left, Right	Events	% Gated	% Total	Mean	Geo Mean
All	0, 1023	9985	100.00	93.81	239.40	230.80
M1	169, 204	4353	43.60	40.90	187.76	187.63
M2	345, 382	746	7.47	7.01	361.70	361.59
M3	204, 345	4674	46.81	43.91	256.95	254.19
M4	81, 169	79	0.79	0.74	132.32	129.86
M5	81, 724	9959	99.74	93.56	238.46	230.47
M6	382, 724	194	1.94	1.82	498.42	488.58

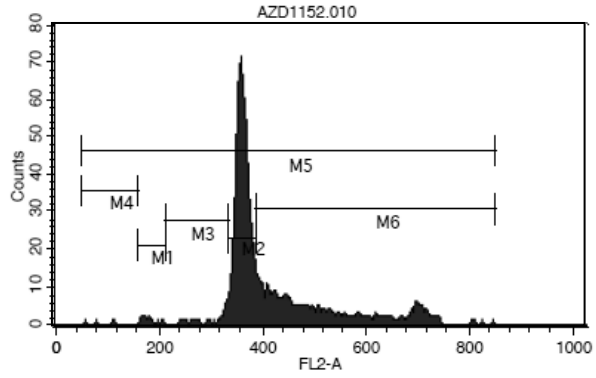

Histogram Statistics

File: AZD1152.010 Log Data Units: Linear Values
Acquisition Date: 28-Jan-15 Gate: G1
Gated Events: 3375 Total Events: 3765
X Parameter: FL2-A (Linear)

Marker	Left, Right	Events	% Gated	% Total	Mean	Geo Mean
All	0, 1023	3375	100.00	89.64	414.49	399.95
M1	157, 210	38	1.13	1.01	178.21	177.78
M2	333, 385	1889	55.97	50.17	358.67	358.49
M3	210, 333	118	3.50	3.13	302.97	300.75
M4	47, 157	20	0.59	0.53	90.70	85.57
M5	48, 847	3360	99.56	89.24	412.84	399.25
M6	385, 847	1311	38.84	34.82	511.83	500.62

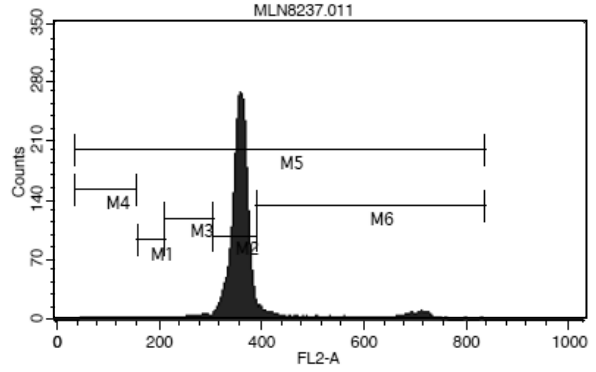

Histogram Statistics

File: MLN8237.011 Log Data Units: Linear Values
Acquisition Date: 28-Jan-15 Gate: G1
Gated Events: 9964 Total Events: 11581
X Parameter: FL2-A (Linear)

Marker	Left, Right	Events	% Gated	% Total	Mean	Geo Mean
All	0, 1023	9964	100.00	86.04	372.79	362.71
M1	157, 210	68	0.68	0.59	184.96	184.34
M2	306, 388	8290	83.20	71.58	354.57	354.28
M3	210, 306	276	2.77	2.38	267.63	266.18
M4	35, 155	120	1.20	1.04	99.85	94.54
M5	35, 833	9949	99.85	85.91	372.03	362.32
M6	388, 833	1215	12.19	10.49	551.73	536.32

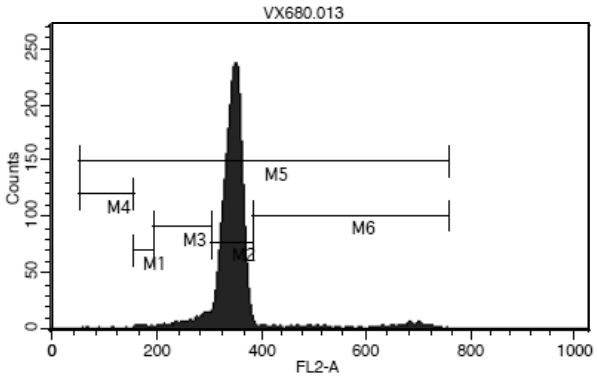

Histogram Statistics

File: VX680.013 Log Data Units: Linear Values
Acquisition Date: 28-Jan-15 Gate: G1
Gated Events: 9996 Total Events: 11483
X Parameter: FL2-A (Linear)

Marker	Left, Right	Events	% Gated	% Total	Mean	Geo Mean
All	0, 1023	9996	100.00	87.05	352.65	346.49
M1	155, 195	65	0.65	0.57	174.06	173.79
M2	304, 386	8734	87.37	76.06	345.29	344.97
M3	195, 304	636	6.36	5.54	267.39	265.81
M4	53, 155	29	0.29	0.25	101.90	97.16
M5	53, 760	9972	99.76	86.84	351.51	345.90
M6	386, 760	523	5.23	4.55	592.66	581.05

Figure S2: Cell cycle results for all compounds, preincubated for 16h with Thymidine.

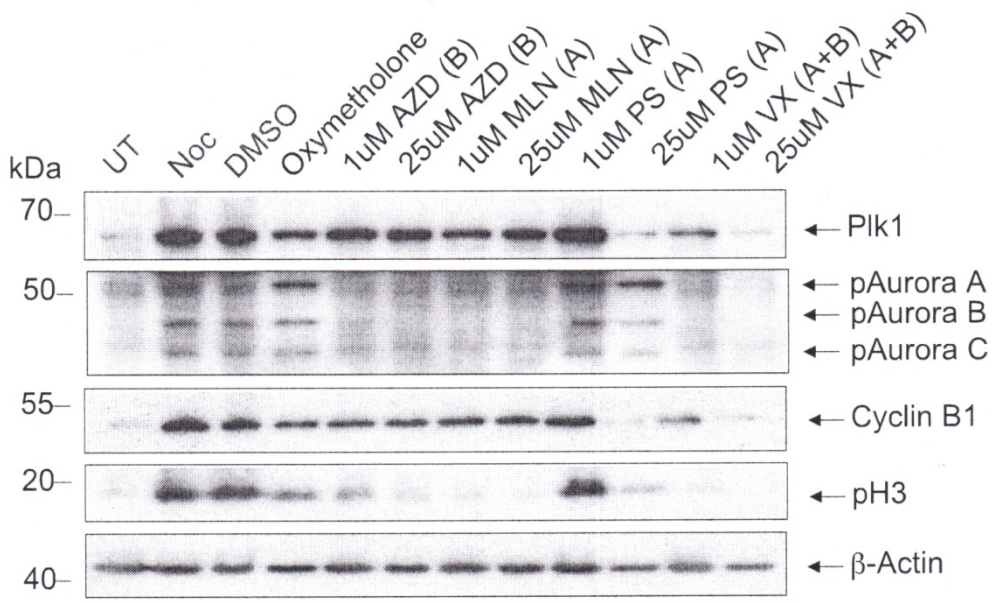

Figure S3: Western blot results for control compounds at 1 and 25 µM.

8. Publications

Co-authorships:

- Schulze, Jörg O., Giorgio Saladino, Katrien Busschots, Sonja Neimanis, Evelyn Süß, Dalibor Odadzic, Stefan Zeuzem, et al. 2016. “Bidirectional Allosteric Communication between the ATP-Binding Site and the Regulatory PIF Pocket in PDK1 Protein Kinase.” Cell Chemical Biology 23 (10): 1193–1205.
- Raab, Monika, Mourad Sanhaji, Larissa Pietsch, Isabelle Béquignon, Amanda K. Herbrand, Evelyn Süß, Santosh L. Gande, et al. 2018. “Modulation of the Allosteric Communication between the Polo-Box Domain and the Catalytic Domain in Plk1 by Small Compounds.” ACS Chemical Biology 13 (8): 1921–31.
- Pabon, Nicolas A., Yan Xia, Samuel K. Estabrooks, Zhaofeng Ye, Amanda K. Herbrand, Evelyn Süß, Ricardo M. Biondi, et al. 2018. “Predicting Protein Targets for Drug-like Compounds Using Transcriptomics.” PLoS Computational Biology 14 (12): e1006651.

9. Acknowledgment

I performed my studies in the Department of Internal Medicine I, Frankfurt University Hospital under the direction of Ricardo M. Biondi. I would like to express my sincerest gratitude to Ricardo, who made it possible for me to write a doctoral thesis in anti-cancer drug research as I always wanted to. I would like to thank him for all the support over the years it took me to finish this thesis, all the positivity and words of motivation, even from Argentina to Switzerland. Also, I would like to thank Evelyn Süss and Larissa Pietsch not only for teaching me the basics of laboratory work and answering every single one of my many questions, but also for being the sweetest colleagues and creating an atmosphere in our lab that made me go to work gladly.

Many thanks also to Jörg Schulze, who made a lot of effort attempting to generate Aurora crystals in complex with my compounds, and Albrecht Piiper, who kindly agreed on being my doctoral advisor and offered help and support whenever needed; to Klaus Strebhardt and Monika Raab for offering their lab and expertise for cell cycle experiments and to Christina Doetsch, who helped me performing those; to Daniel Pastor-Flores, who tested my compounds on Saccaromyces cervesiae; to Pedro Alzari, who made it possible for me to perform MST experiments at Institut Pasteur in Paris, and Mariano Martinez, who was a big help at Institute Pasteur. Thanks to Carlos Camacho who offered the opportunity to take part in his latest publication. Last but not least, thanks to Stefan Zeuzem for offering me the chance to perform my thesis at the department of Internal Medicine and to the department for paying a small salary during the time I worked in the lab.

10. Schriftliche Erklärung

Ich erkläre ehrenwörtlich, dass ich die dem Fachbereich Medizin der Johann Wolfgang Goethe-Universität Frankfurt am Main zur Promotionsprüfung eingereichte Dissertation mit dem Titel

Identification and characterization of allosteric inhibitors of Aurora Kinase A for innovative drug discovery for cancer therapy

in dem Zentrum der Inneren Medizin, Medizinische Klinik I unter Betreuung und Anleitung von Dr. Albrecht Piiper mit Unterstützung von Dr. Ricardo Biondi ohne sonstige Hilfe selbst durchgeführt und bei der Abfassung der Arbeit keine anderen als die in der Dissertation angeführten Hilfsmittel benutzt habe. Darüber hinaus versichere ich, nicht die Hilfe einer kommerziellen Promotionsvermittlung in Anspruch genommen zu haben.

Ich habe bisher an keiner in- oder ausländischen Universität ein Gesuch um Zulassung zur Promotion eingereicht*. Die vorliegende Arbeit wurde bisher nicht als Dissertation eingereicht.

Vorliegende Ergebnisse der Arbeit wurden (oder werden) in folgendem Publikationsorgan veröffentlicht:

Schulze JO, Saladino G, Busschots K, et al. Bidirectional Allosteric Communication between the ATP-Binding Site and the Regulatory PIF Pocket in PDK1 Protein Kinase. Cell Chem Biol. 2016;23(10):1193-1205. doi:10.1016/j.chembiol.2016.06.017.

_____ _____

(Ort, Datum) (Unterschrift)

*) im Falle des Nichtzutreffens entfernen